SPring-8

# INDUSTRIAL APPLICATIONS

## Outline

1. Why did we start promoting industrial use?
2. Industrial support organization
3. Program for the industry supported by MEXT
   a. *Trial Use Program*
   b. *Strategic Program for Utilization of Advanced Large-Scale Research Facilities*
4. Public Beamlines for industrial applications
5. Highlights of industrial research works
6. User satisfaction
7. Summary

**Norimasa Umesaki**
Industrials Application Division, JASRI/SPring-8

10th SPring-8 Anniversary

# Why did we start promoting industrial use?

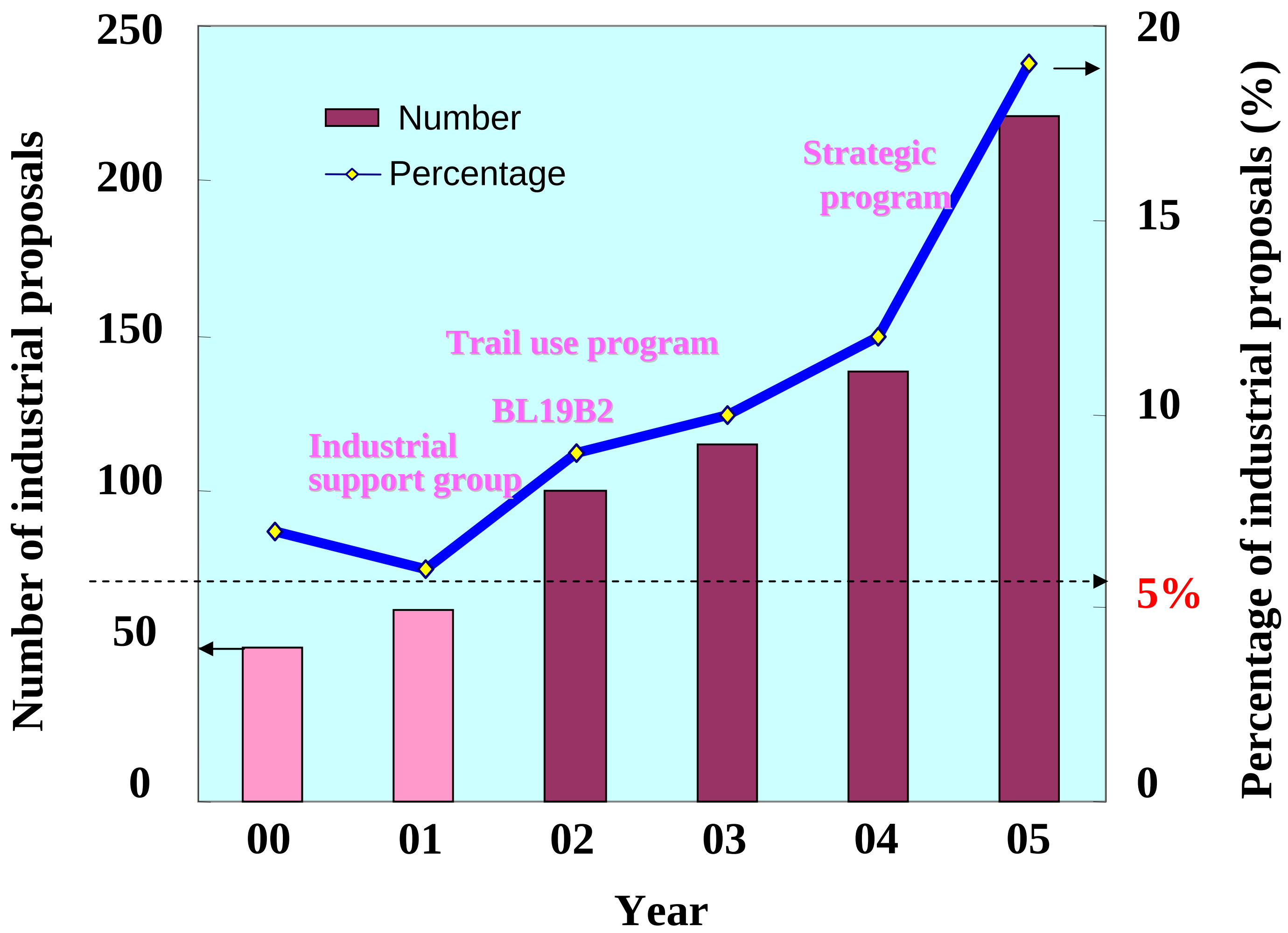


**The annual trend of the Number and Percentage of Industrial Research Proposals from the Companies.**

# Support Organization for Industrial Use

- Since fiscal 2001, ***the Industrial Application/Utilization Support Group*** started with three coordinators, eight technical staff and three in the secretariat.
- In April 2003, ***the Industrial Application/Utilization Support Group*** was reorganized in order to enhance support for the industrial users with four coordinators, seven technical staff and two in the secretariat.
- In April 2005, in order to cope promptly with various forms of utilization by industrial application users and reinforcement of support for beamline utilization in future, the group became a division called ***the Industrial Application Division***, and has been keeping its dynamic activities so far.

# Staff of Industry Application Division

**The industry application division** was organized at JASRI/SPring-8 in April 2001.

- **Hard Materials Science:**

**4 coordinators**

Dr. Y. Watanabe (Semiconductor materials)
Dr. S. Komiya (Electronics devise)
Dr. N. Umesaki (Metal, inorganic, etc.)
Dr. T. Hashimoto (Structural steel)

- **Soft Matter Science:**

**4 coordinators**

Dr. M. Sugiura (Catalysis science)
Dr. T. Ninomiya (Chemical analysis)
Dr. Y. Ohashi (Crystallography )
Dr. K. Horie (Polymer materials)

**6 beamline scientists and 10 engineers**

Secretariat (3 people)

# Services Provided by Industry Application Division

- Promotion of industrial use
- Interface between companies and SPring-8
- Consultation on industrial subjects
- Training meetings and courses
- Technical and scientific support
- Management of public beamlines BL14B2, BL19B2 and BL46XU
  - Industrial applications
- Collaboration with companies
- Workshops and research meetings

# Promoting Programs for Industrial Use

## - To increase the number of industrial users and application fields -

| Phase I (2001, 2003-2005) | Phase II (2005-present ) |
|---|---|
| ***Trial Use Program*** | ***Strategic Program*** *for Utilization of Advanced Large-scale Research Facilities* |
| Adopted proposals: **40** proposals/year | Adopted proposals: **125** proposals/year |
| Adoption Priority**: new industrial users** | Adoption Priority**: new industrial users** |
| Proposal according to several analytical methods | Proposal according to industrial application fields |
| Support: 3 coordinators, 6 beamline staff | Support: 8 coordinators, 16 beamline staff |

**(Financial support of MEXT)**

# Annual Trend of Number of People and Companies using SPring-8

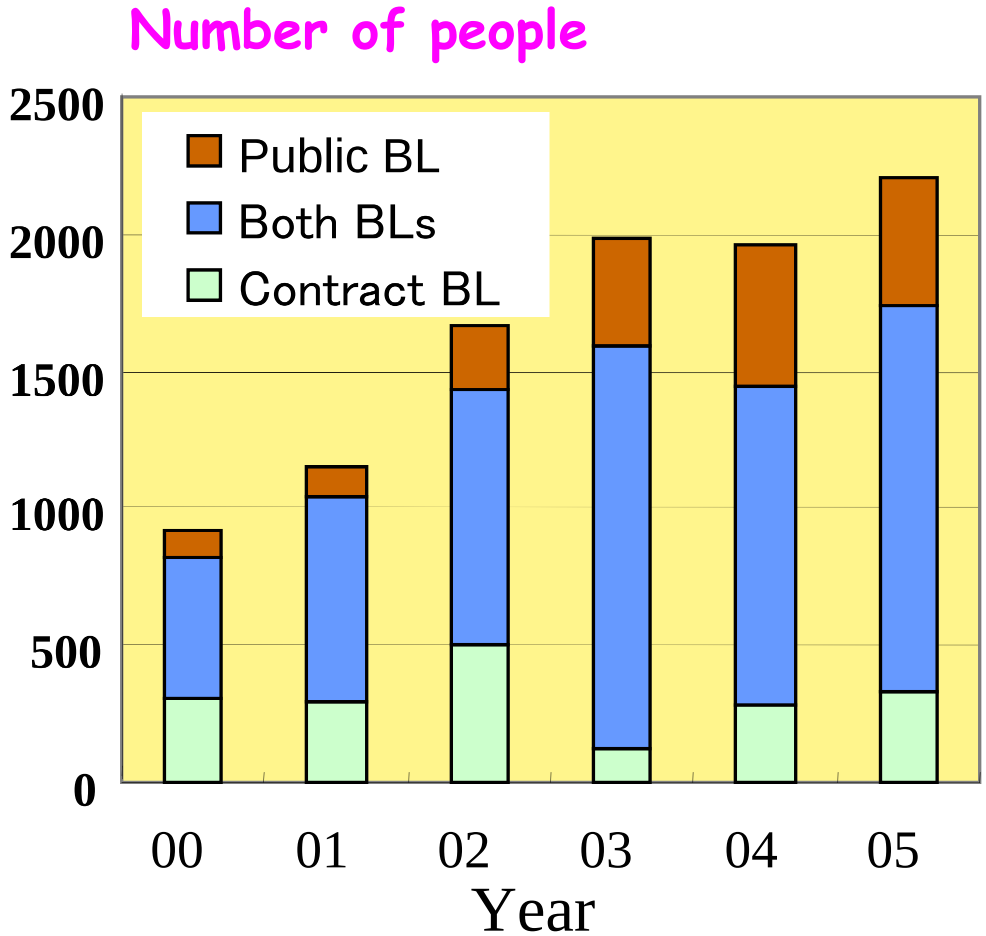


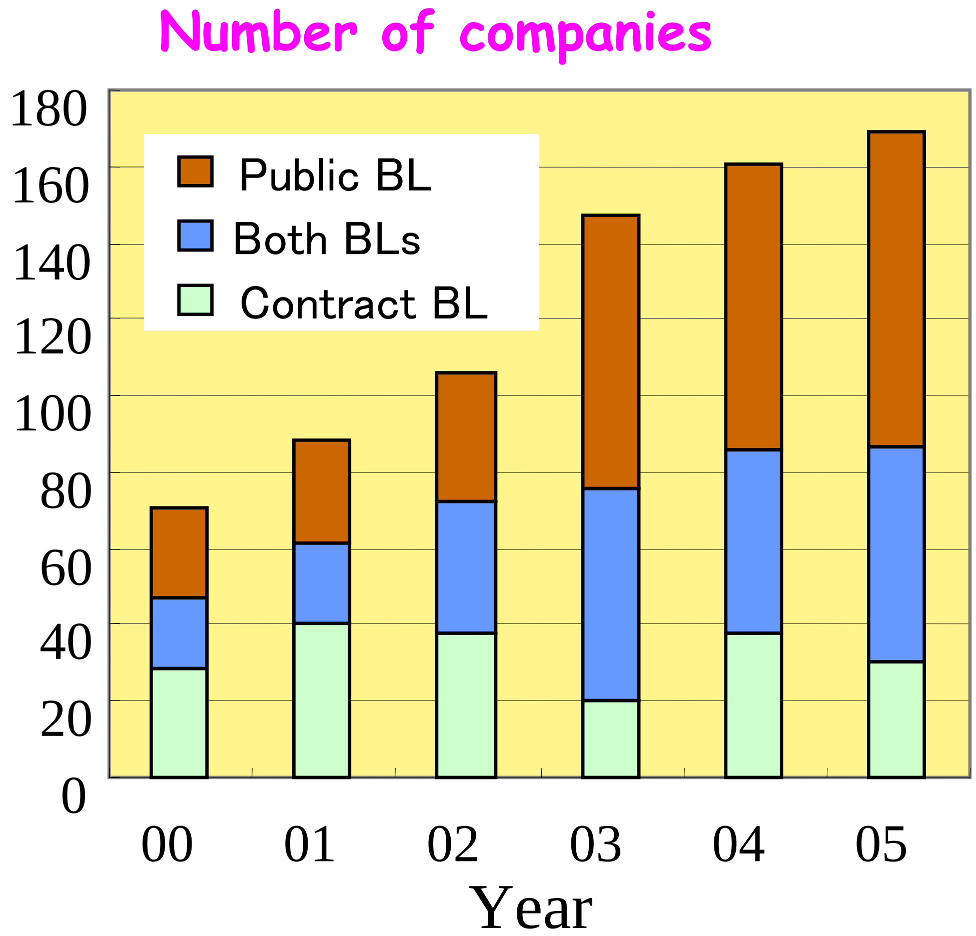

# The Annual Trend of the Number and Percentage of Industrial Research Proposals from the Companies

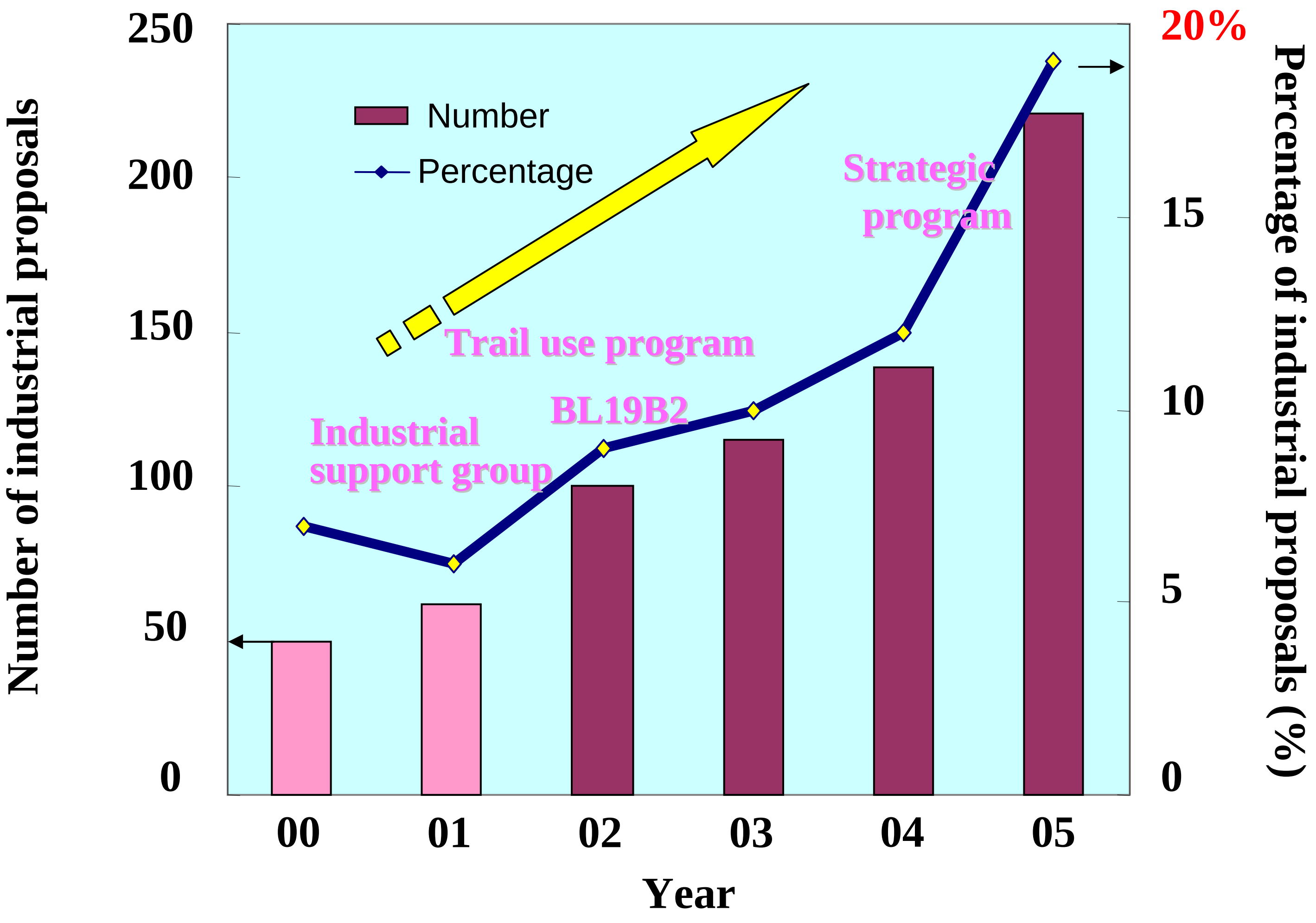

# Industrial Applications

SANYO Electric, SUMITOMO ELECTRIC, SONY, TOSHIBA, NEX, HITACHI, FUJITSU, Fuji Electric, Mistubishi Electric, Panasonic, NTT, Canon, RICOH, TAIYO YUDEN, etc.

TOYOTA CENTRAL R&D LABS., DAIHATSU, MATSUDA etc.

Kawasaki, KOBELCO, SUMITOMO Metals, Nippon Steel, JFE Steel CO., MITSUBISHI HEAVY INDUSTRIES, TOSHIBA, MITSUBISHI MATERIALS, AsahiKASEI, AKO KASEI CO., SRI, TOYOBO, SUMITOMO CHEMICAL, FUJIFILM, NISSAN CHEMICAL INDUSTRIES, MITSUBISHI RAYON CO., TAKIRON etc.

## Electronics

- Films for ULSI,
- Semiconductors
- HDD, DVD
- Semiconductor laser

## Automobile

## Metals & Soft materials

…uction materials

…ctional polymer

**2,300 users**

**Easy Accessibilyty**

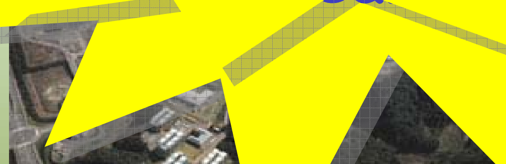

## Energy & Environment

- Batteries: fuel cell & Li-ion
- Nuclear power material
- Analysis of contamination elements
- Catalysts for environment

TOYOTA, TOYOTA CENTRAL R&D LABS., Honda Motor Co., DAIHATSU, MATSUDA, NISSAN ARC, KANSAI ELECTRIC POWER CO., TOKYO GAS, GS Yuasa Co., TOHO GAS, DAISO Co., NIPPON OIL CO., etc.

## Material Analysis

TRC, Kobelco research Inst., NITTECH RESEARCH, Sumitomo Metal Technology Inc., Mitsui Chemical Analysis & Consulting Serve Inc., MCRC, etc.

## Life science

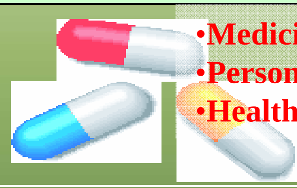

- Medicine
- Personal care products
- Health care

Astellas, Eisai, DAINIPPON SUMITOMO PHARMA, SHIONOGI & Co., Meiji, Mochida Pharmaceutical Co., Kao Co., SUNSTAR, LION, P&G, INAX, SHISEIDO, Kanebo, KOSE, MENARD, Takeda Pharmaceutical Co., etc.

# Utilization of SR of SPring-8

| Feature | Advantage |
| --- | --- |
| Ultra-bright | Ultra-trace element analysis; Quick analysis |
| Highly direction | Micro-area analysis; High resolution analysis |
| Energy selectivity | Element selection analysis |
| High energy | Deep part analysis |

# Interaction of X-rays with Matter

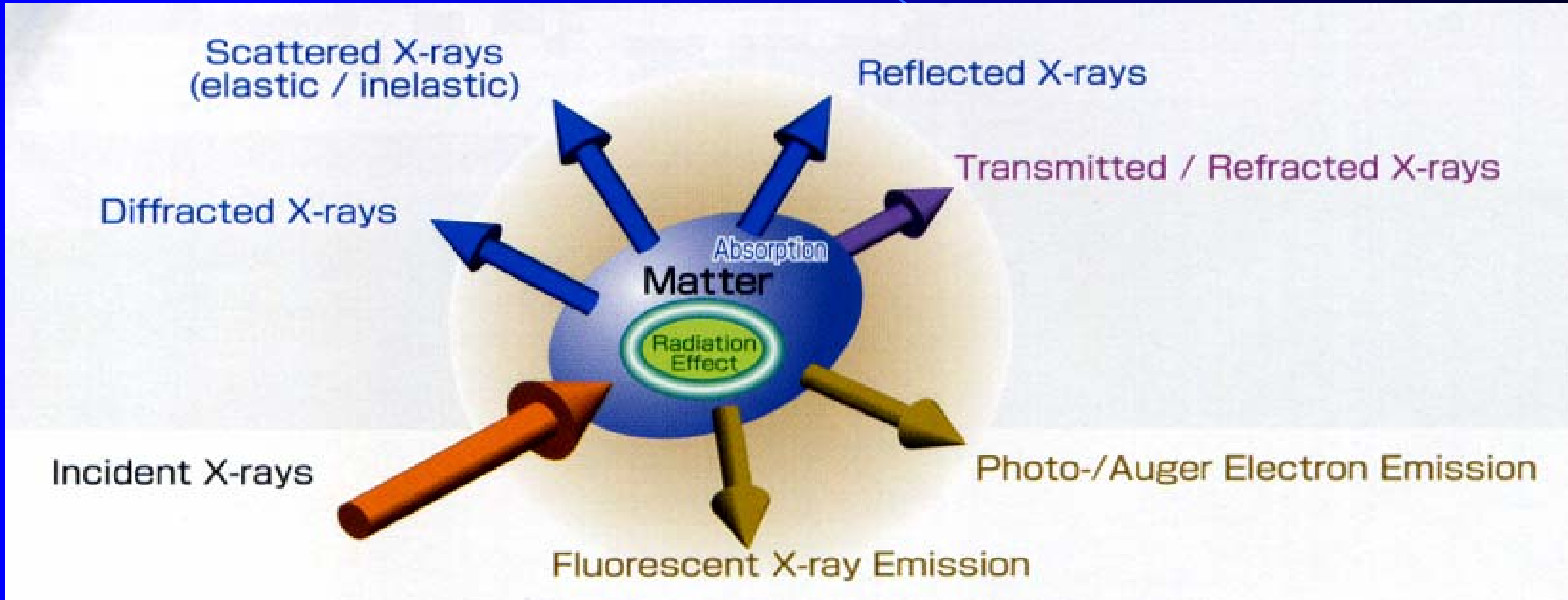


- **Diffraction / Scattering X-rays**: the atom arrangement of the material and electronic density distribution or the time fluctuation of the atom
- **Transmitted / Refracted X-rays**: Microstructure observation of micron size and submicron size of materials and biological substance
- **Spectroscopic Analysis**: Electronic structure and ultra-trace element analysis

# Research Methods Used in the SR Science

## X-ray Diffraction and Scattering

- Macromolecular crystallography
- X-ray diffraction under extreme conditions
- X-ray powder diffraction
- Surface diffraction
- Small angle scattering
- Medium angle scattering
- X-ray magnetic scattering
- X-ray diffuse scattering
- Residual stress analysis
- Nuclear resonant scattering/Nuclear excitation
- X-ray Optics

## X-ray Imaging

- Refraction-contrast imaging
- Phase-contrast imaging
- X-ray microtomography
- X-ray fluorescence microscopy
- X-ray microscopy
- X-ray topography
- X-ray holography
- Photoelectron emission microscopy (PEEM)

## Spectroscopy and Spectrochemical Analysis

- Photoelectron spectroscopy
- Atomic and molecular spectroscopy
- Compton scattering/Compton magnetic scattering
- X-ray inelastic scattering
- X-ray fluorescence spectroscopy
- XAFS (X-ray absorption fine structure)/X-ray absorption spectroscopy
- X-ray magnetic circular dichroism
- X-ray photon correlation spectroscopy
- Infrared spectroscopy

## Radiation Effect

- Material processing
- Radiation biology

**High performance analysis tool → Many functions utilization**

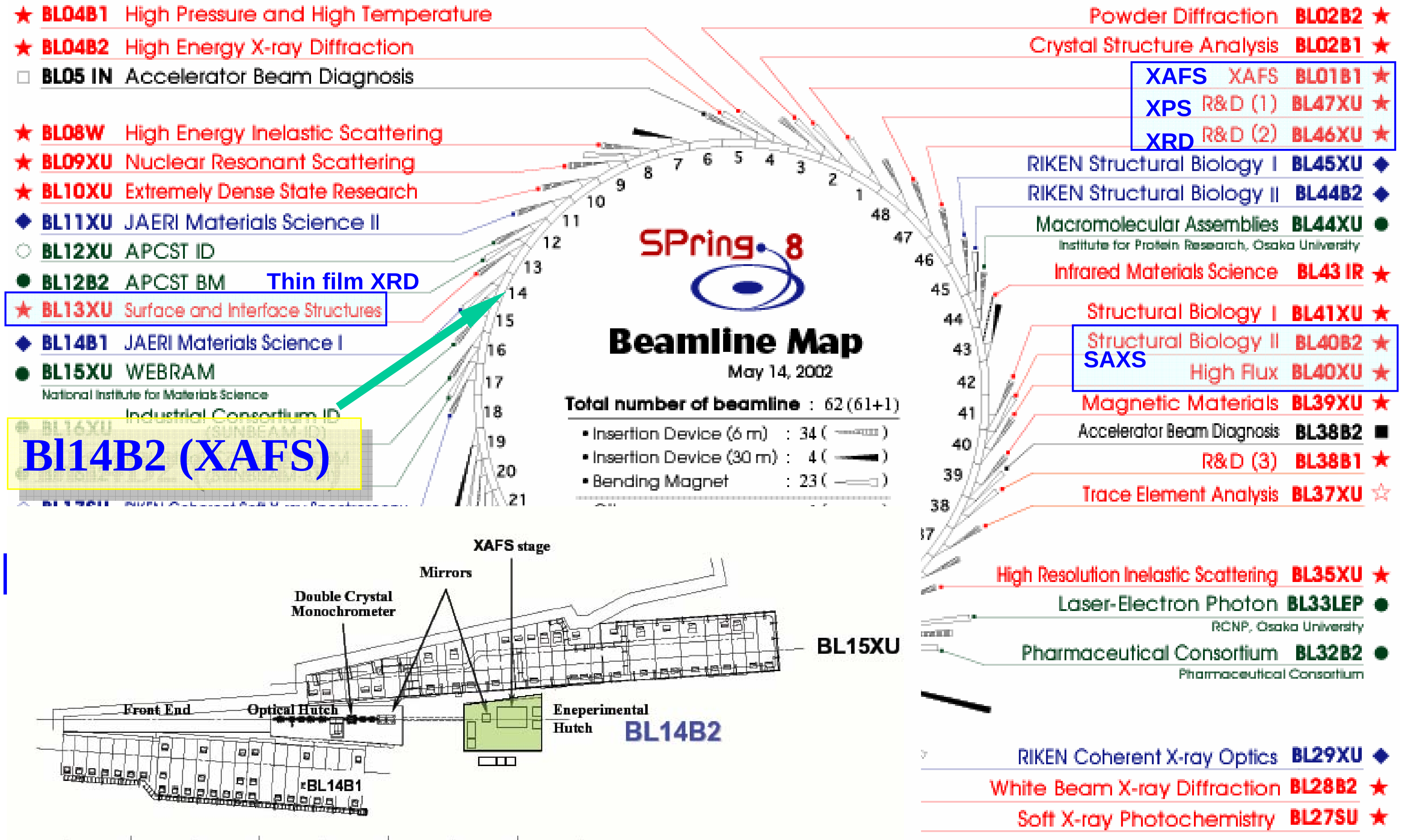


| | | Beamline | | | Total |
|---|---|---|---|---|---|
| | | Contract Beamlines | RIKEN Beamlines | Accelerator Beam Diagnostic Lines | |
| Operation | 25 | 14 | 7 | 2 | 48 |
| Planned or Construction | 0 | 0 | 0 | 0 | 0 |
| Total | 25 | 14 | 7 | 2 | 48 |

☆ ○ ◇ □ : Planned or Under construction

# Engineering Science Research Beamline (BL19B2)

Standard double Si crystal monochromater of SPring-8

Energy range 4 -111KeV

## 1st Station: XAFS

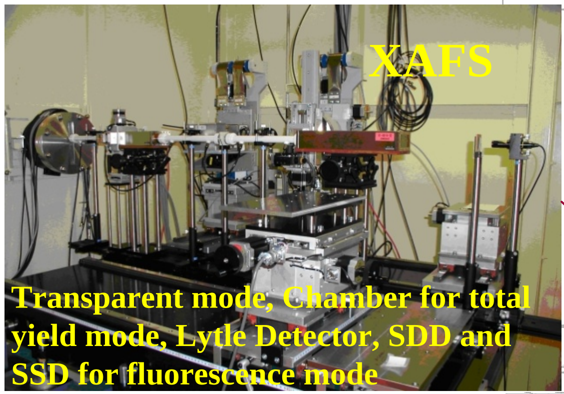


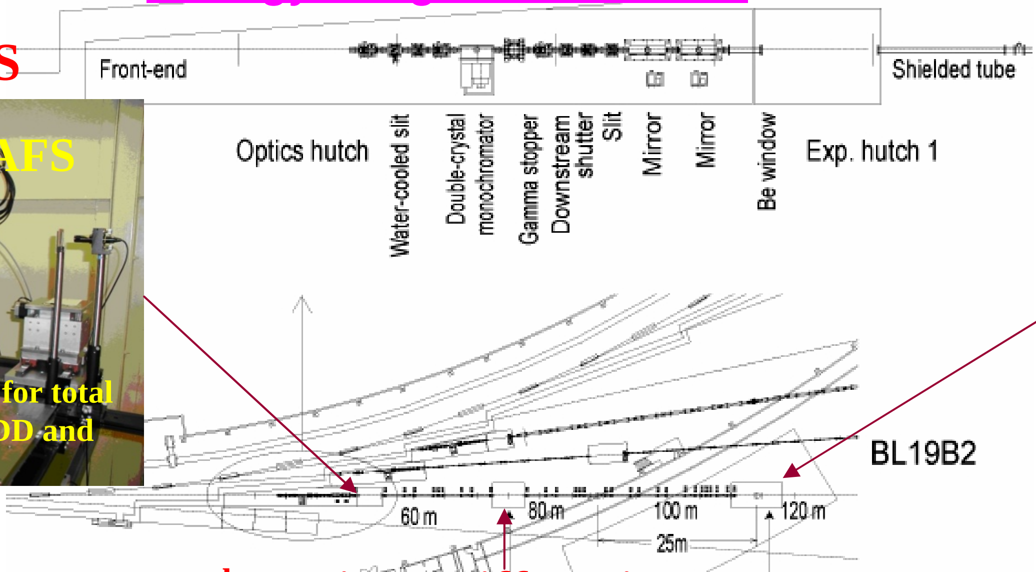


## 3rd Station: Imaging

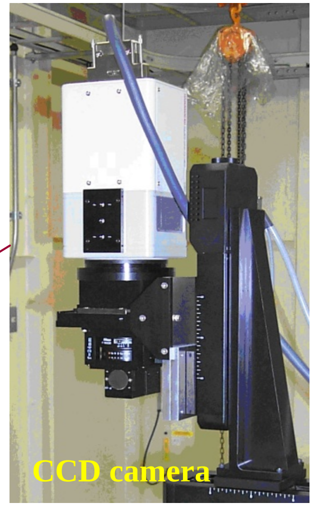


## 2nd Station: Diffraction: XRD


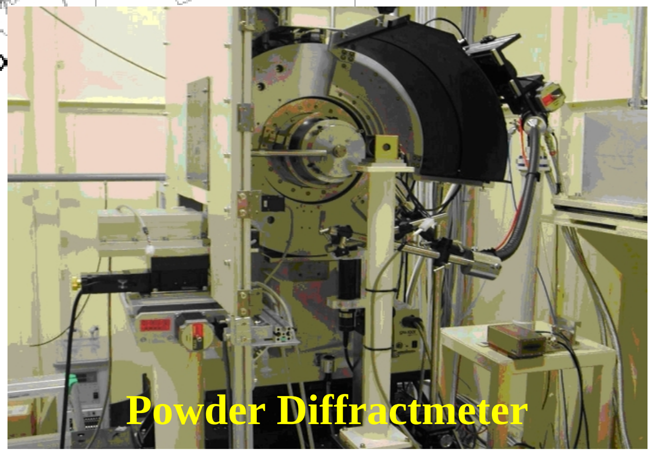

SPring-8

# INDUSTRIAL APPLICATIONS

## Outline

1. Why did we start promoting industrial use?
2. Industrial support organization
3. Program for the industry supported by MEXT
   a. *Trial Use Program*
   b. *Strategic Program for Utilization of Advanced Large-Scale Research Facilities*
4. Public Beamlines for industrial applications
5. Highlights of industrial research works
6. User satisfaction
7. Summary

**Norimasa Umesaki**
Industrials Application Division, JASRI/SPring-8

10th SPring-8 Anniversary

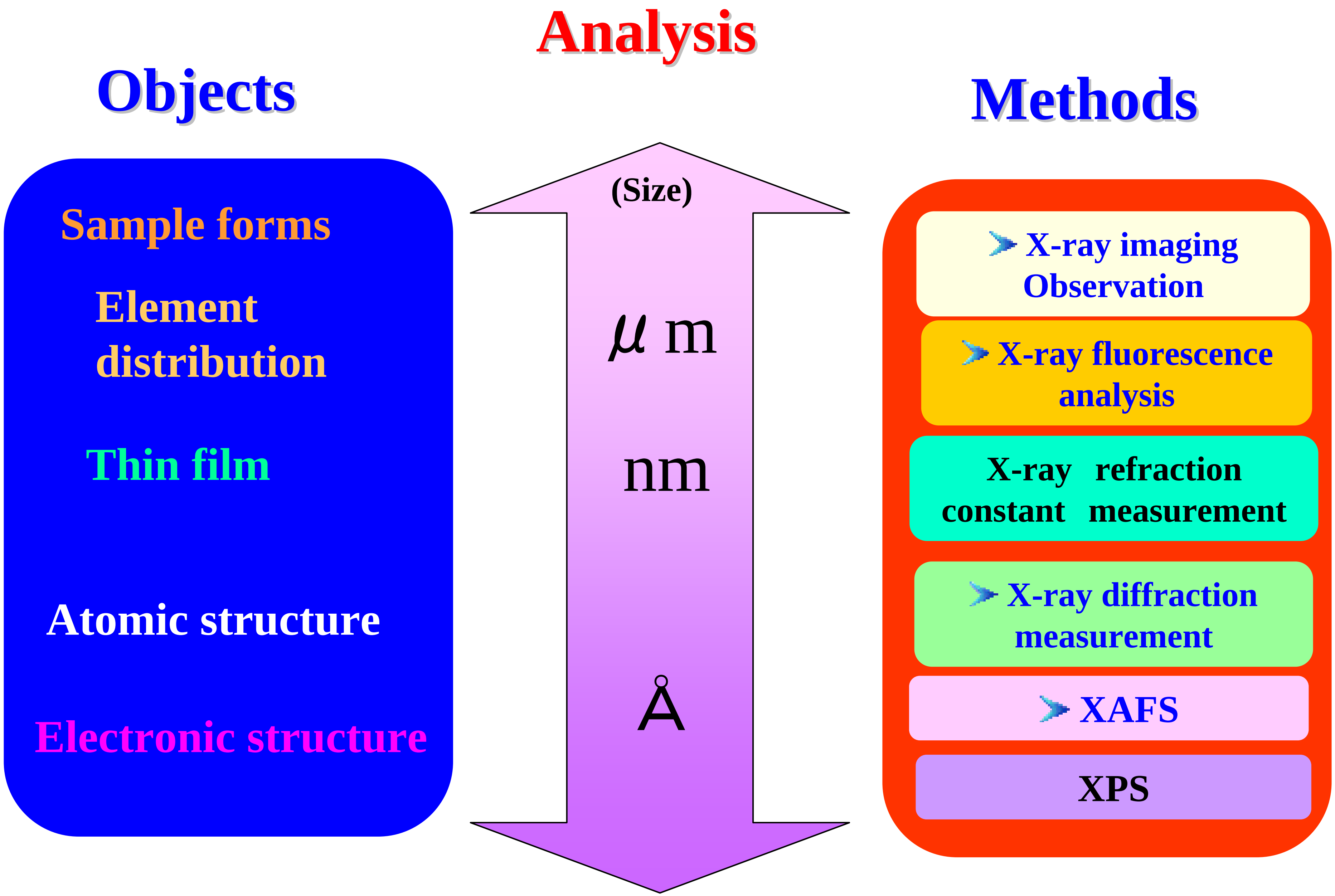
Analysis
Objects
Methods
Sample forms
Element distribution
Thin film
Atomic structure
Electronic structure
(Size)
μ m
nm
Å
X-ray imaging Observation
X-ray fluorescence analysis
X-ray refraction constant measurement
X-ray diffraction measurement
XAFS
XPS

**➤ X-ray Imaging**

When X-rays penetrate in the substance, we can observe X-ray absorption and refraction images through substrate.

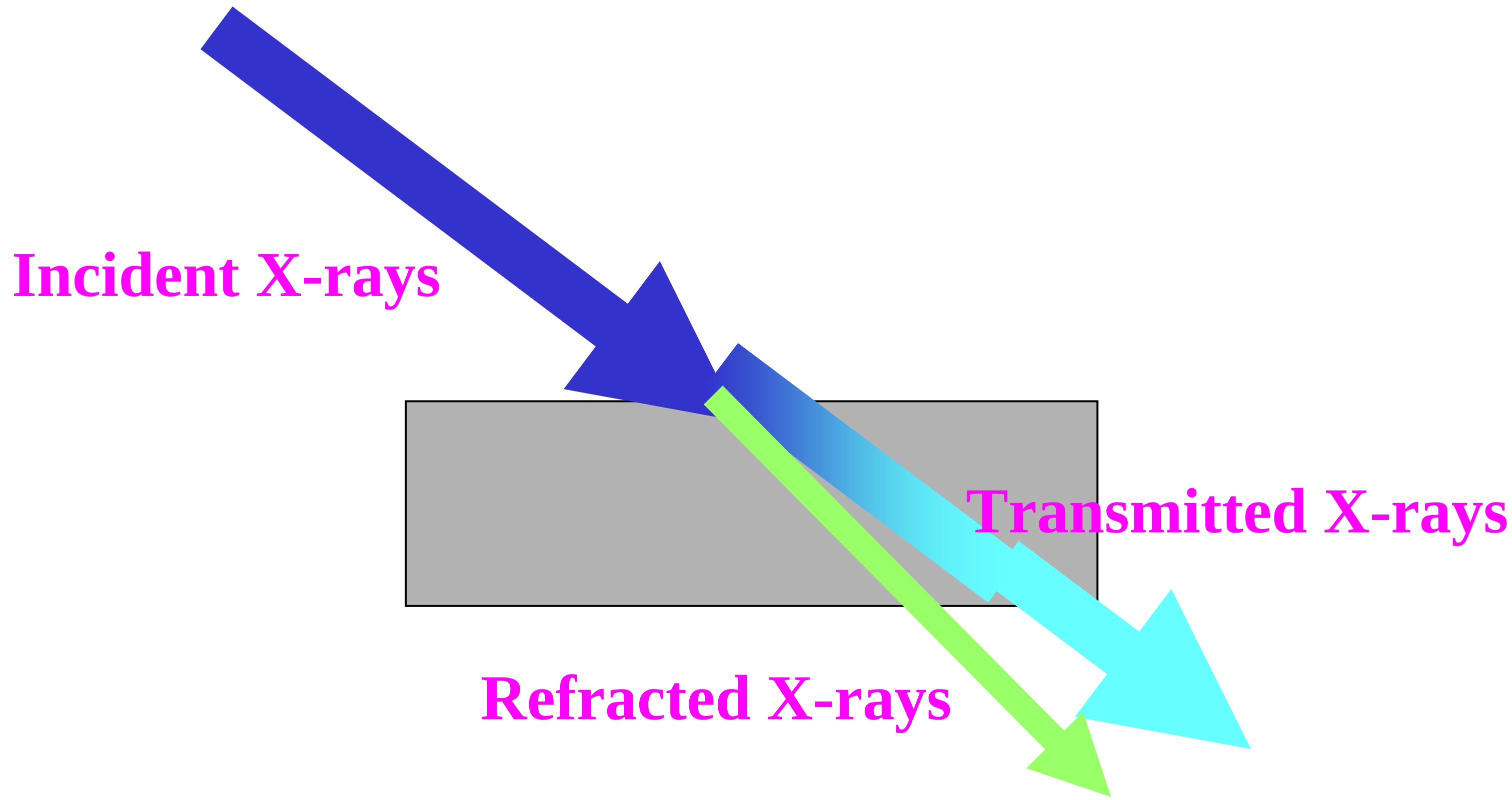

**$\sim \mu$ m**

Morphological Observation

X-ray Imaging

# Observation of contact behavior between glass-fibers in rubber and ice by refraction-contrast image

## Example 2

DUNLOP
SUMITOMO RUBBER INDUSTRIES, LTD.

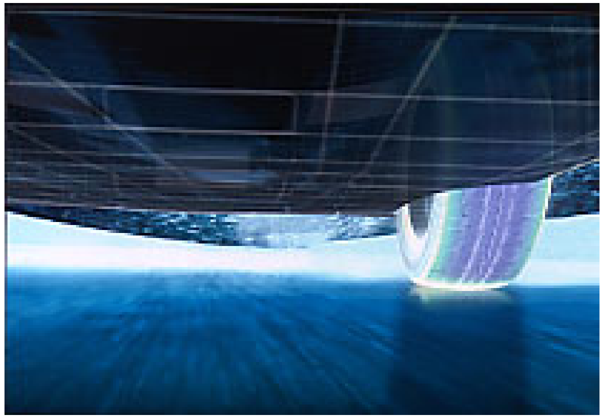

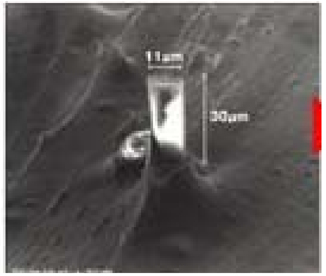

SEM image of implanted glass fiber (33 $\mu$ m diameter)

Glass fibers implanted in tires for frozen road

**The behavior of glass fibers on ice was unknown.**

# Experiments (3rd Station of BL19B2)

## Refraction-contrast imaging of glass fibers in rubber

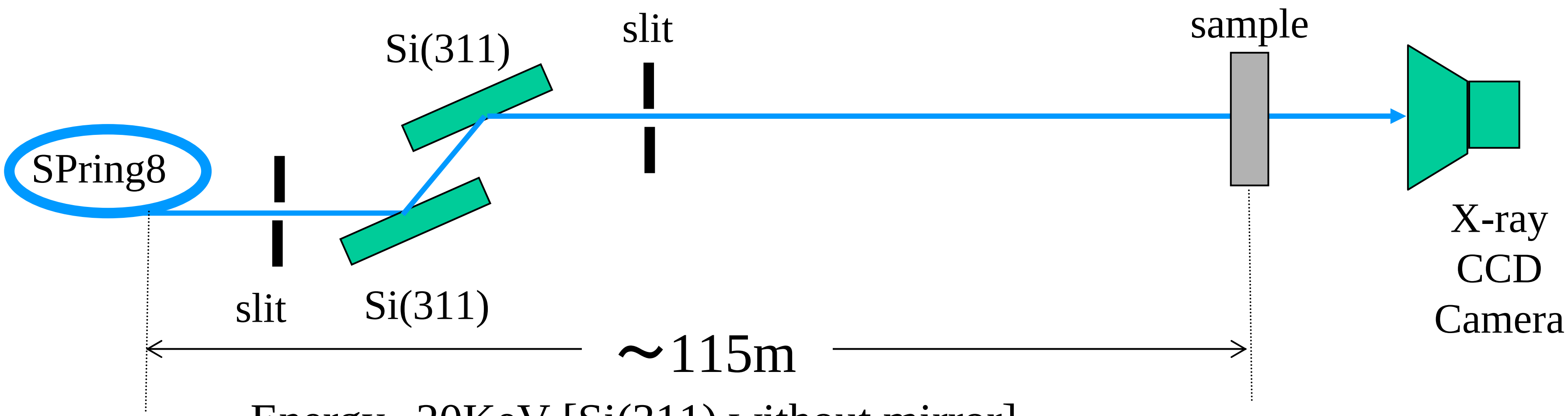


Energy 20KeV [Si(311) without mirror]

Distance between sample and detector : 4m

Active area of detector : 10mm × 10mm

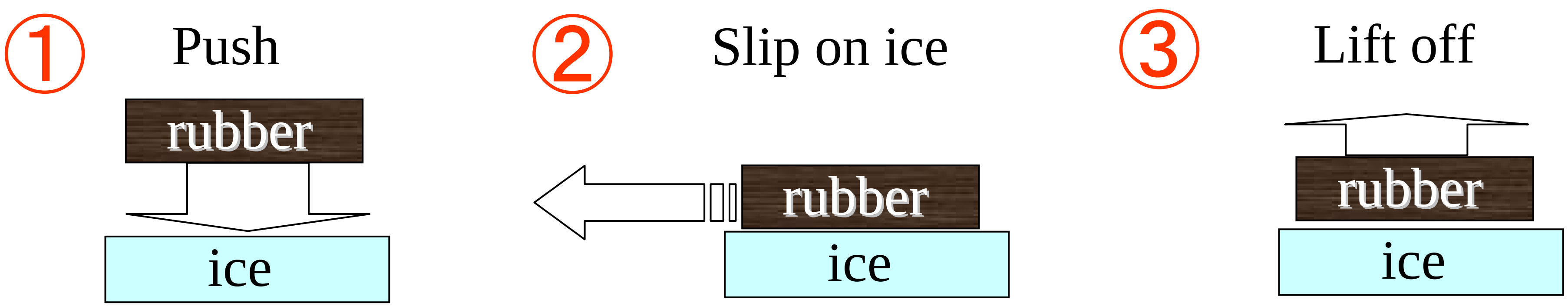

# Experiments (3rd Station of BL19B2)

## Compression and shearing machine

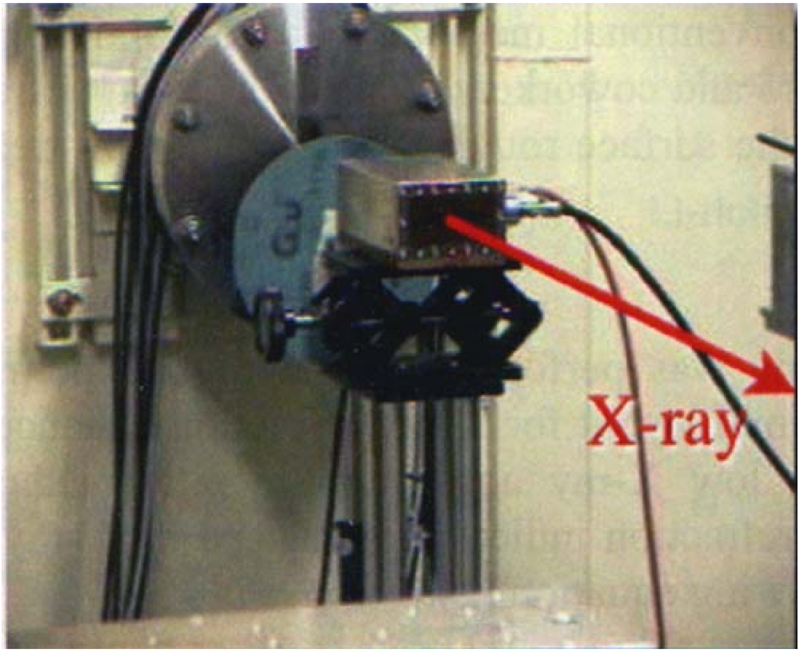


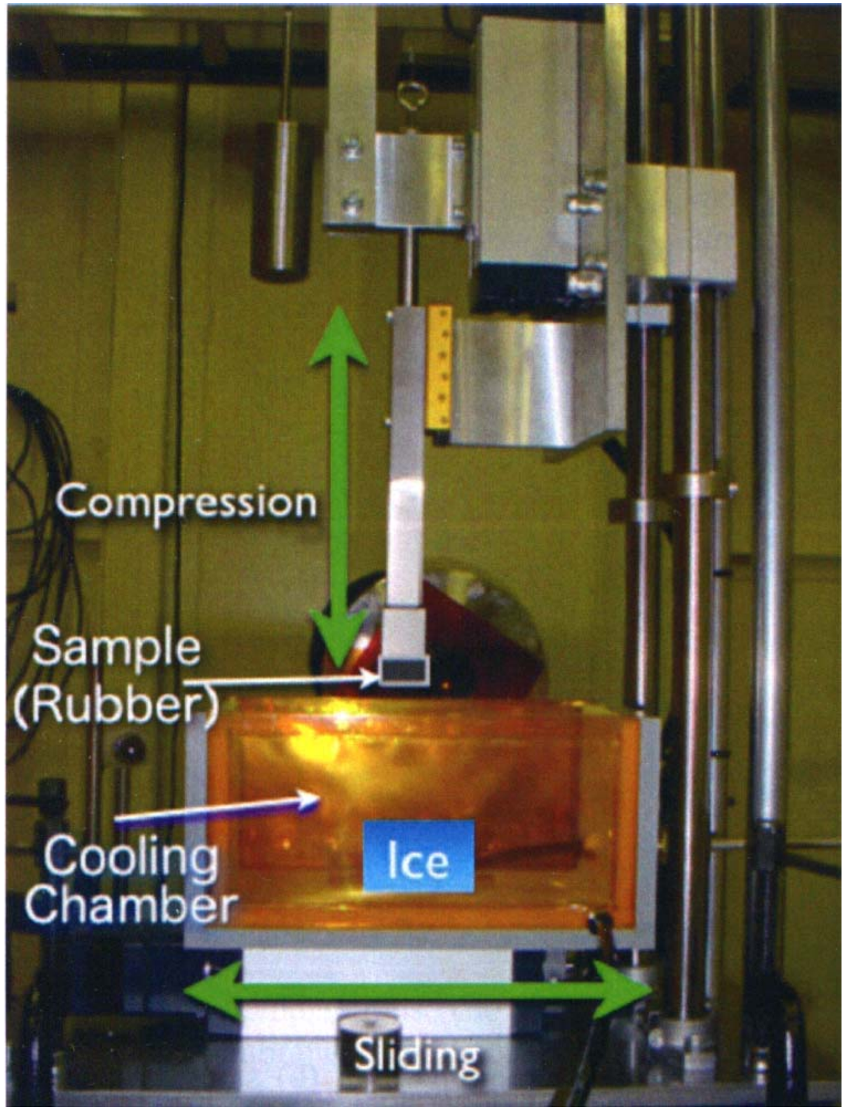

# Observed refraction contrast image

Rubber

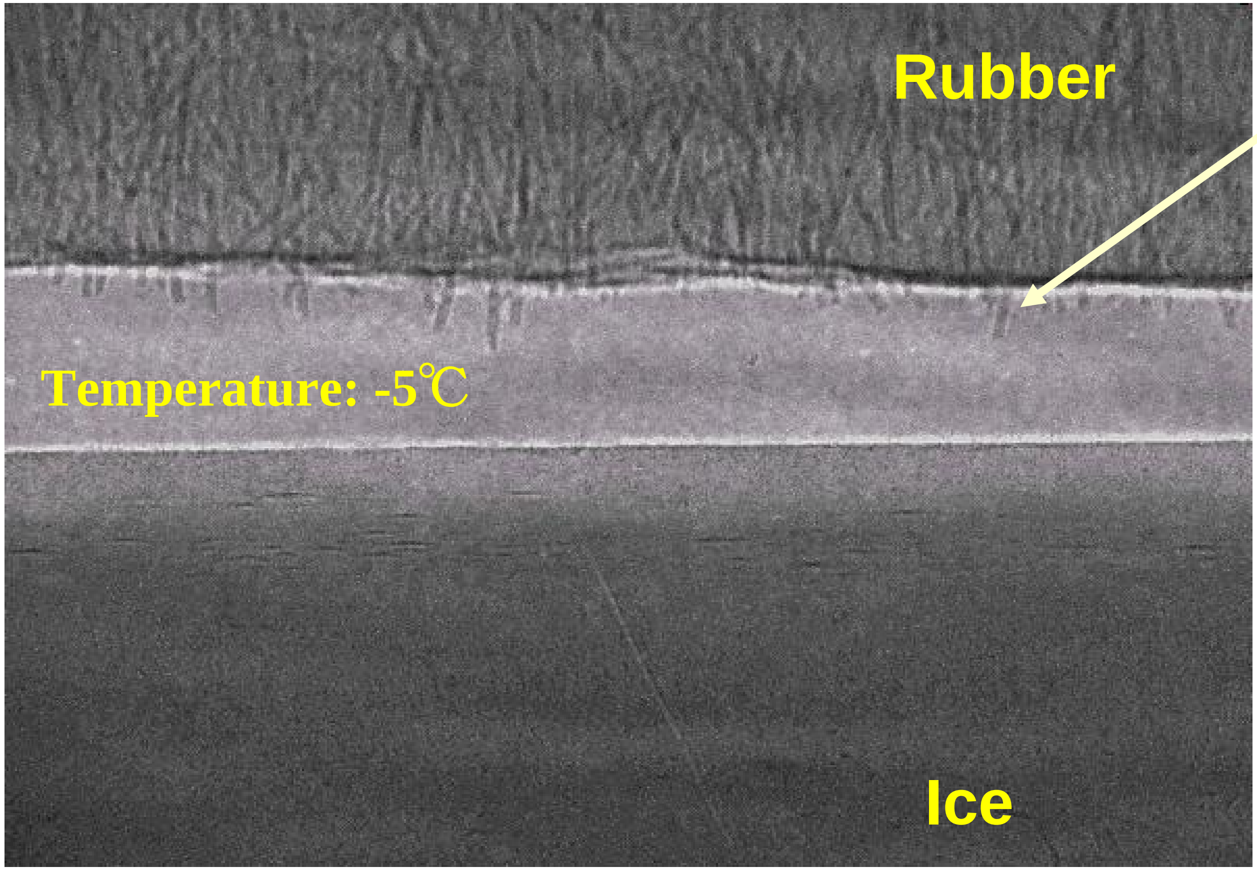


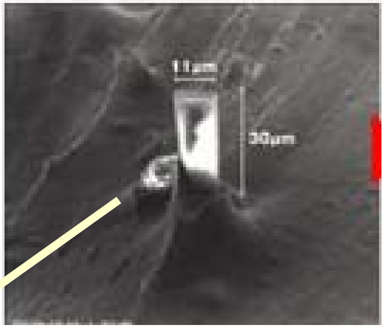

Glass fiber

Ice

**Shapes of glass fibers were clearly observed.**

# Real-time imaging of rubber and ice contact

## Scheme

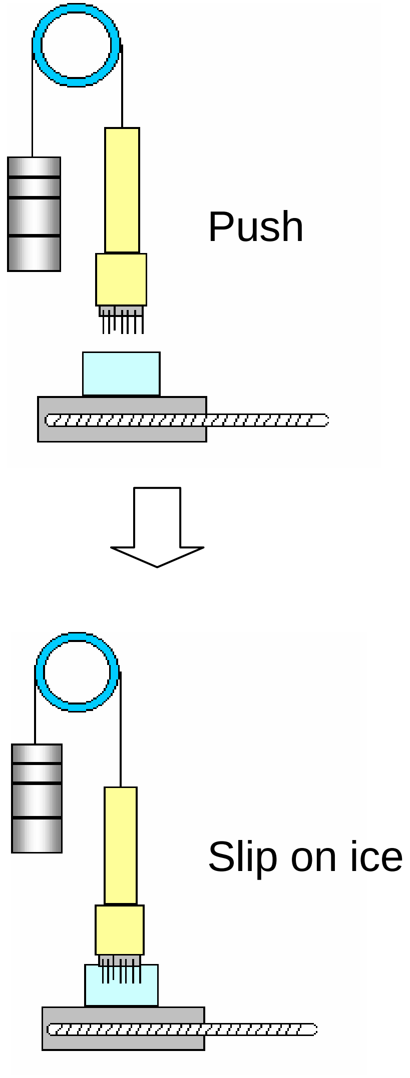


## A result of observation

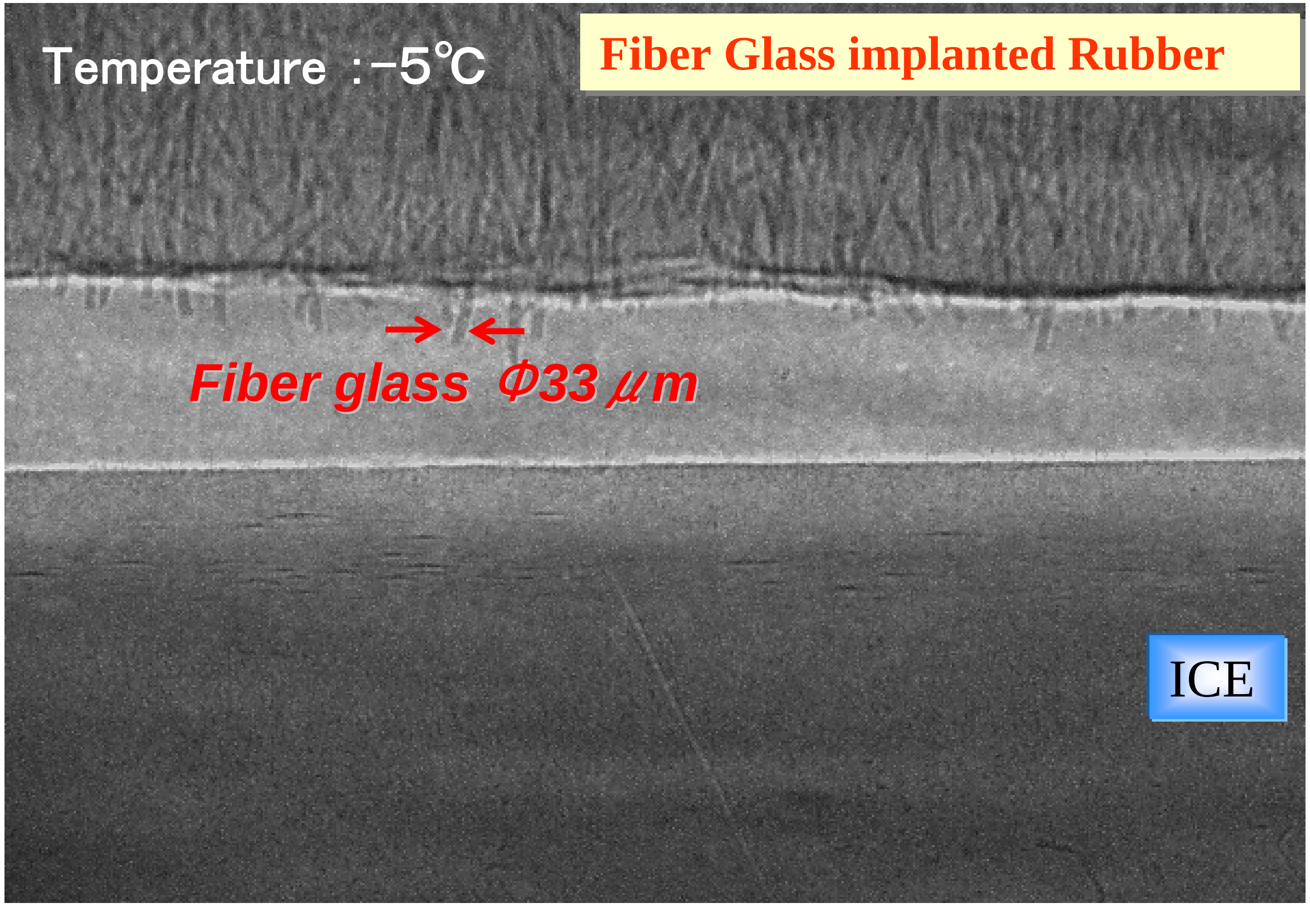


***Fibers don't transform, nor break.***

# Real-time imaging of rubber and ice contact

## Scheme

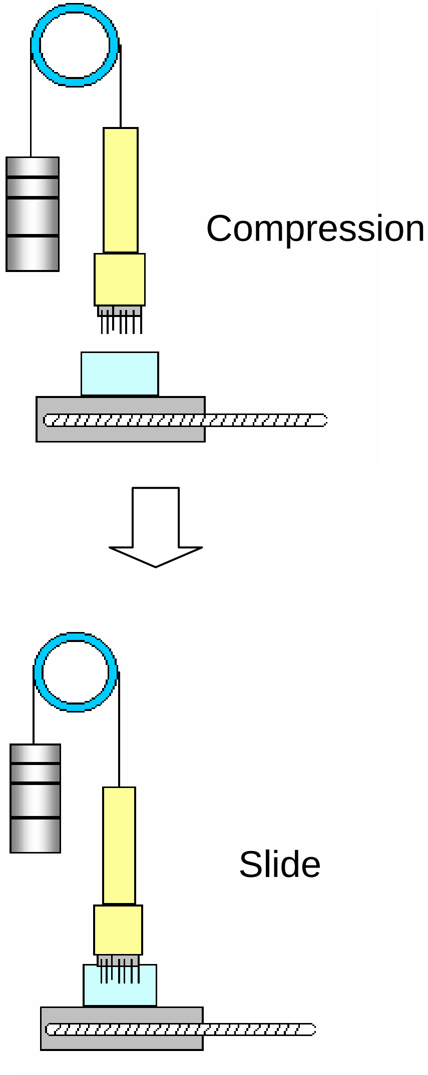


## A result of observation

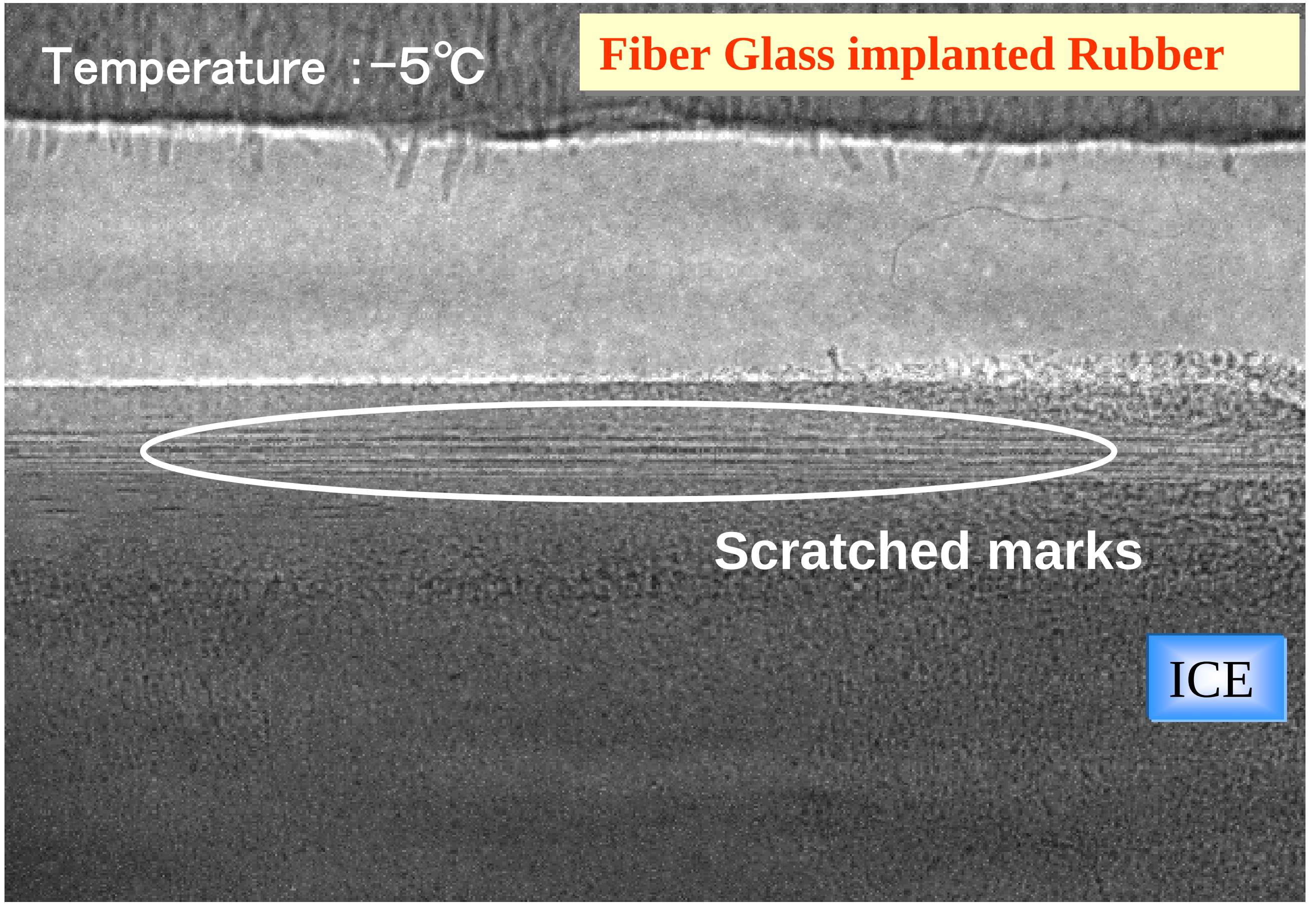


***Direct observation of fiber glass behavior on ice is proving the engineering simulations for the development of a high-performance tire.***

# Observation of contact behavior between glass-fibers in rubber and ice by refraction-contrast image

## Summary

- **Glass fibers drill into ice.**
- **Almost glass fibers were removed from the ice without breaking.**
  - *Observed images were used in a promotion video to advertise tires*

# In situ X-ray Radiography for Compression Test of Foam Aluminum

Kobelco Research Institute, Inc., Shinko Wire Co., Ltd. And Kobe Steel Ltd.

**Crashworthiness**

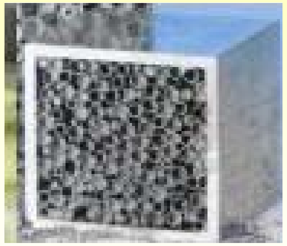

Human safety

33keV

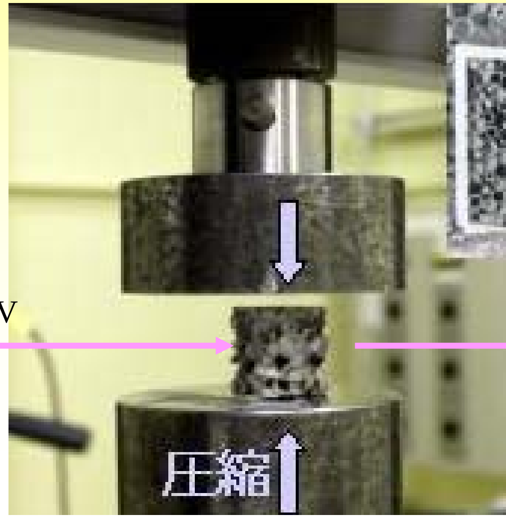


1280×1024pixel CCD camera with a 6.7 μm pixel size

CCD

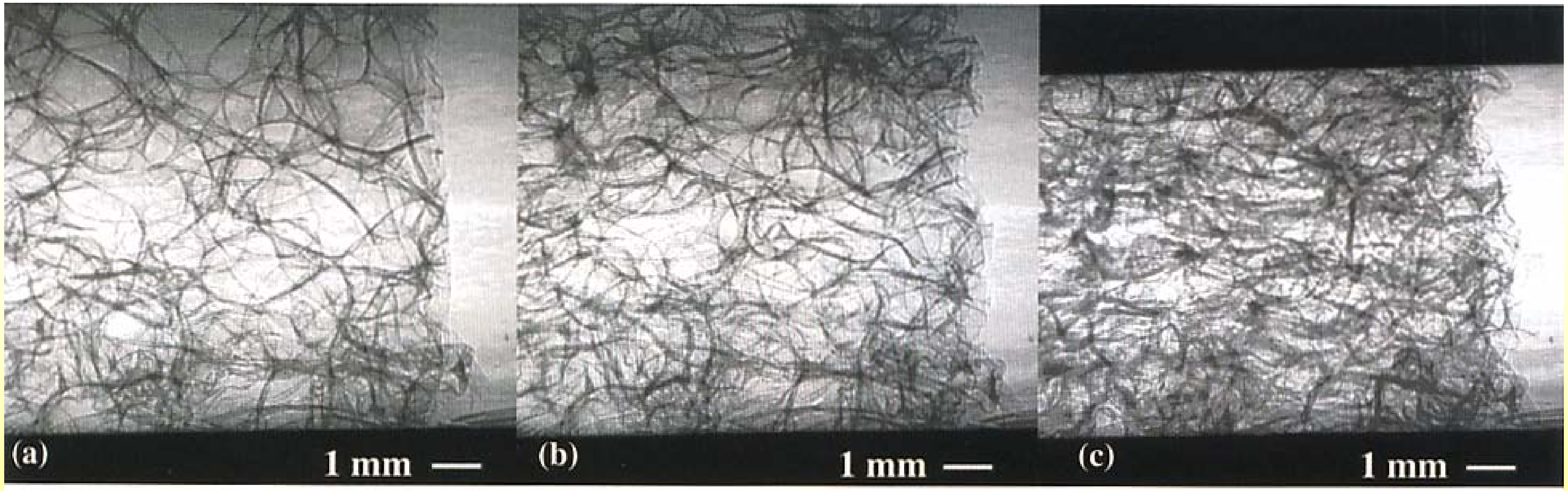


*Fig. 2. Three scenes of an in situ image monitored by X-ray radiography when a compression test is done on foam aluminum. (a) Foam aluminium begins to collapse at top and bottom. (b)Foam aluminium is collapsing. The center keeps its shape. (c) All the foams seem to be almost destroyed.*

When X-rays irradiate to the substance, we can observe florescent X-ray emission, photo electron emission and absorption form surface and bulk of the material.

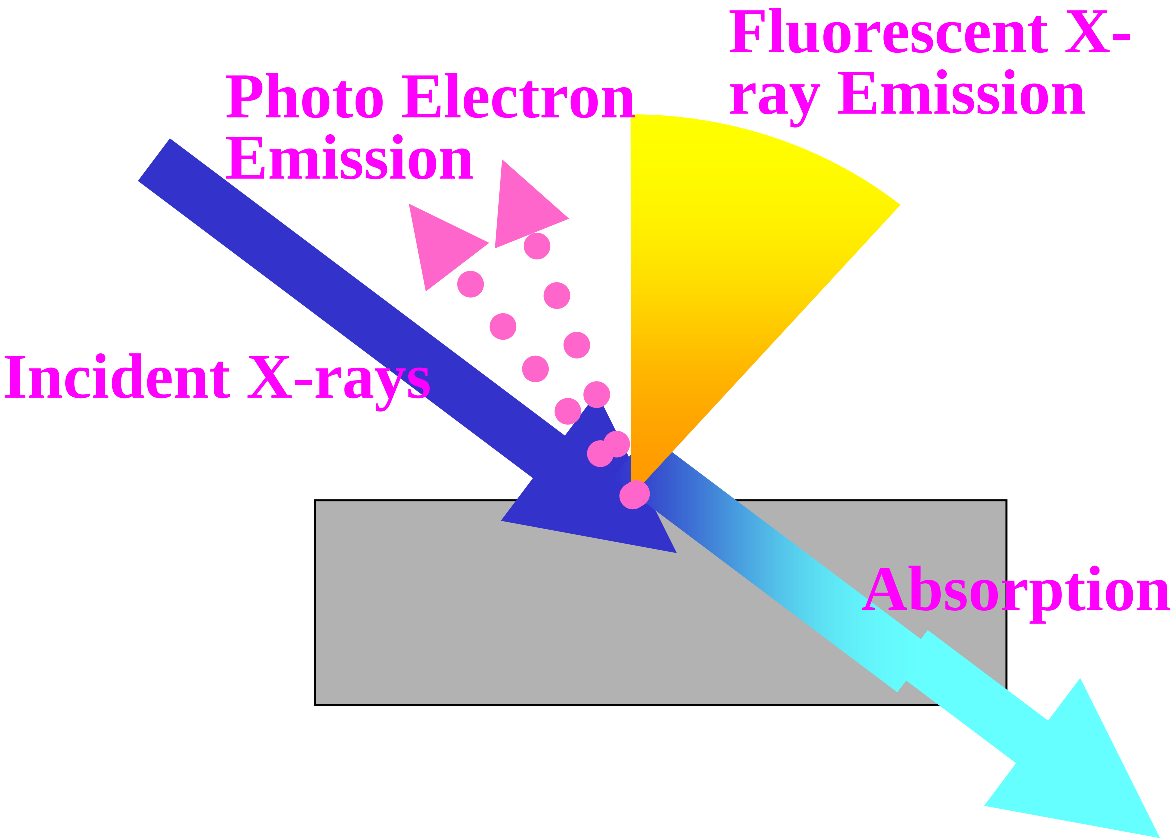


- X-ray Imaging
- **X-ray Fluorescence Analysis**
- **X-ray Absorption Fine Structure (XAFS)**
- **X-ray Photoelectron Spectroscopy (XPS)**

**~$\mu$m**

Element Analysis

**X-ray Fluorescence Analysis**

# SPring-8 affects to Archeology

AD220~280: Three Countries struggles for supremacy in China. They have a literature saying a set of 100 mirror were given to messenger from Japan. In Japan, long argument continues where is the origin of Japan. There exist two candidates. The oldest literature in Japan is written in AD712.

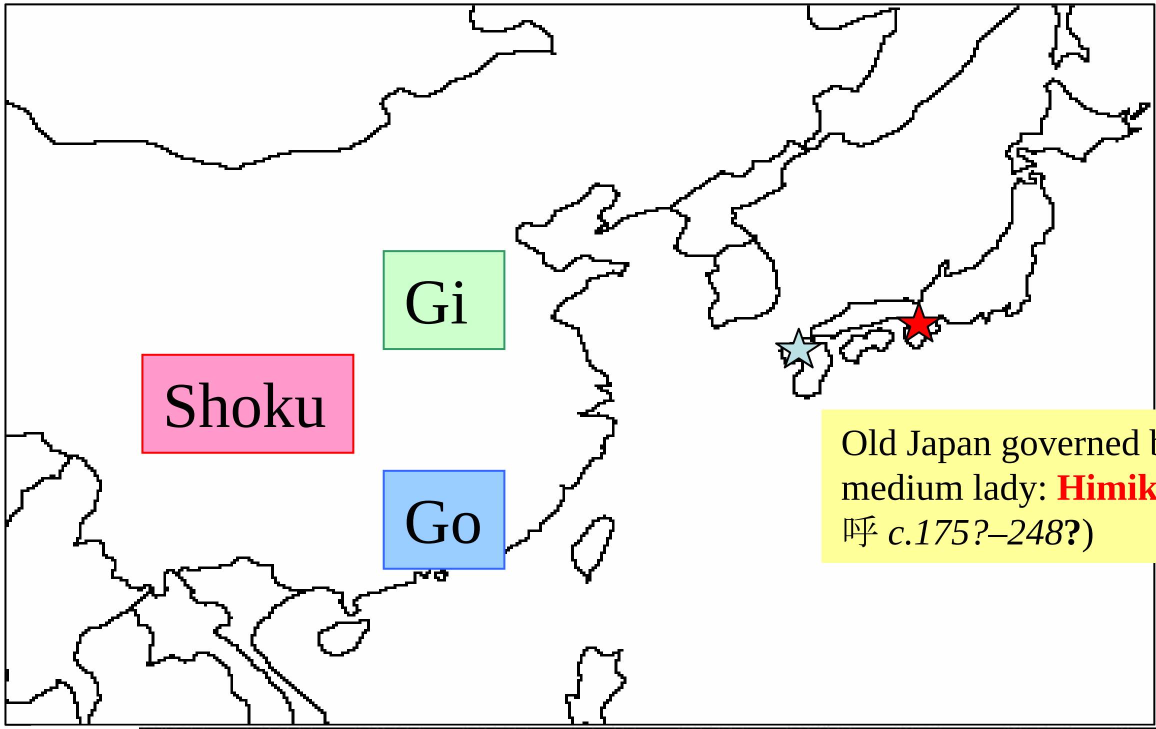


Old Japan governed by medium lady: **Himiko** (卑弥呼 *c.175?–248*?)

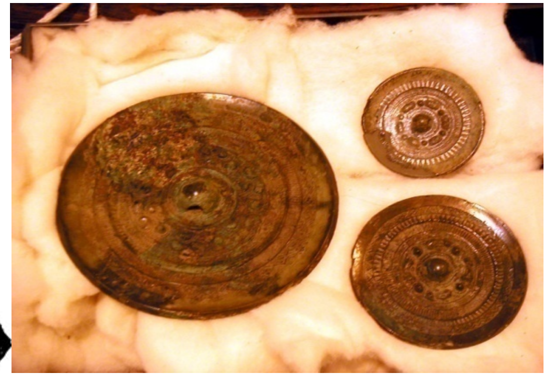

Where is the origin of ancient bronze mirror “Triangular-rim mirror” ?

Location of Yamataikoku is one of the most controversial topics in Japanese history.

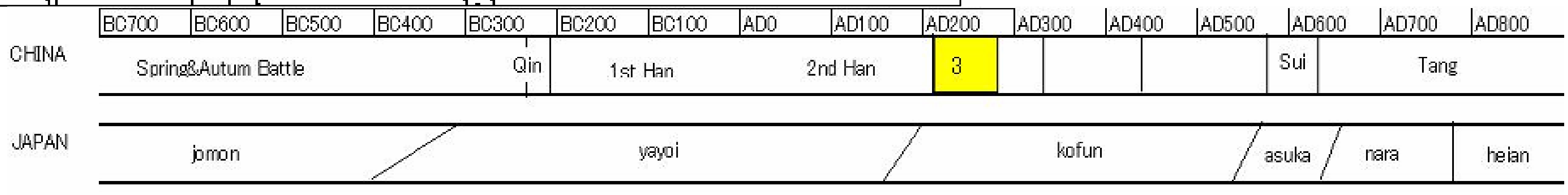

# 中国古代青銅鏡年表

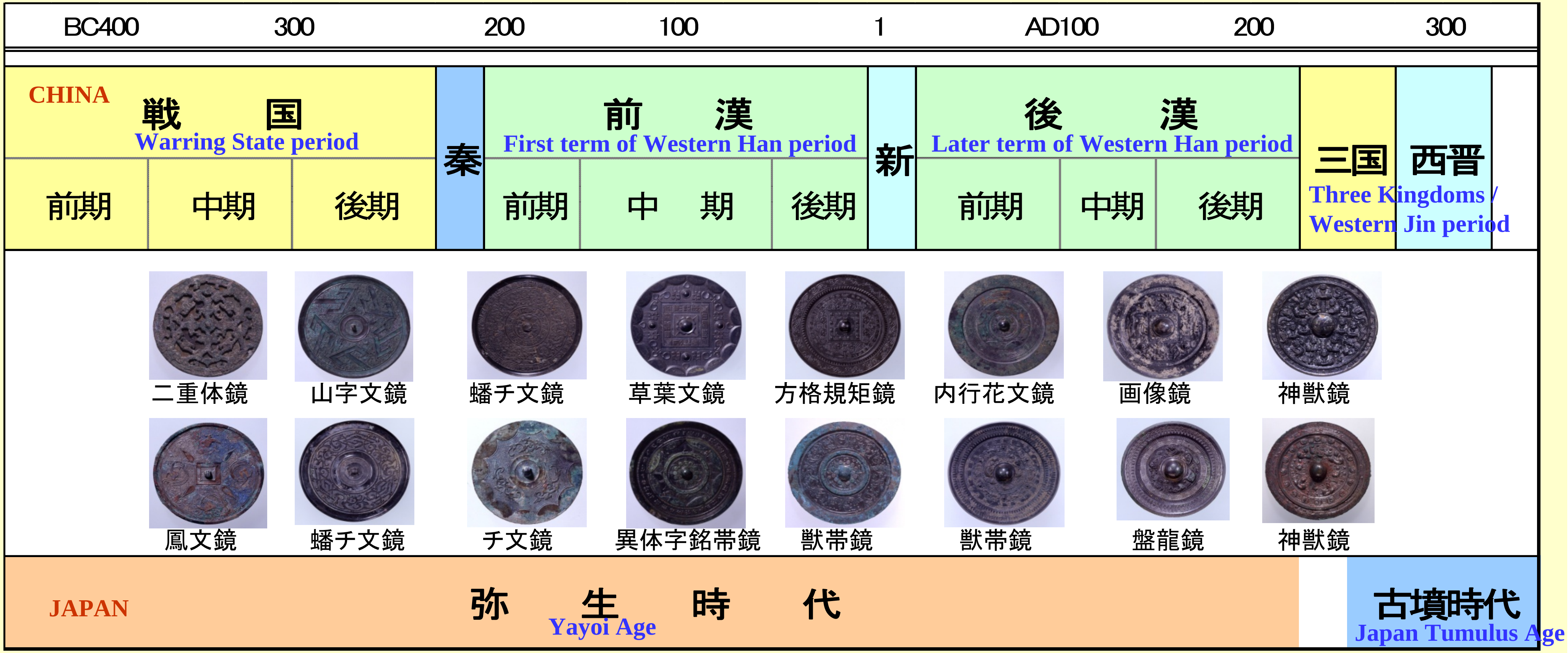


戦国時代(**Warring State period**)：**BC5c～BC221**　秦時代 (**Qin Dynasty period**)：**BC221～BC206**

前漢時代(**First term of Western Han period**)：**BC206～BC7**　新時代：BC7～AD25

後漢時代(**Later term of Western Han period**)：**AD25～AD221**　三国・西晋時代

(**Three Kingdoms / Western Jin period**)：**AD221～AD317**

# 三角縁神獣鏡(紀元3世紀)

**"Triangular-rim mirror"**
(AD3c)

# Mirror with triangle edge and Gods & Beats design

Museum of Sumitomo, JASRI, Sumitomo Metals

1. 三角縁三神五獣鏡(M23)

2. 三角縁三神五獣鏡(M24)

3. 三角縁四神四獣鏡(M25)

4. 三角縁四神四獣鏡(M112)

All 8 mirrors come from Japanese ancient tomb.

5. 三角縁二神二獣鏡(M116)

6. 三角縁三神三獣鏡(M33)

7. 三角縁三神二獣鏡(M118)

8. 三角縁三神三獣鏡(M119)

# BL19B2 (SPring-8)
# エネルギー分散型蛍光X線スペクトロメーター

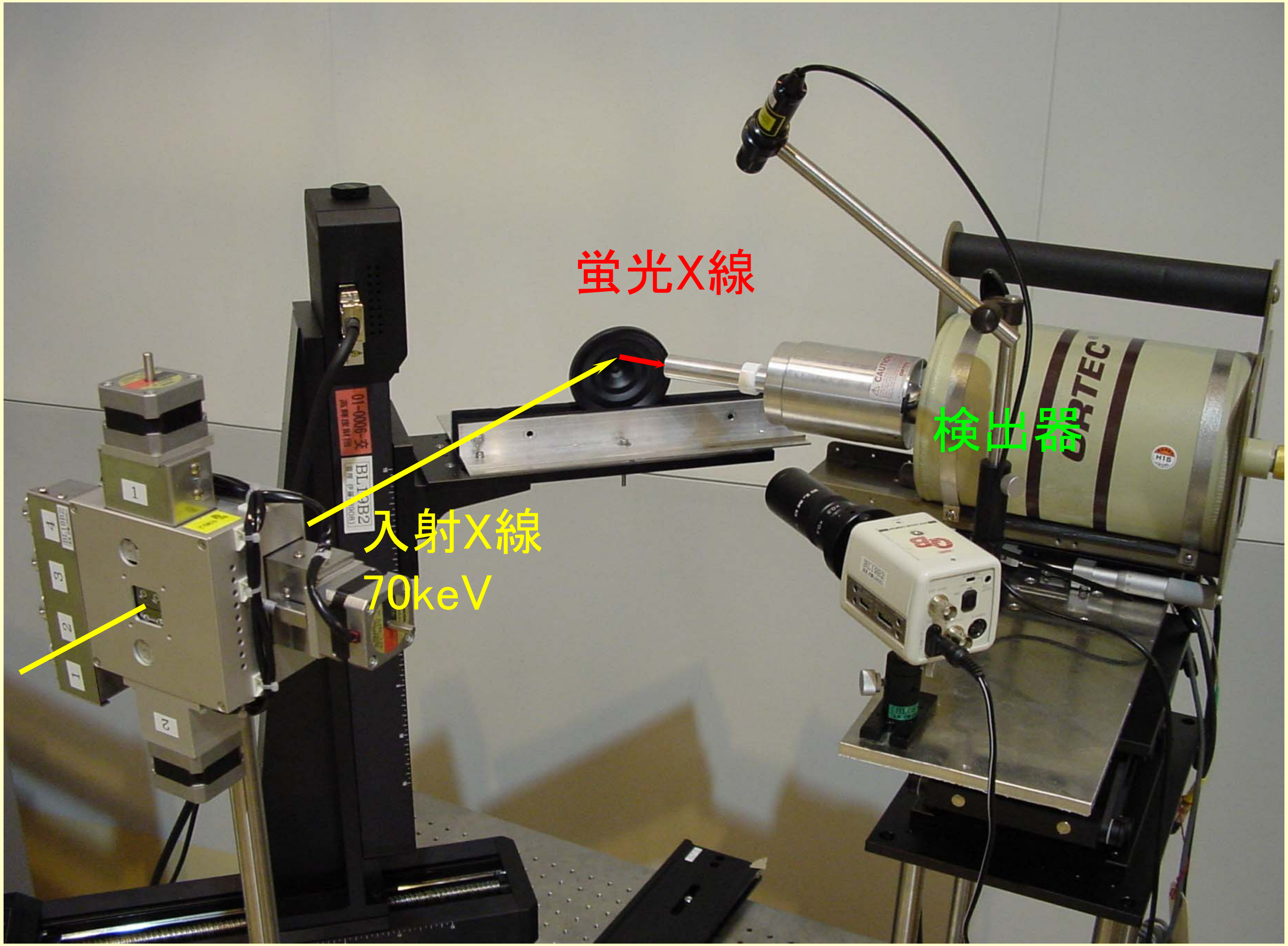

# 表面状態の違いによる数値の変動状況

三角縁三神五獣鏡（M24)鏡面上で、表面状況の異なる84点を測定する。

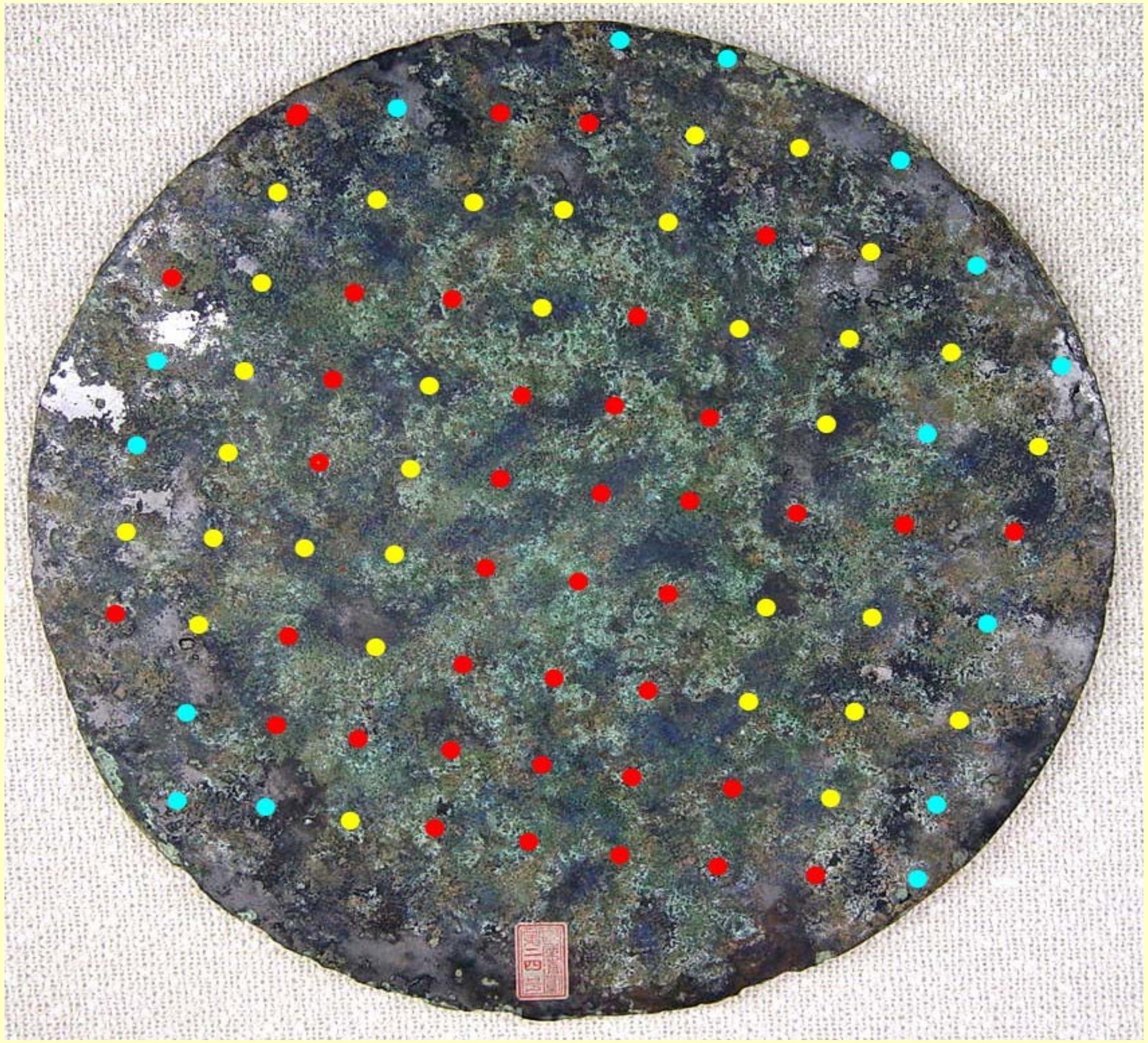

- 青：ほぼ地金と考えられる部分
- 黄：薄い錆に覆われている部分
- 赤：厚い錆に覆われている部分

厚い錆に覆われている部分

薄い錆に覆われている部分

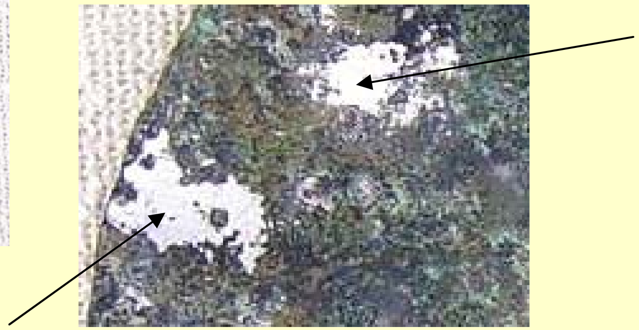

ほぼ地金と考えられる部分

# Distribution of Impurities in Bronze Mirror by Fluorescence at Spring-8

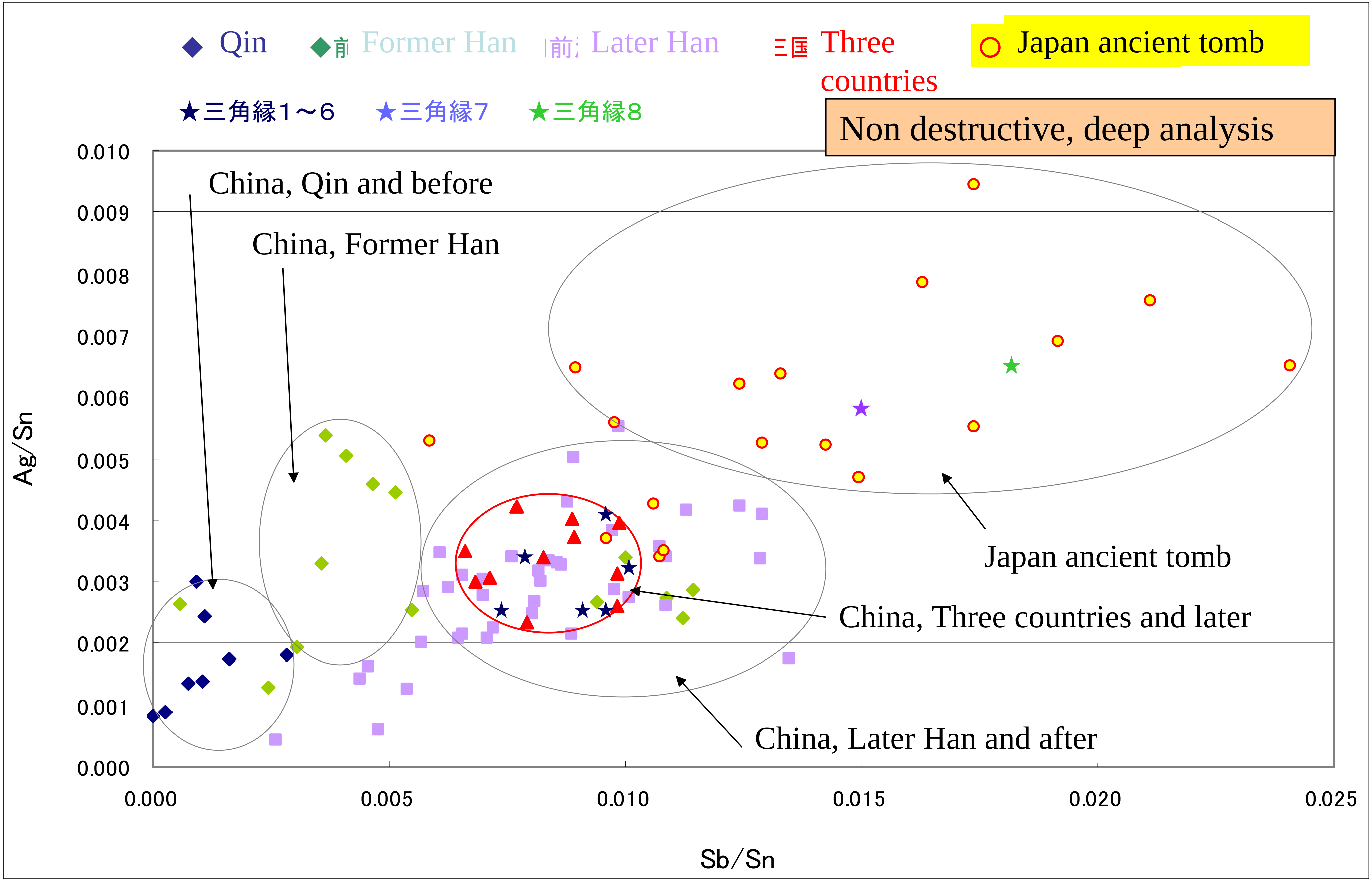

When X-rays irradiate to the substance, we can observe X-ray diffraction and scattering form surface and bulk of the materials.

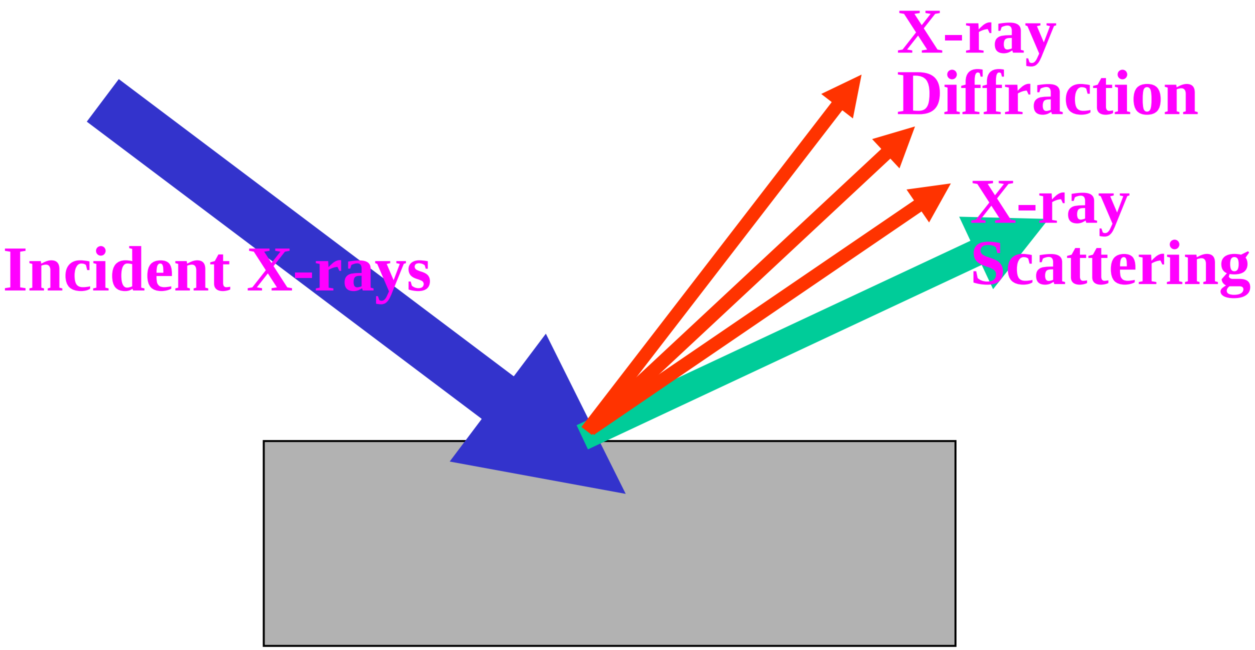


- X-ray Imaging
- X-ray Fluorescence Analysis
- X-ray Reflectometry
- **X-ray Diffraction/Scattering**
- X-ray Absorption Fine Structure (XAFS)
- X-ray Photoelectron Spectroscopy (XPS)

~Å

Structural Analysis at atomic Level

X-ray Diffraction/Scattering

# Highlights of Industrial Researches carried out at BL19B2

- **Example 1**

  *In-situ* Observations of Formation of Fe-Zn Intermetallic Compounds during Galvannealing Process by XRD

- **Example 2**

  Grazing Incidence X-ray Diffraction of Amorphous $SiO_x$ Thin Film

- **Example 3**

  *In Situ* Observation for Weld Solidification Process of Carbon Steel Metals

# In-situ Observation of Alloying of Galvanized Steel

## Example 1

- Galvanized Steel: good corrosion protection
- ➡ Used for outer body of cars

SUMITOMO METAL INDUSTRIES,LTD.

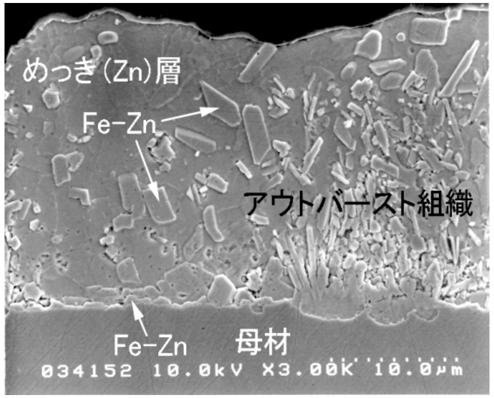


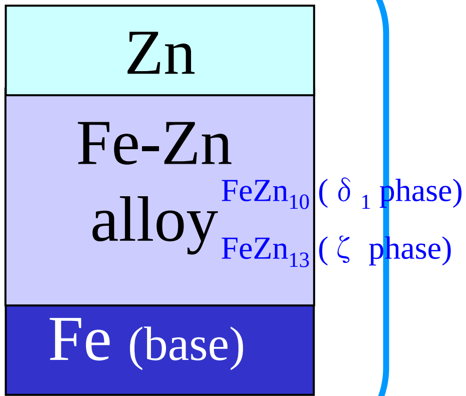


- Property of galvanized steel is strongly depends on kind of Fe-Zn intermetallic compounds ($FeZn_{10}$: $\sigma_1$ phase and $FeZn_{13}$: $\zeta$ phase) at interface.
- ➡ $\delta_1$ ($FeZn_{10}$) phase is preferable.

# Process of galvanization

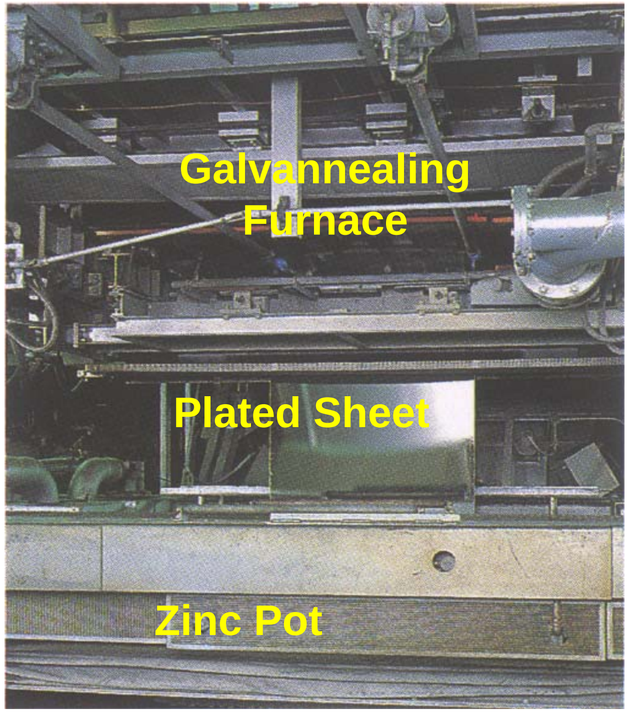


Dipping in molten Zn

↓

Annealing (galvannealing)

(forming alloy )

How (When) $\delta_1$ phase forms in annealing process?

In-situ observation of forming alloys during annealing process

# Experiments (2nd Station of BL19B2)

## In-situ observation of alloying of galvanized steel

### 1. Sample

Zn-0.14mass%Al galvanized steel, and pure Zn galvanized steel

### 2. Annealing (alloying)

IR Lamp annealing from backside of sheet

### 3. Diffraction experiment

- Energy 38.68keV (Si(111) , without mirror)
- Rapid 2$\theta$ scanning

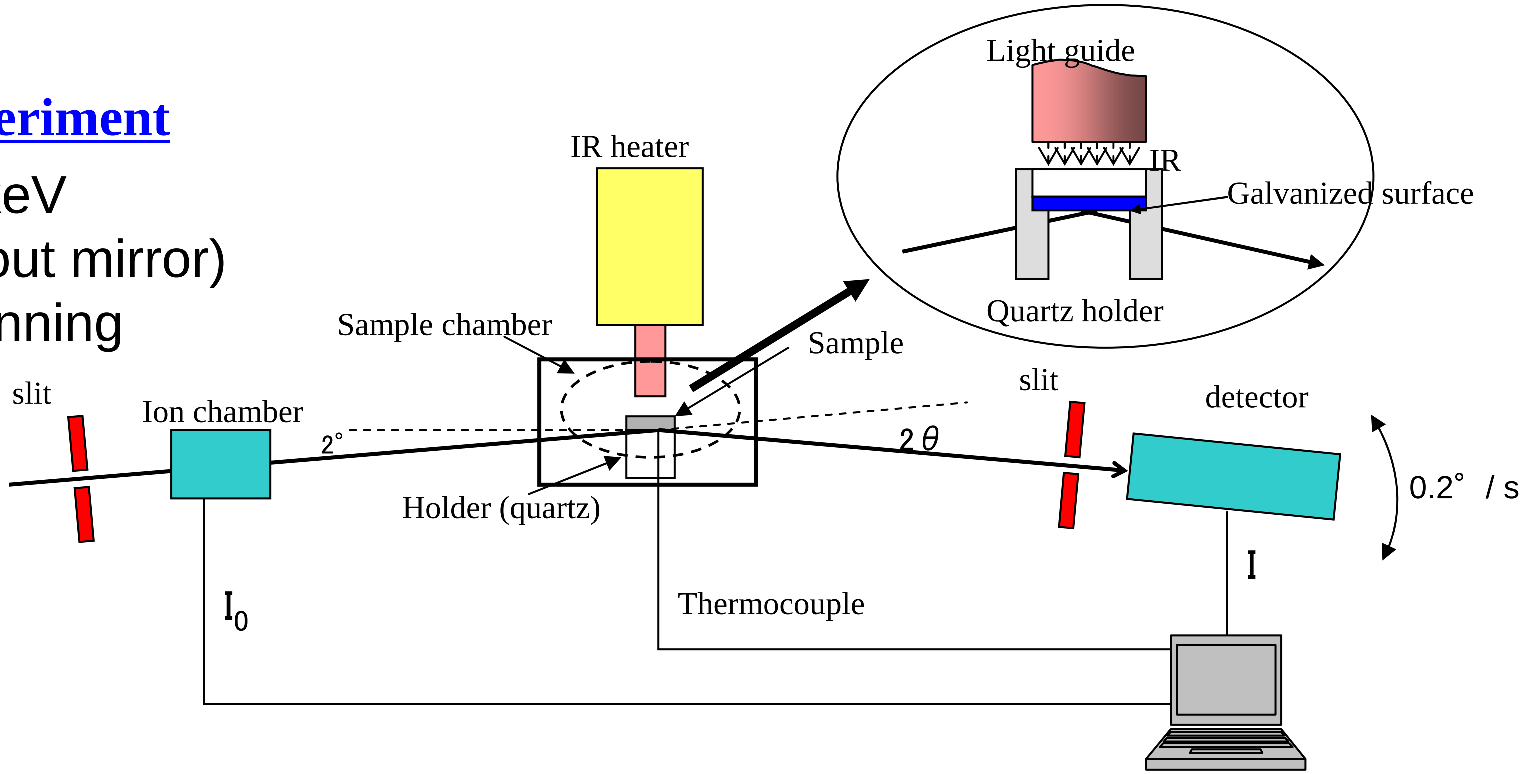

# Variation of diffraction profiles to annealing time

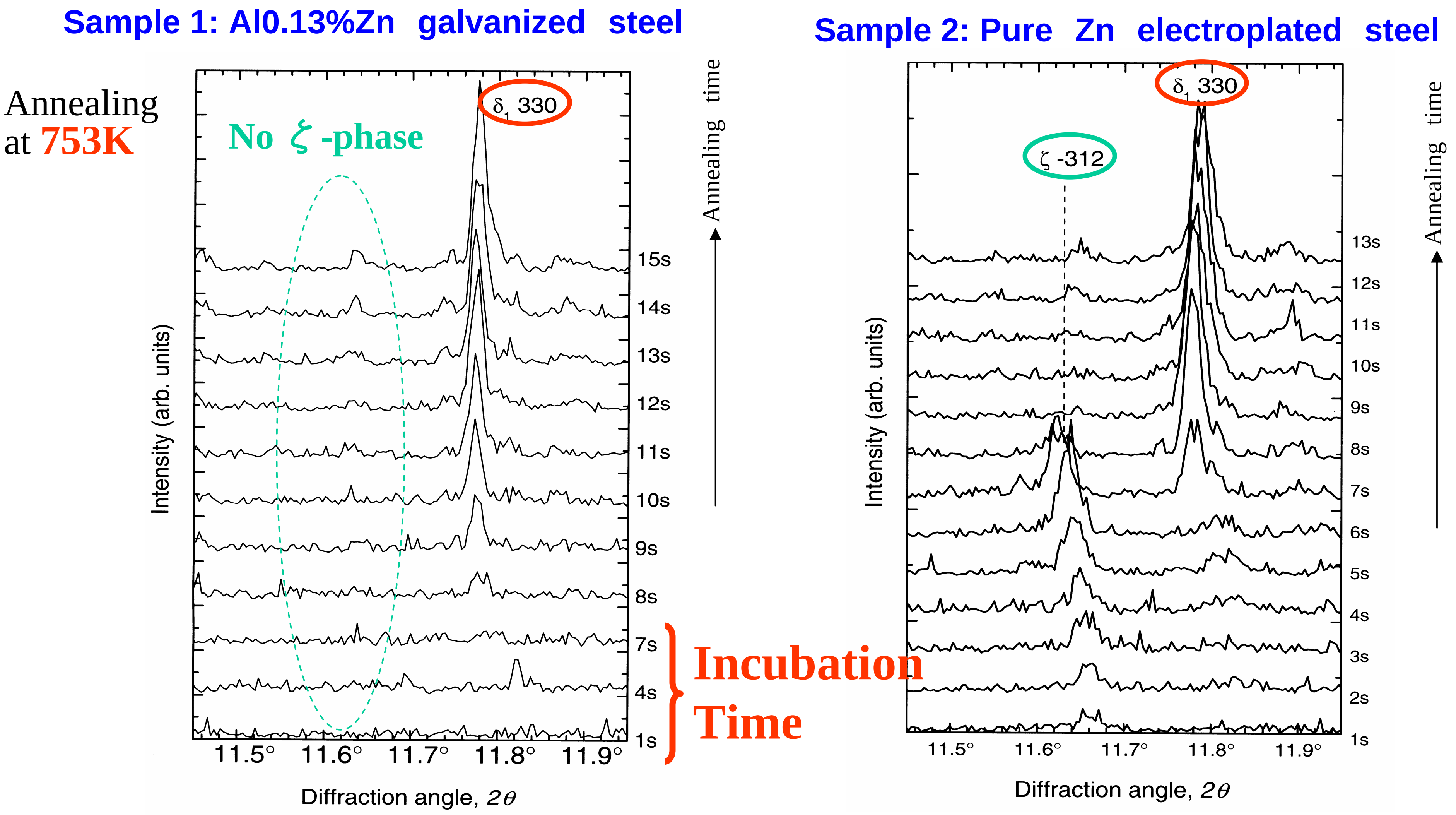


A. Taniyama, M.Arai, T. Takayama, M. Sato, Material Transaction Vol.45, No. 7 (2004) p.2326

# Dependences of diffraction intensities on annealing time

A) Zn-0.14mass%Al

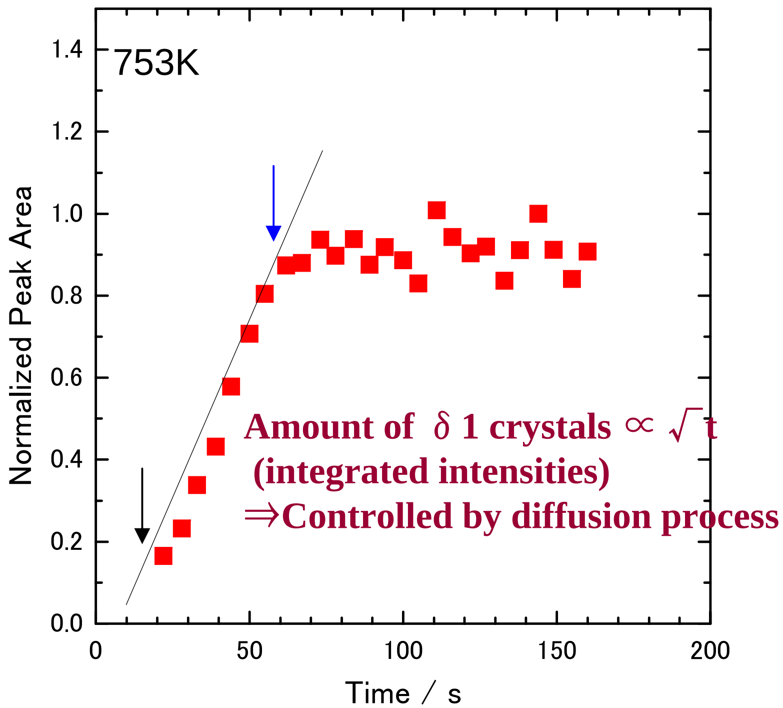


B) Pure Zn

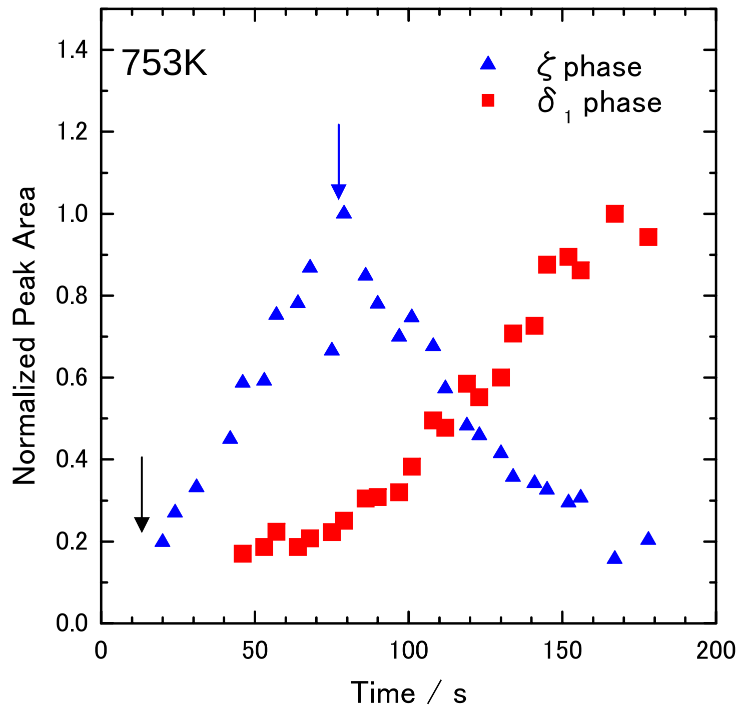


A) <u>Zn-0.14mass%Al galvanized steel</u>: **Alloying of Al containing galvanized steel was completed in 70 seconds at 753K.**

- Suggesting **layer-by-layer forming of alloy**

B) <u>Pure Zn galvanized steel</u>: **The of ζ phase in galvanized with pure Zn decreased after 70 sec.**

SPring-8

# Dependences of diffraction intensities on annealing time

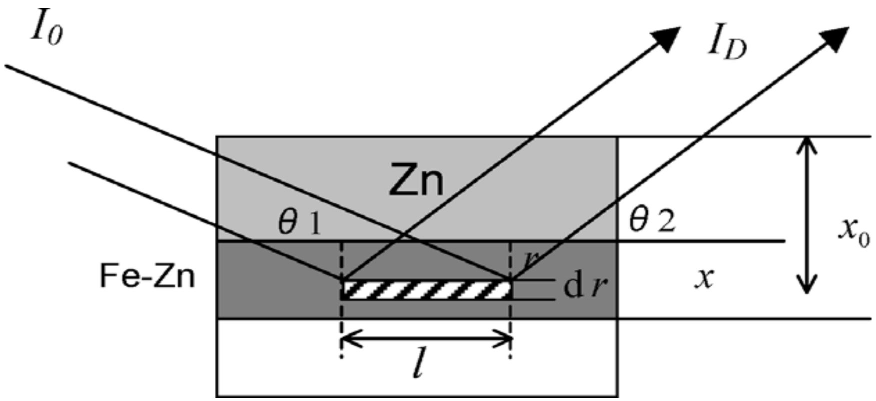


$$\frac{I_D(x)}{I_D(x_0)} = \exp(-\mu_1(x_0 - x)\beta)\frac{1-\exp(-\mu_2 x\beta)}{1-\exp(-\mu_2 x_0\beta)} \quad (\beta = 1/\sin\theta_1 + 1/\sin\theta_2)$$

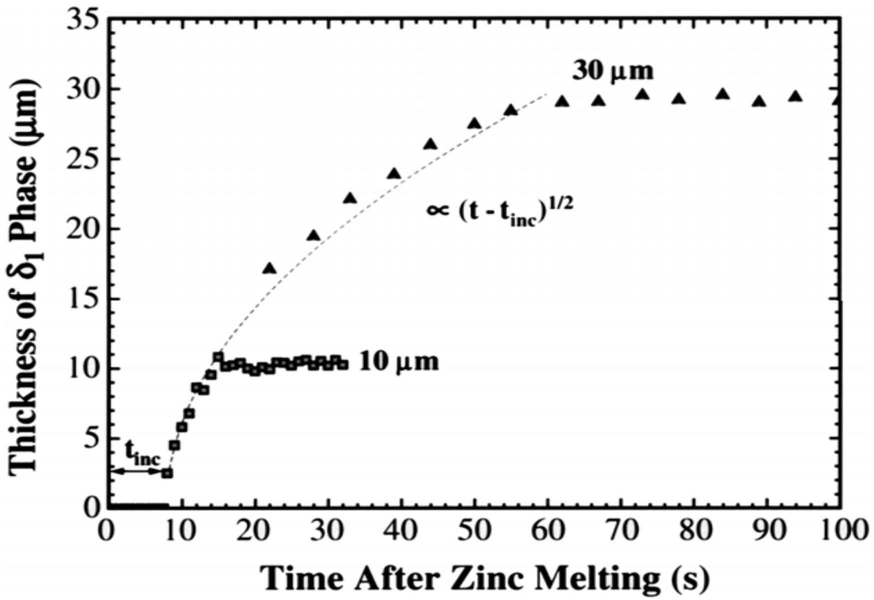


Assuming that the $\delta_1$ phase grows in a layer-by-layer manner, the time dependence of thickness was estimated as shown in this equation.

The estimated thickness of the $\delta_1$ phase increased by the parabolic law with annealing time, taking into account the incubation period ($t_{inc}$).

These results suggest that the growth of $\delta_1$ phase is dominated by a diffusion of Fe atoms and Zn atoms in the coating.

# In-situ observation of alloying of galvanized steel

## Summary

- Only p… ferable … ase … rmed in Al containi…
- Al… … as compl…
- Obs… … to be proportiona… … time.
  - ➡Suggesting … er-by … yer forming of alloy

This experimental result is very useful for the quality control in the actual galvanized process.


- A. Taniyama, M. Arai, T. Takayama and M. Sato: "*In-Suit* Observation of Growth Behavior of Fe-Zn Intermetallic Compounds at Initial Stage of Galvaannealing Process", Mat. Trans., **47**(2004) 2326.

# Grazing Incidence X-ray Diffraction of Amorphous $SiO_x$ Thin Film

## Example 2

### Grazing incidence X-ray Scattering (GIXS)

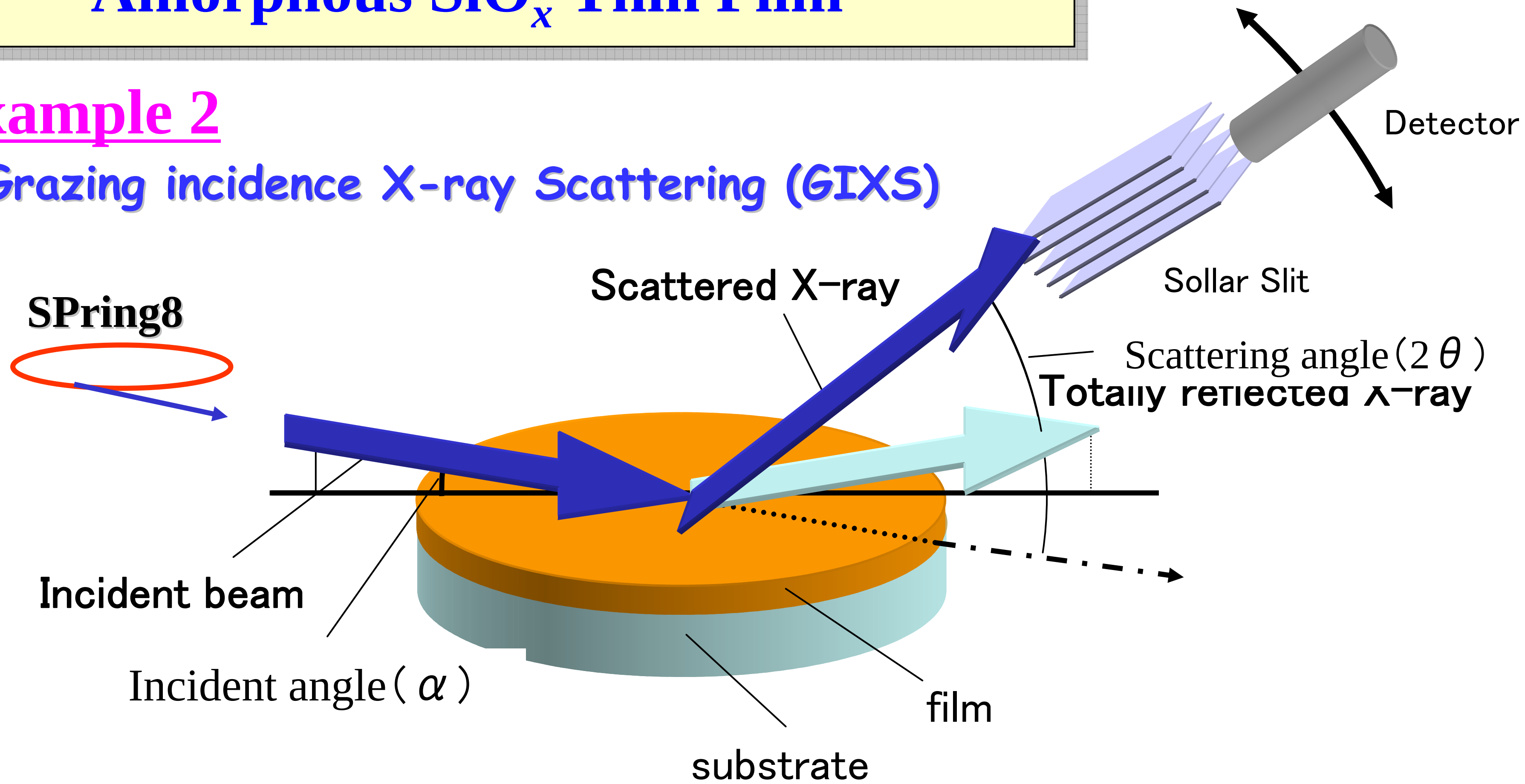


**Reducing background from substrate by grazing incidence (lower than critical angle)**

**High sensitivity to the films on substrate**

# Preparation of $SiO_x$ Film

- **$SiO_x$ film deposited on Si wafer**

**ECR plasma sputtering with flowing $O_2$ gas 1 sccm**

These films are used for anti-reflection coating film

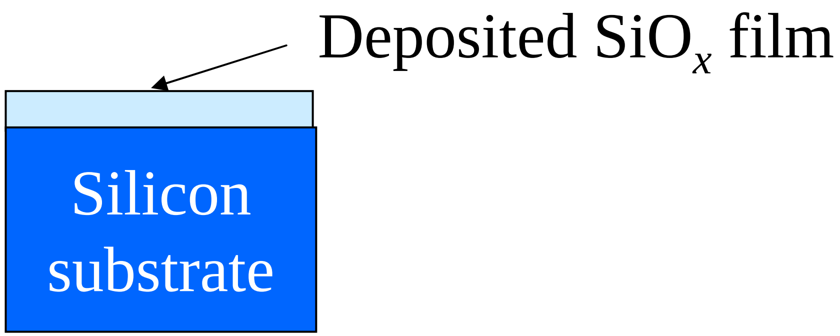


- **Reference : bulk silicate glass plate**

# Characterization of the $SiO_x$ film

## Reflectivity of the $SiO_x$ film

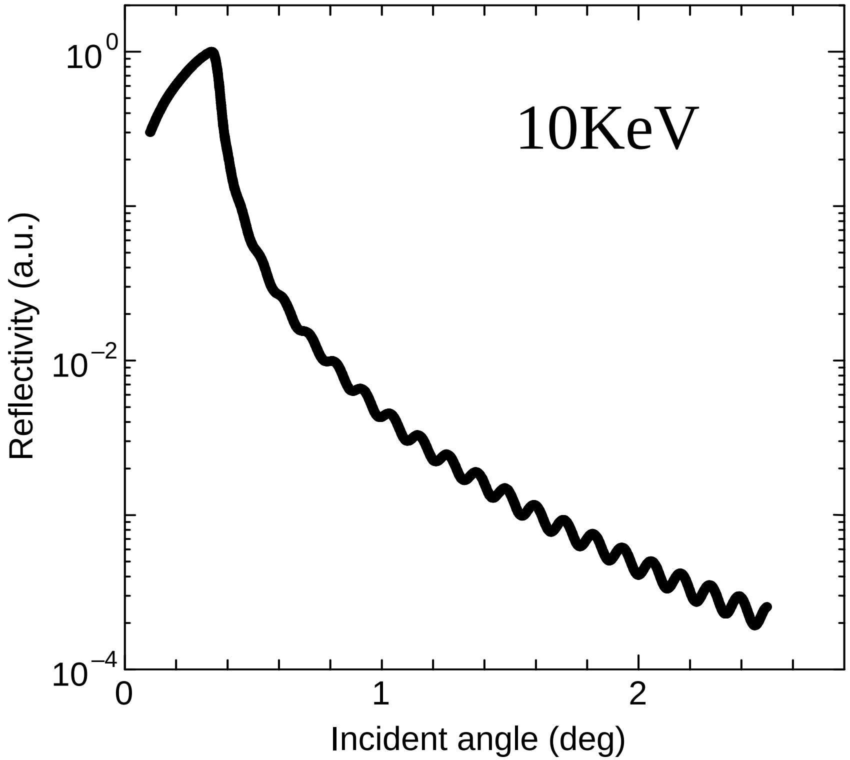


| | |
|---|---|
| Thickness | 58.6 nm |
| Roughness | 0.5 nm |
| Density | 2.154 $g/cm^3$ |

Observed at BL16B2 in SPring8

## Visible Ellipsometry (He-Ne laser)

Refractive index 2.6 absorption coefficient 0.13

# Incident angle & penetration depth

Dielectric constant is less than 1 for X-ray

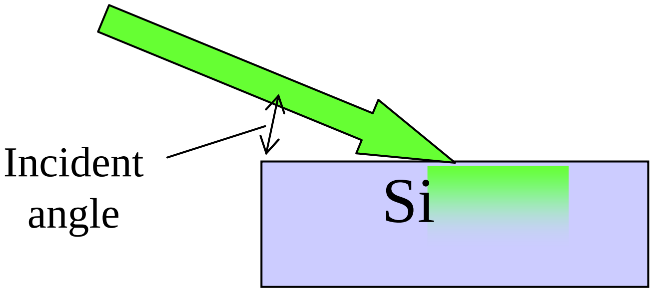


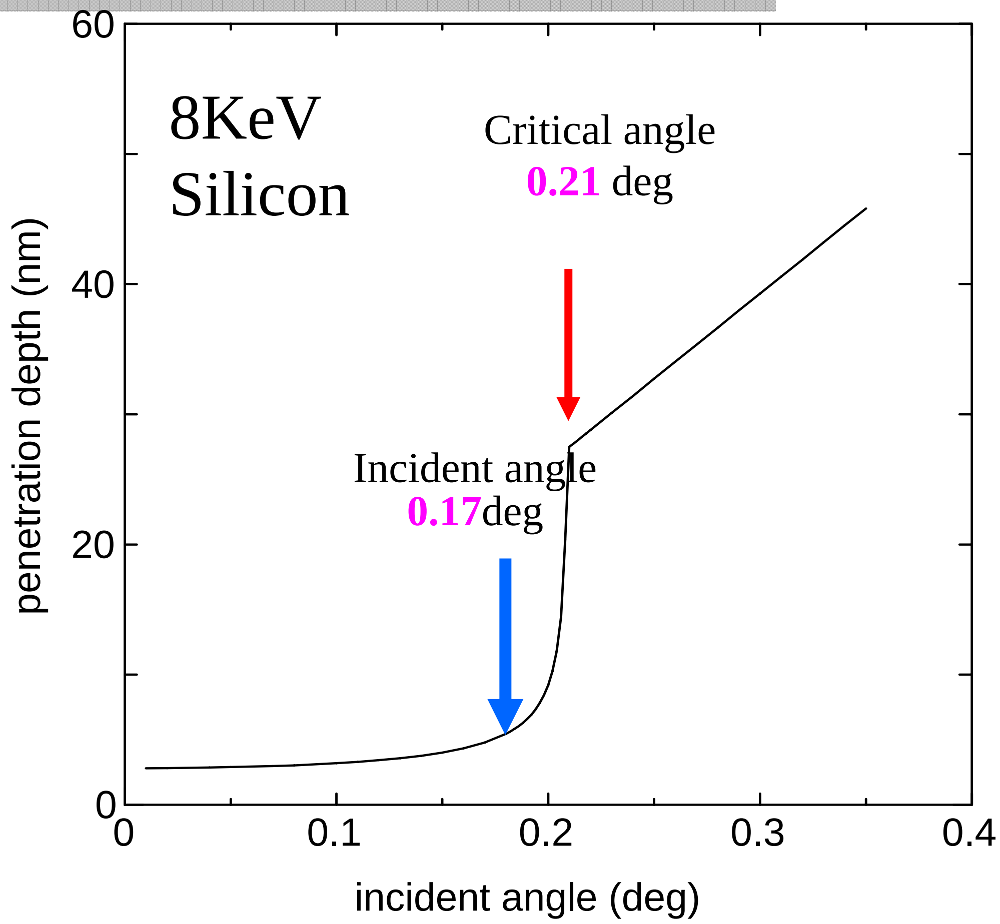


Penetration depth is several nanometers under the critical angle

**High surface sensitivity**

# Set up for GIXS

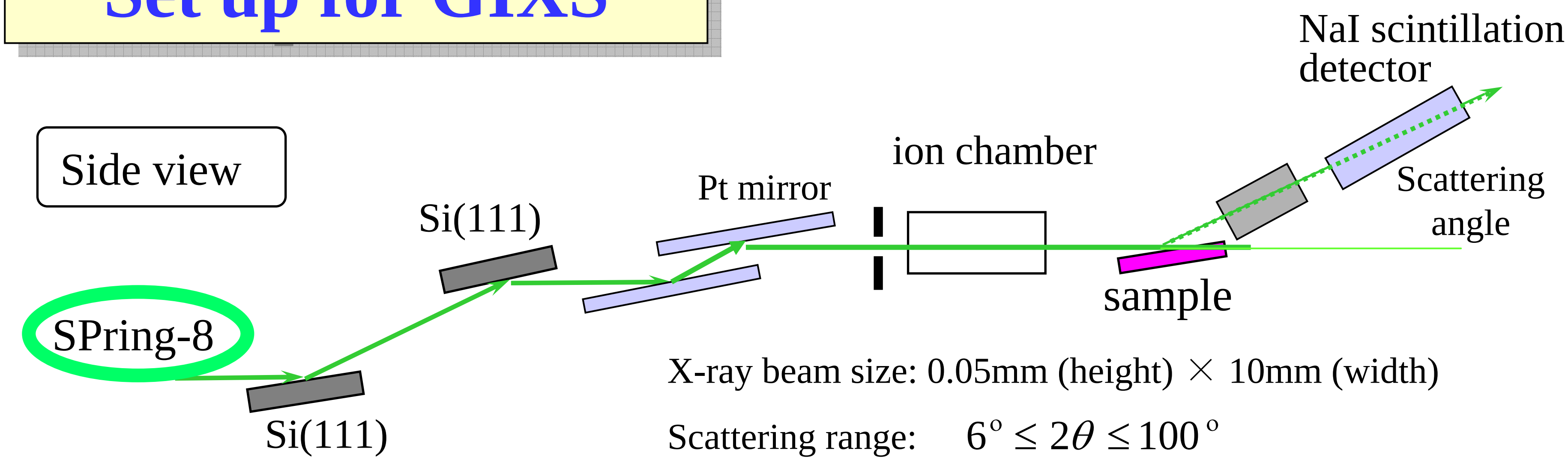


X-ray beam size: 0.05mm (height) × 10mm (width)

Scattering range: $6^\circ \le 2\theta \le 100^\circ$

8KeV　　Incident angle　0.17°

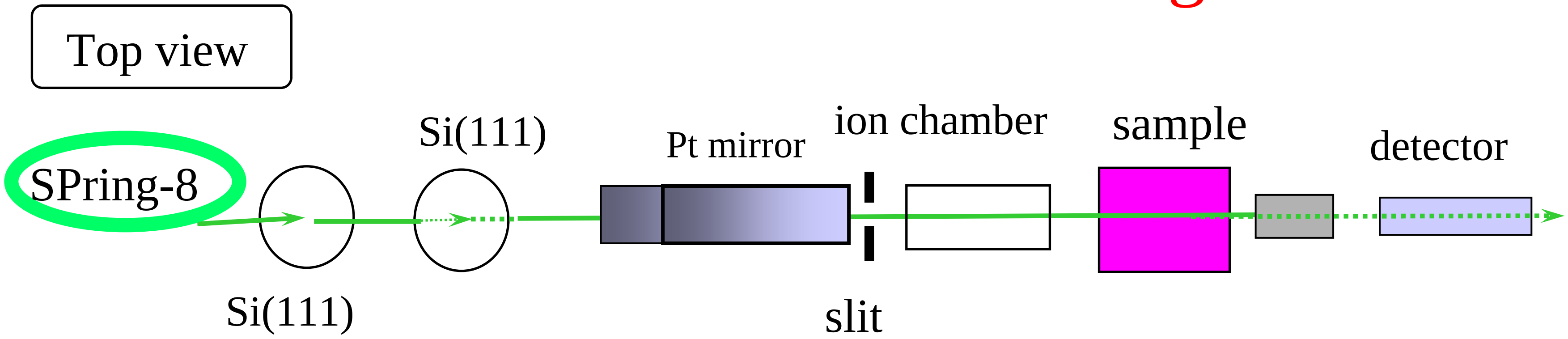


SPring8　BL19B2

# Instrumentation

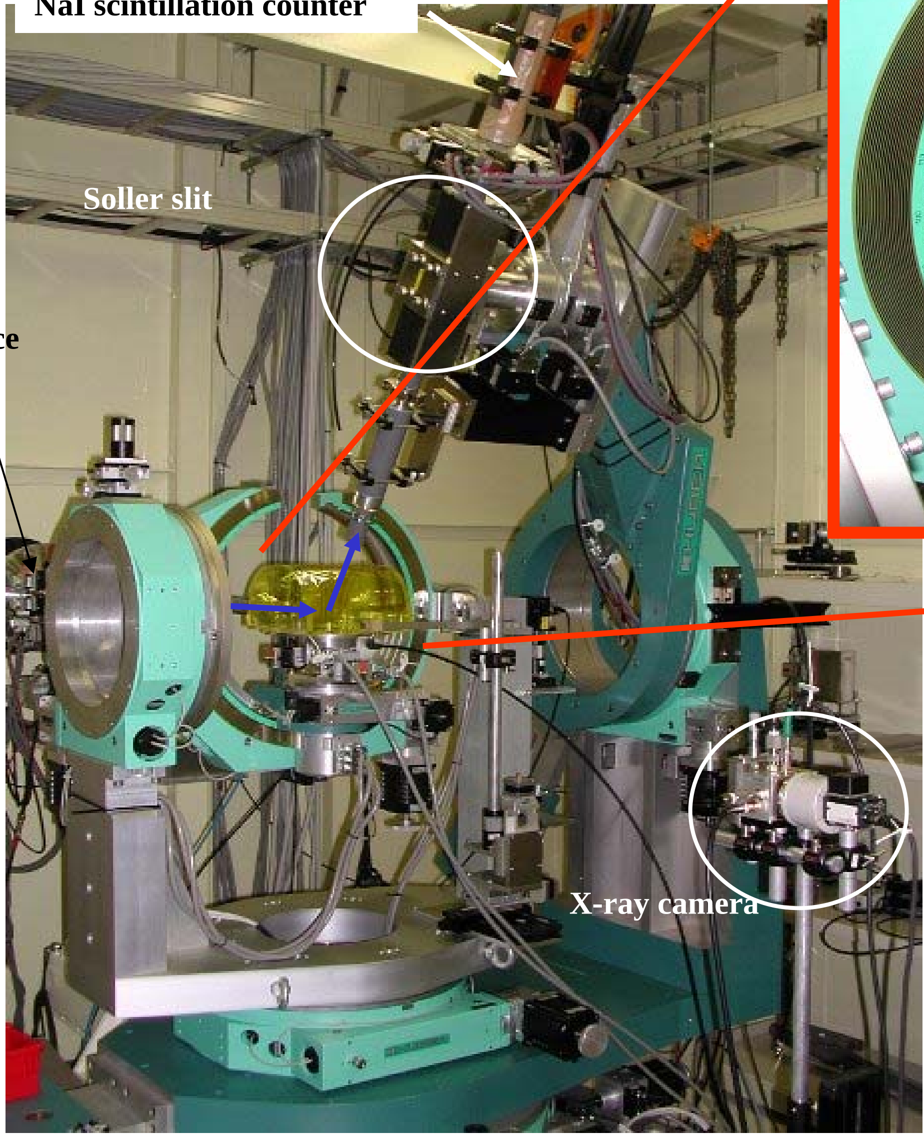


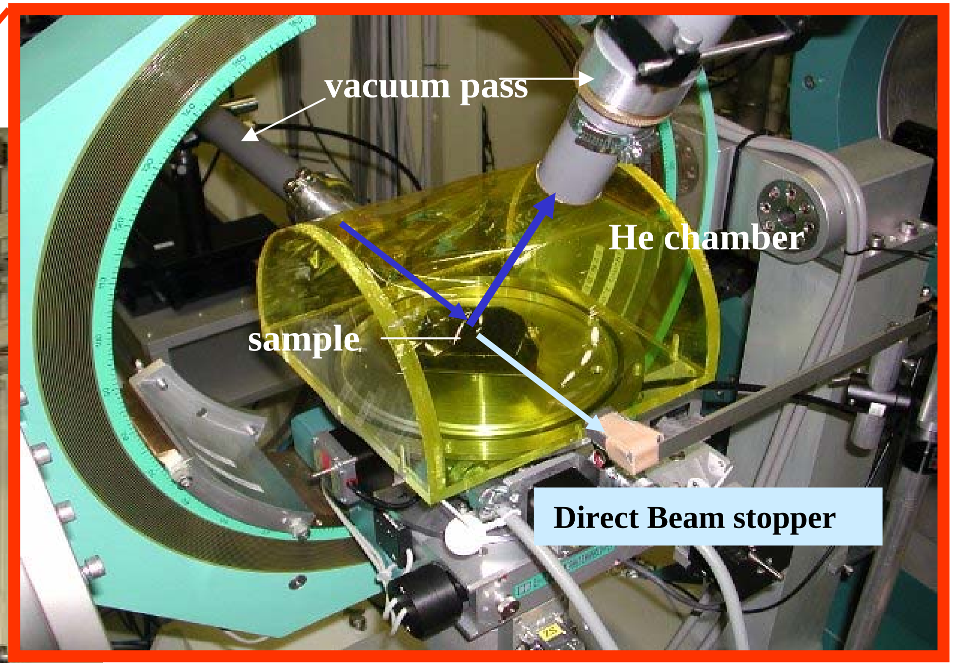


## SPring8　BL19B2

Divergence slit

Width × Height＝10.5× 0.05mm

Divergence of Soller slit　0.2 deg

Receiving slit

Width×Height＝10.0× 15.0mm

# Real Space Correlation Functions

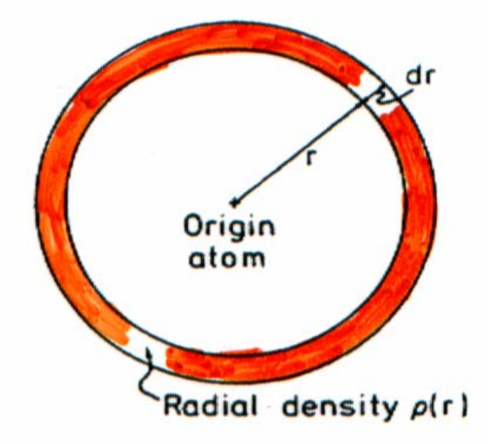


The number of neighbours between r and r+dr is given by $g(r) = 4\pi^2 \rho(r)$

**Radial distribution function (r.d.f):**

$$4\pi r^2 \rho(r) = 4\pi r^2 \rho_0 + \frac{2r}{\pi}\int_{Q_{\min}}^{Q_{\max}} Q \cdot i(Q) \sin rQ dQ$$

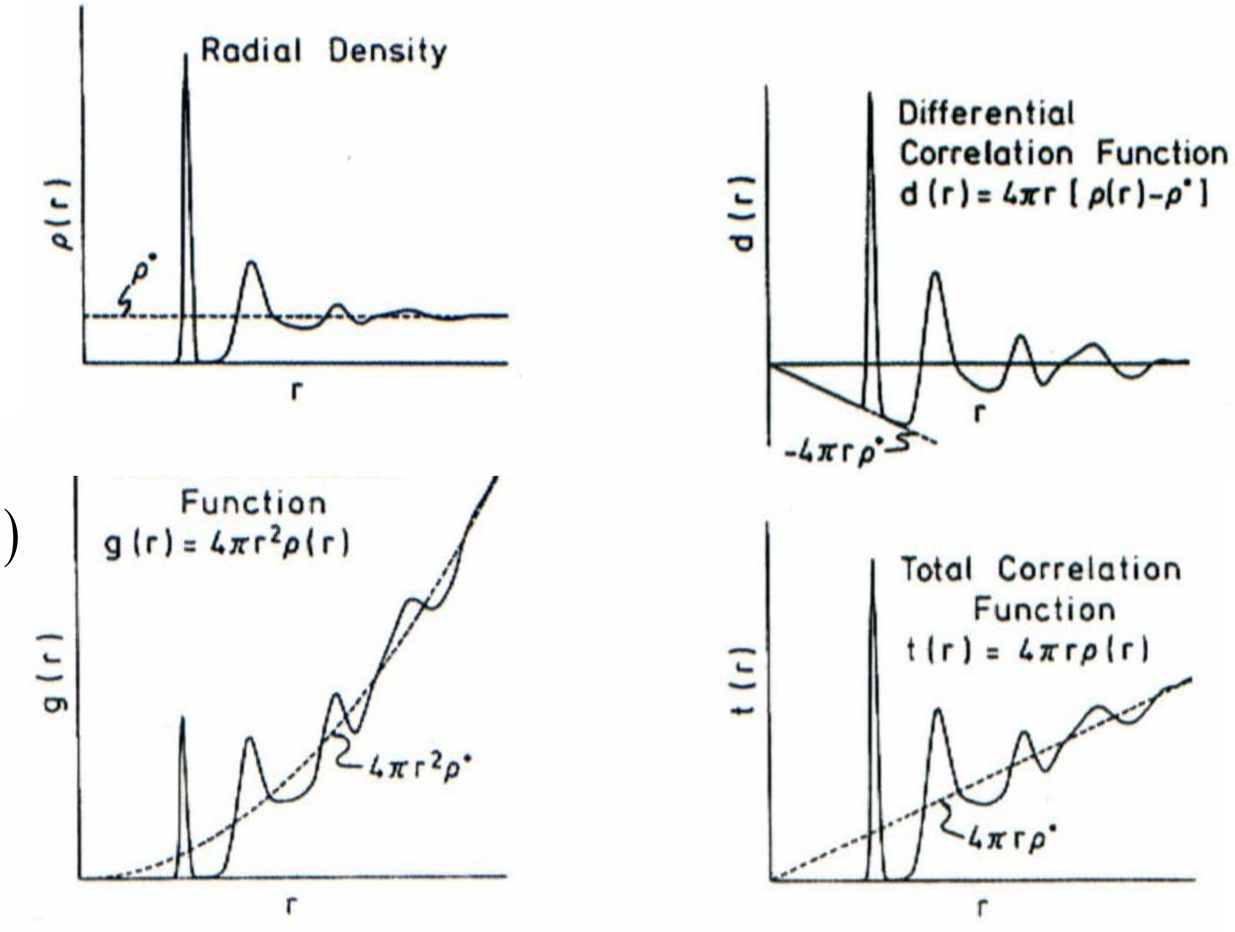


Real space correlation functions for a monatomic amorphous solid.

## Atomic Structure of Glass ?

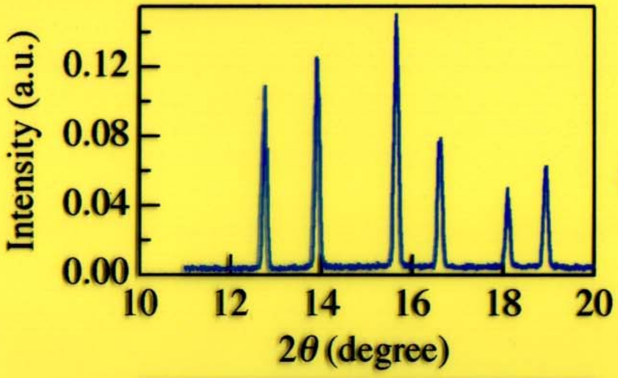


***Crystal***

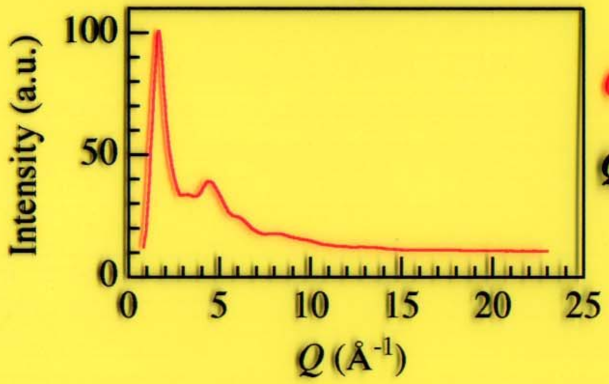


***Glass*** ➡ ***Disordered***

***Q*: *Momentum transfer*** (Å$^{-1}$)

$$Q = \frac{4\pi \sin\theta}{\lambda}$$

### Faber-Ziman total structure factor $S(Q)$

$$\frac{d\sigma_a}{d\Omega} = \langle \bar{b} \rangle^2 \left[ S(Q) - 1 \right] + \langle \overline{b^2} \rangle$$

$$\langle \bar{b} \rangle = \sum_i x_i \overline{b}_i$$

$$\langle \overline{b^2} \rangle = \sum_i x_i \overline{b}_i^{\,2}$$

$$S(Q) = \sum_{ij} \sqrt{x_i x_j}\, \overline{b}_i \overline{b}_j \frac{S_{ij}(Q)}{\langle \bar{b} \rangle^2}$$

$x_i$: concentration of the $i$th componet
$b$: scattering length

$$S(Q) = aS_{ii}(Q) + bS_{ij}(Q) + cS_{jj}(Q)$$

$$g(r) = ag_{ii}(r) + bg_{ij}(r) + cg_{jj}(r)$$

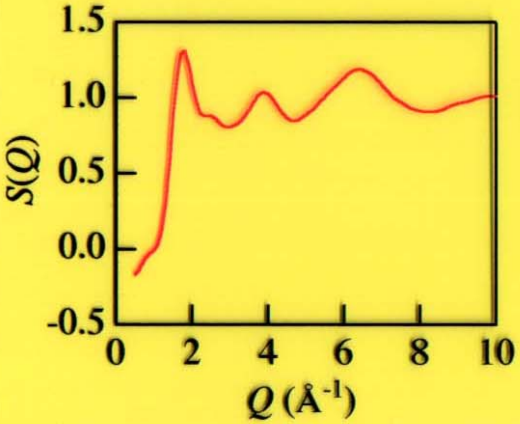


**F. T. R.**

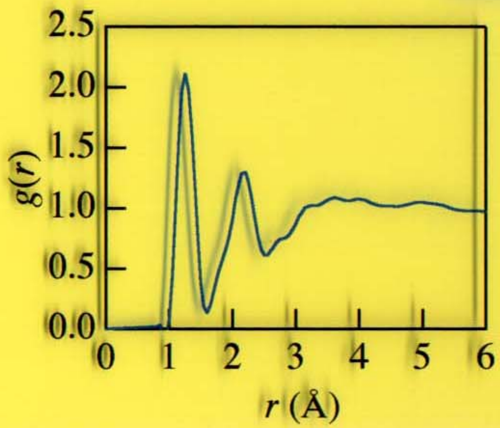


### Total pair distribution function $g(r)$

$$g(r) = \frac{1}{2\pi^2 r\rho} \int_0^{Q_{\max}} Q\left[ S(Q) - 1 \right] \sin(Qr)\, dQ + 1$$

$\rho$: atomic density (Å$^{-3}$)

**Fourier transformation (F. T. R.) from *Q* space to *r* space**

# HIGH ENERGY X-RAY STUDY ON THE STRUCTURE OF VITREOUS $B_2O_3$

K. Suzuya, S. Kohara, Y. Yoneda and N. Umesaki: Phys. Chem. Glasses, **41** (2000), 282.

## $B_2O_3$ glass

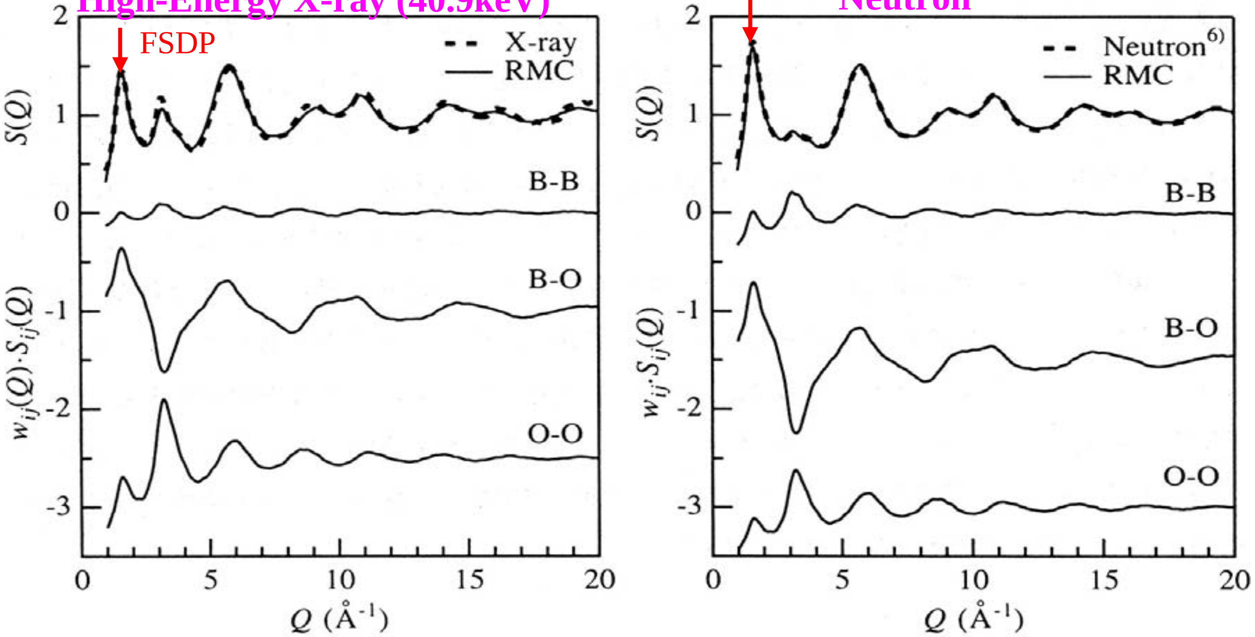


Fig. 7 Total and partial structure factors $S(Q)$ of vitreous $B_2O_3$. $w_{ij}$: neutron weighted partial coefficient, $w_{ij}(Q)$: X-ray weighted partial coefficient

- Neutron data from A. C. Hannon, D. I. Grimley, R. A. Hulme, A. C. Wright and R. N. Sinclair: J. Non-Cryst. Solids, **177** (1994) 299.

## $B_2O_3$ glass

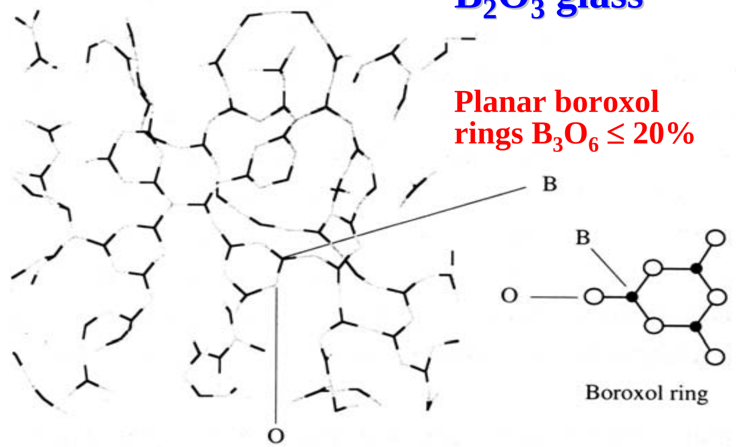


Fig. 8 Slice through a RMC configuration (10Å× 10Å×10Å) of vitreous $B_2O_3$.

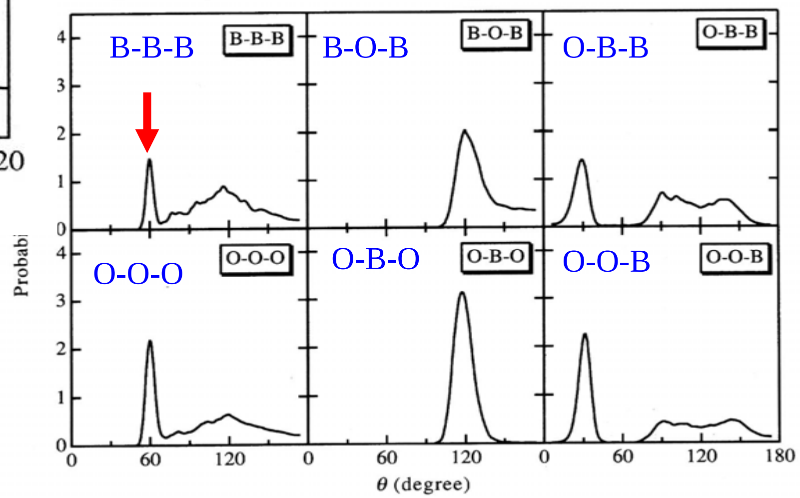


Fig. 6 Bond angle distribution for $B_2O_3$ glass

FSDP:First Sharp Diffraction Peak

# Observed X-ray diffraction profiles

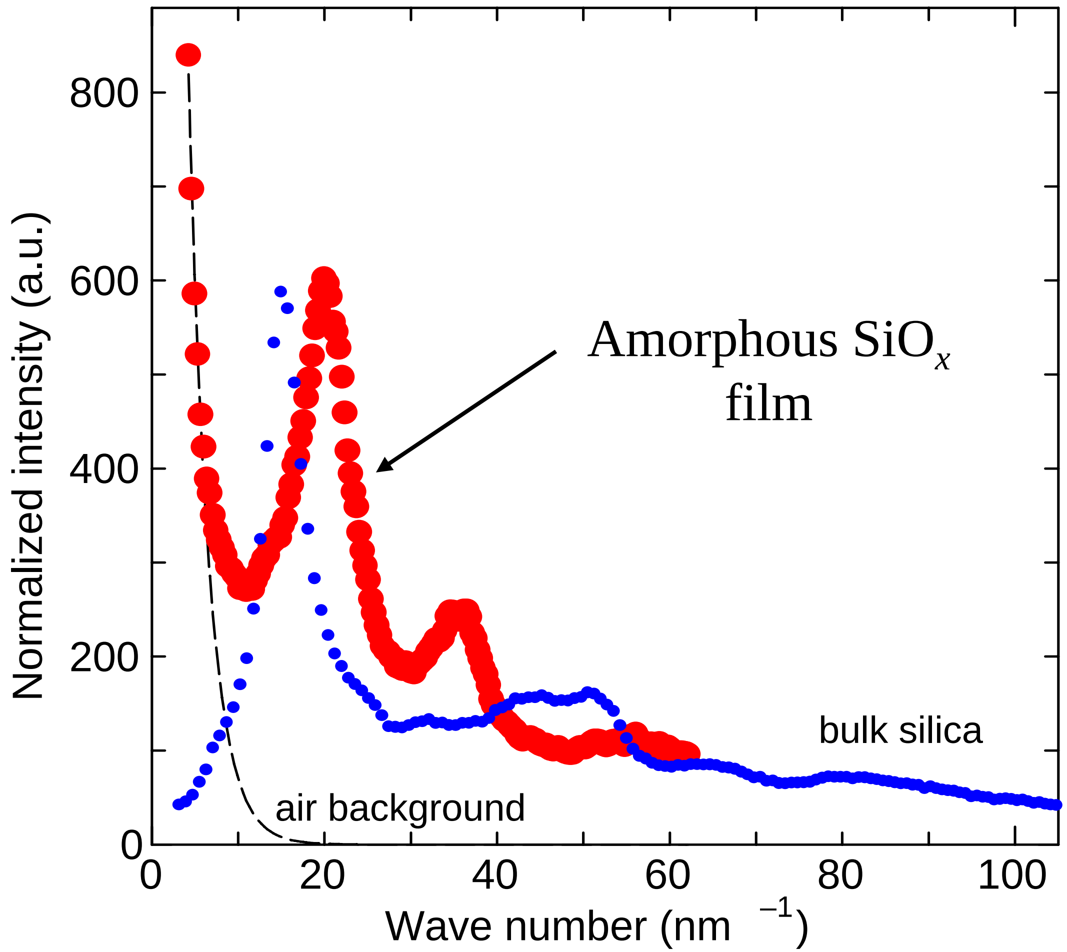


<u>Clear difference from bulk silica</u>

# Interference function

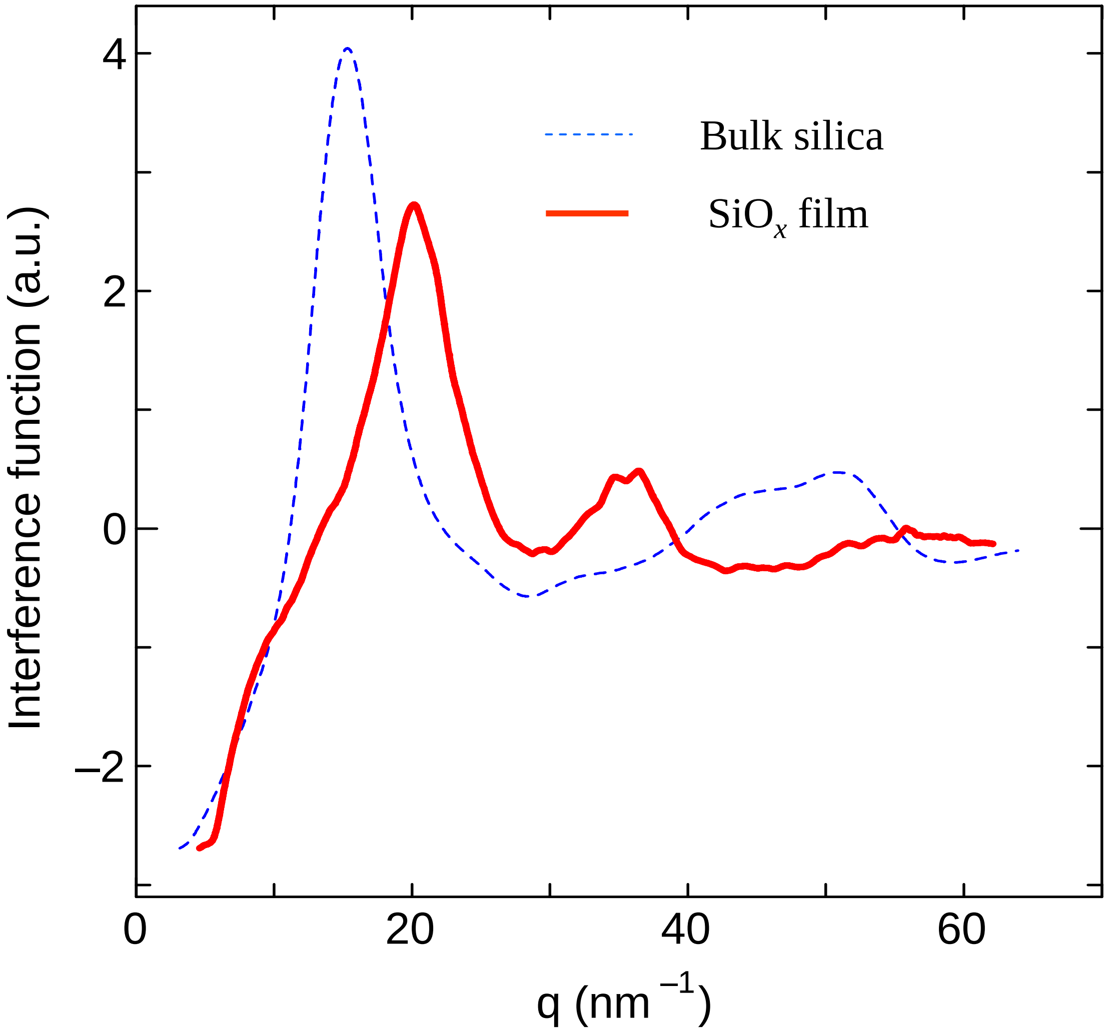


Interference function:

$$\boldsymbol{S(q)=\alpha I(q)-\Sigma f_i^2}$$

$$( \quad q = 4\pi \sin\theta/\lambda)$$

# RDF of the deposited amorphous $SiO_x$ film

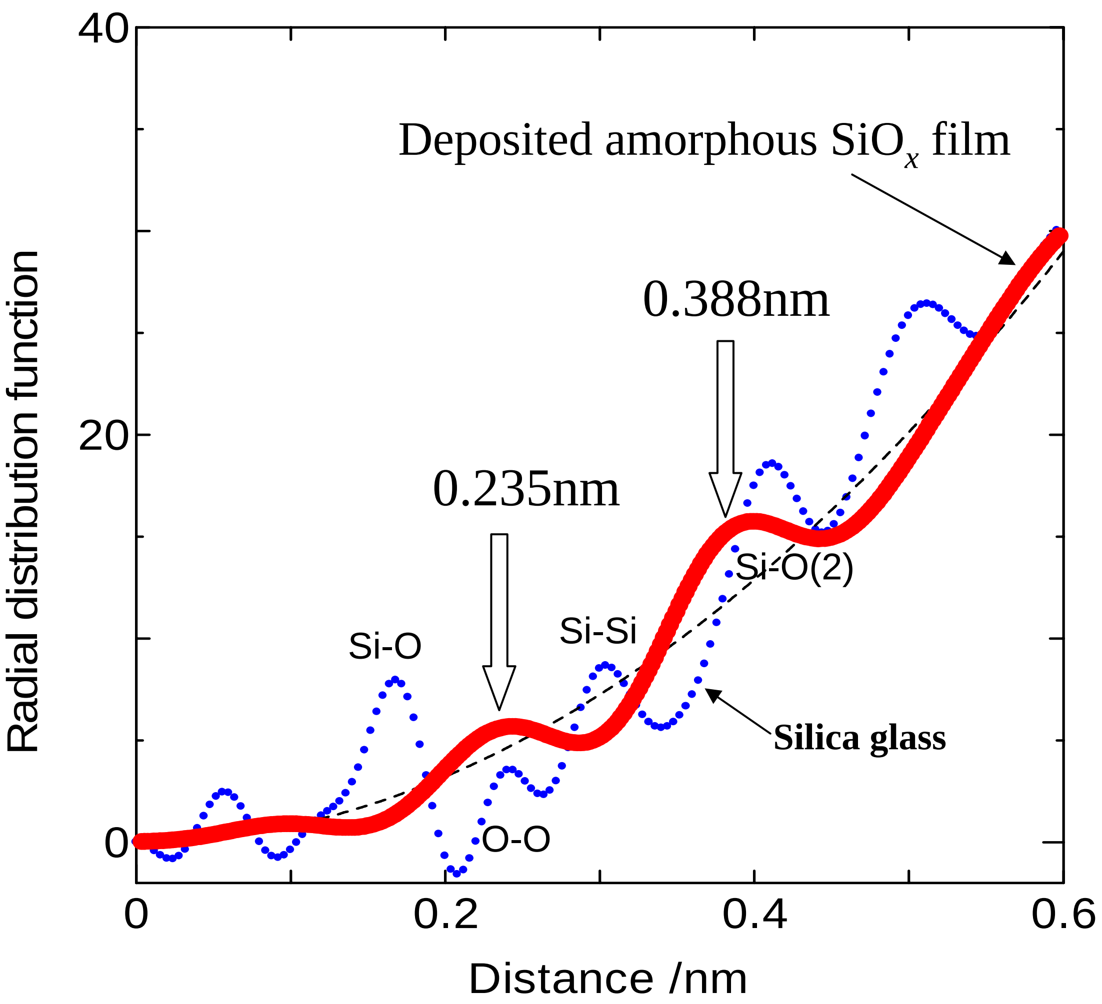


The RDF of the SiOx film has the peaks at 0.235nm and 0.388nm. As for silicon crystal, the interatomic distances of the first and second nearest neighbors are 0.235nm and 0.384nm. However, there is no indication of the pair correlations of third and forth nearest neighbors in silicon crystal in the RDF of the film. This result suggests that the film is composed of tetrahedron formed by silicon. Thus it is considered that silicon atoms of the film are partially oxidized.

Tetrahedron of Si crystal

| | |
|---|---|
| 1st nearest | 0.235nm |
| 2nd nearest | 0.385nm |

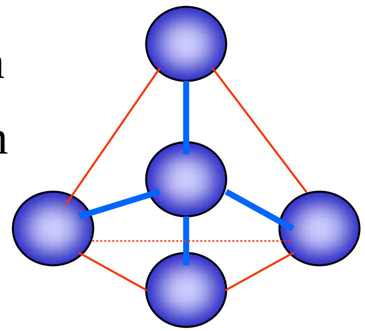

**The film is composed of Si tetrahedra** (not Si-O tetrahedra)

# Summary

- **Studying $SiO_x$ film deposited on Si substrate by ECR sputtering with grazing incidence X-ray scattering (GIXS).**
- **The radial distribution function derived from scattering profile revealed that the $SiO_x$ film was composed of silicon tetrahedra.**
- **It is concluded that silicon atoms of the film are partially oxidized.**
- **GIXS is a valuable technique to study the structure of amorphous thin film.**

# *In-situ* observation for weld solidification process of carbon steel metal

SUMITOMO METAL INDUSTRIES,LTD.

**Solidification Crack**

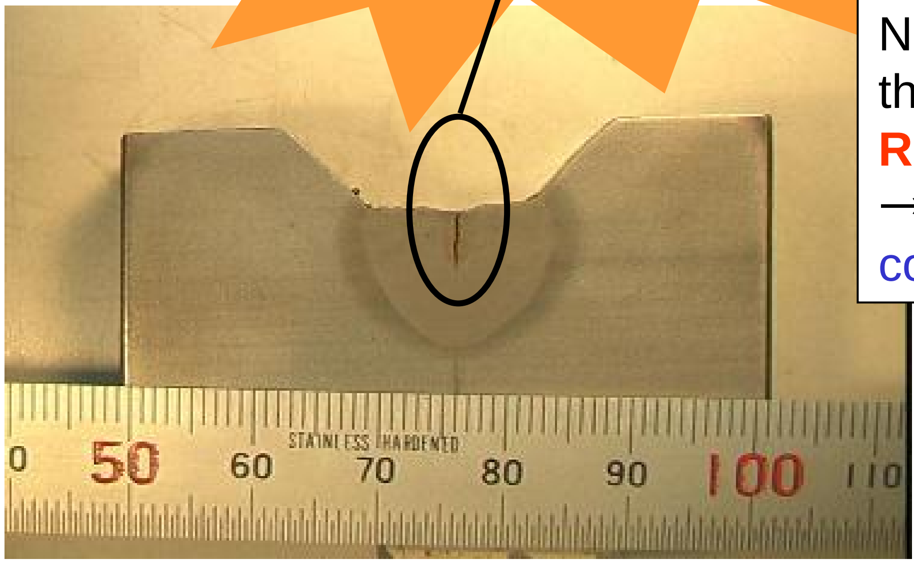


Countermeasure

Narrowing the solidification temperature range where the ductility of the steel decreases：

**Raising the solidification temperature**

→Control of the phase evolution during the rapid cooling by the matrix composition of the steel

**Guideline for the material design**

***In-situ*** **observation of weld solidification process during the rapid cooling（～500K/sec)**

# Time resolved X-ray diffraction measurement by Silicon Pixel Detector

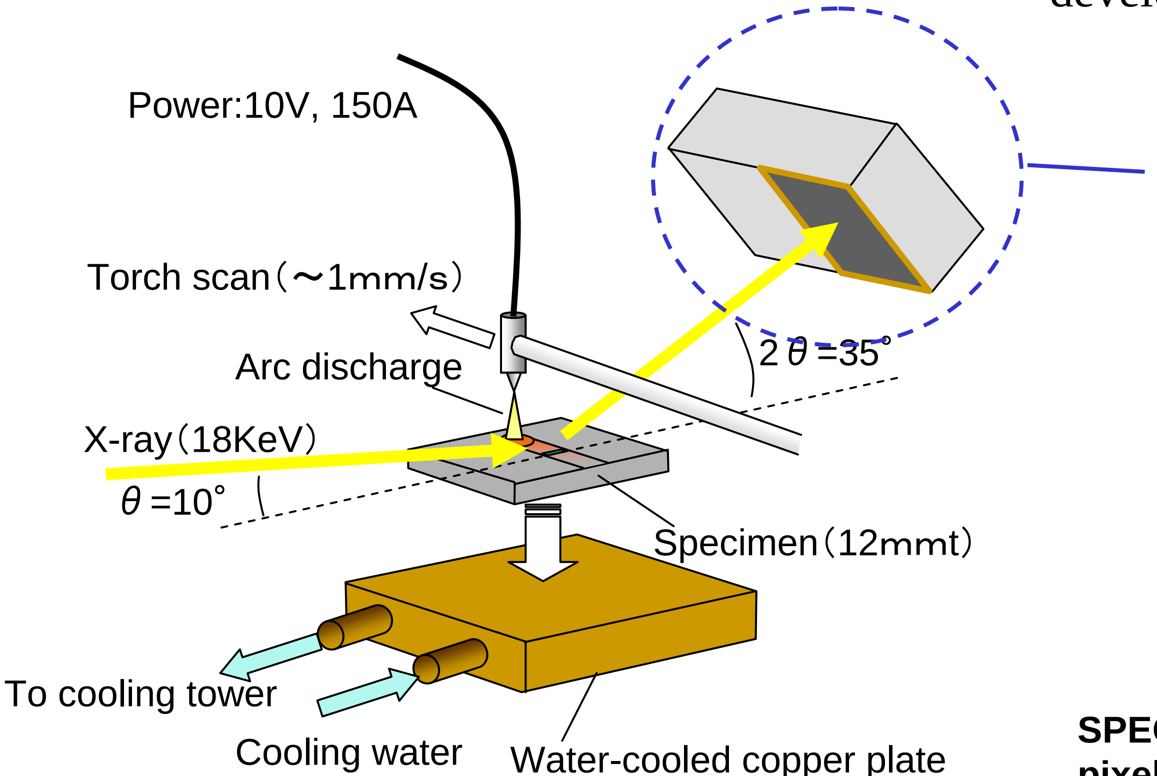


## PILATUS

developed by PSI（SLS）&JASRI（SPring-8）

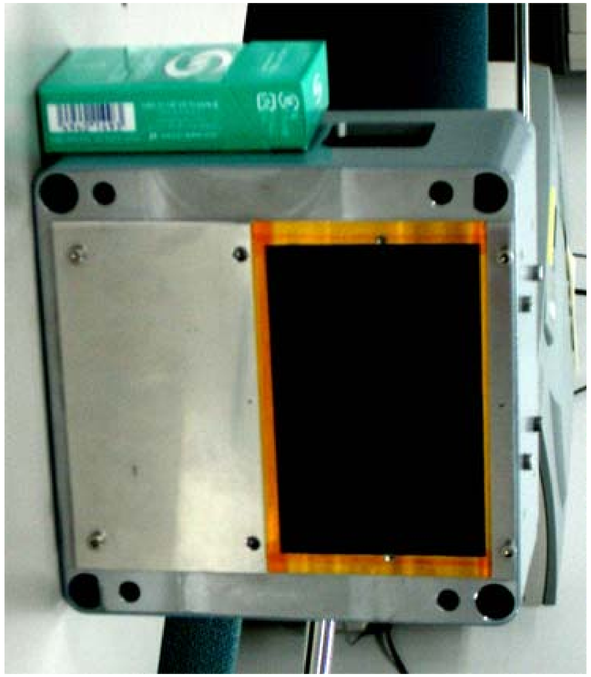

**SPEC**:

| | |
|---|---|
| **pixel size** | **217 μm** |
| **Number of pixel** | **366×157** |
| **area of detector** | **79.4mm×34.mm** |
| **Digital clock** | **10MHz** |
| **readout time** | **6.7msec** |

**Upgraded version PILATUS II has been installed at 2006.**

# *Layout of experiment*

## BL46XU Multi-axis Diffractometer

Upstream side view

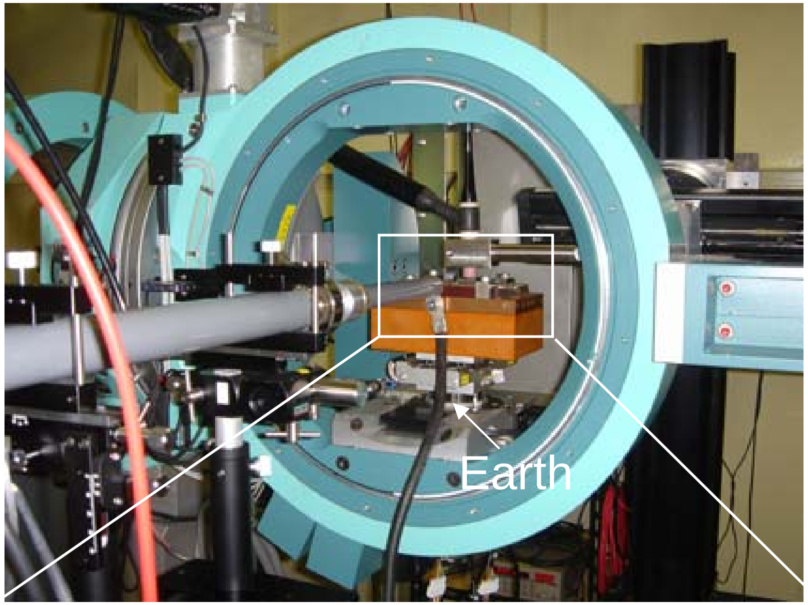


Downstream side view

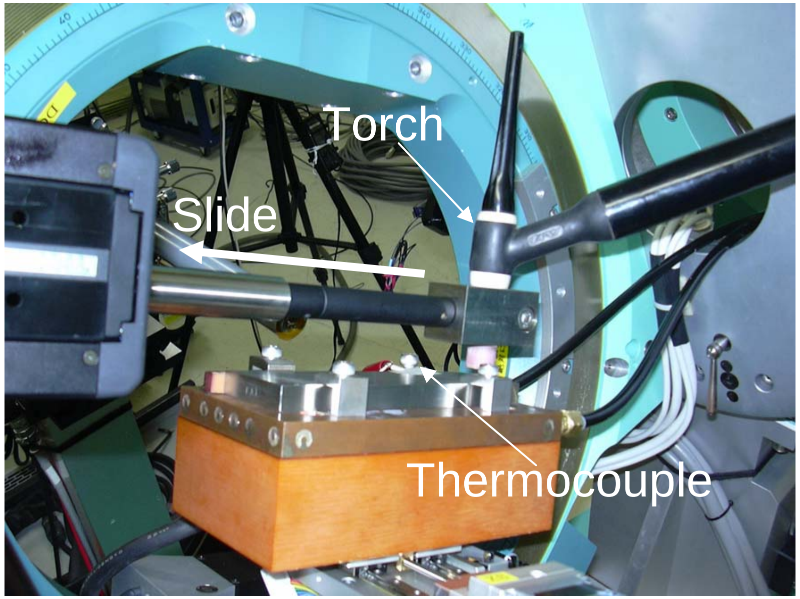


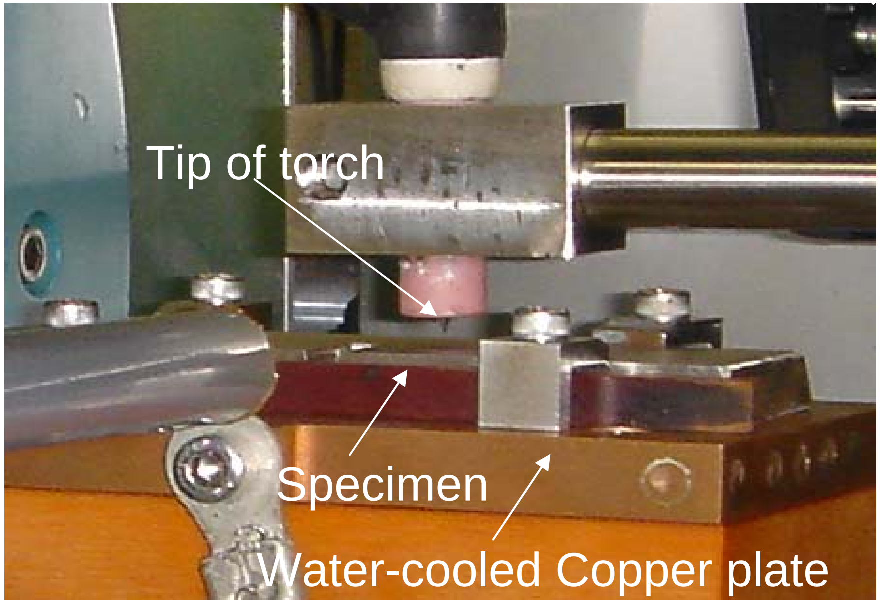


Time change of temperature with the torch motion

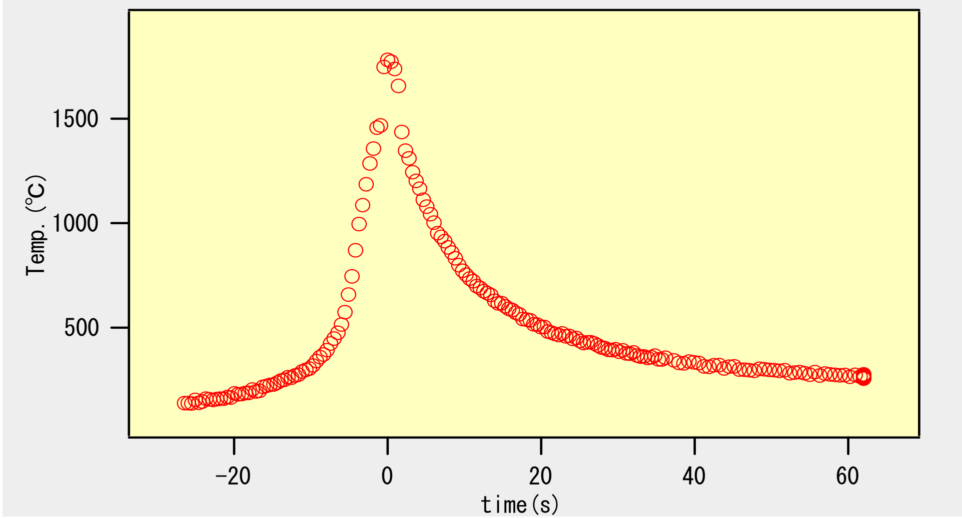

# Variation of diffraction profiles during solidification II

**Low Alloy steel**

**total：4sec**

Complicated phase evolution
with solid transformation

It is impossible to investigate the solidification process by the ex-situ observation of quenched solidification microstrucures.

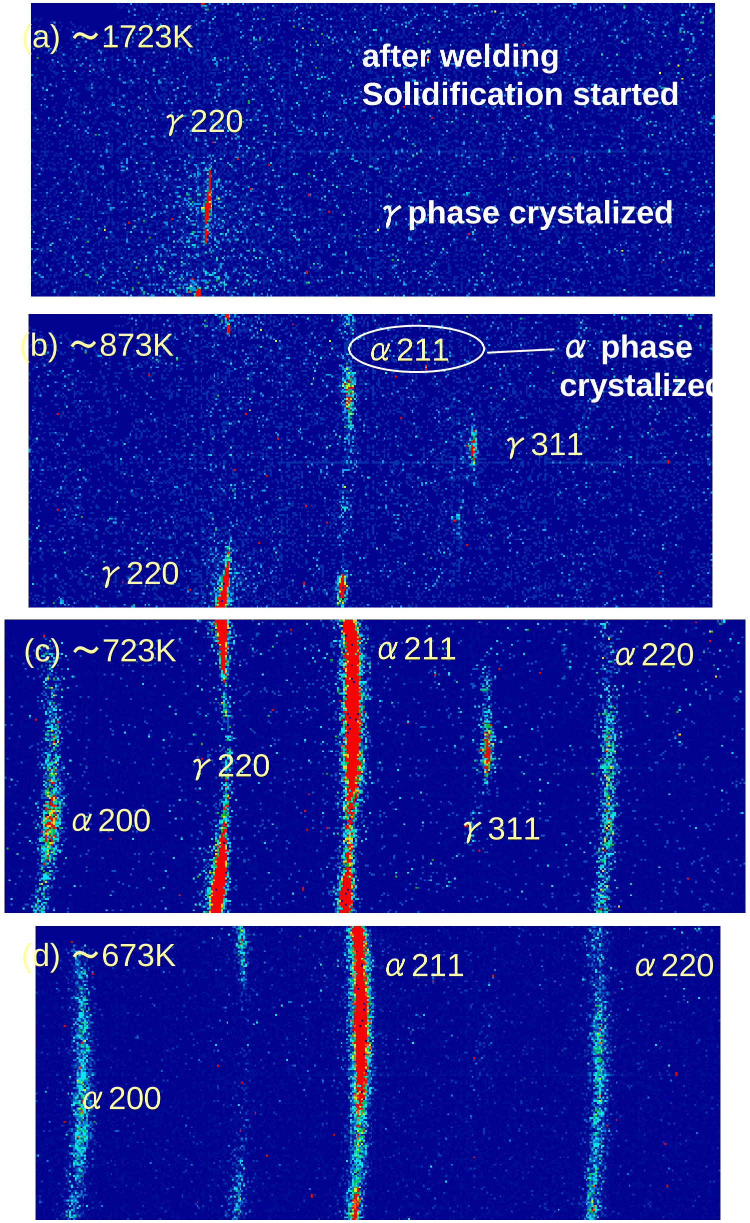

# Variation of diffraction profiles during solidification I

## High Alloy steel (AF mode)

Total time：4sec

**Calculated Phase Diagram**

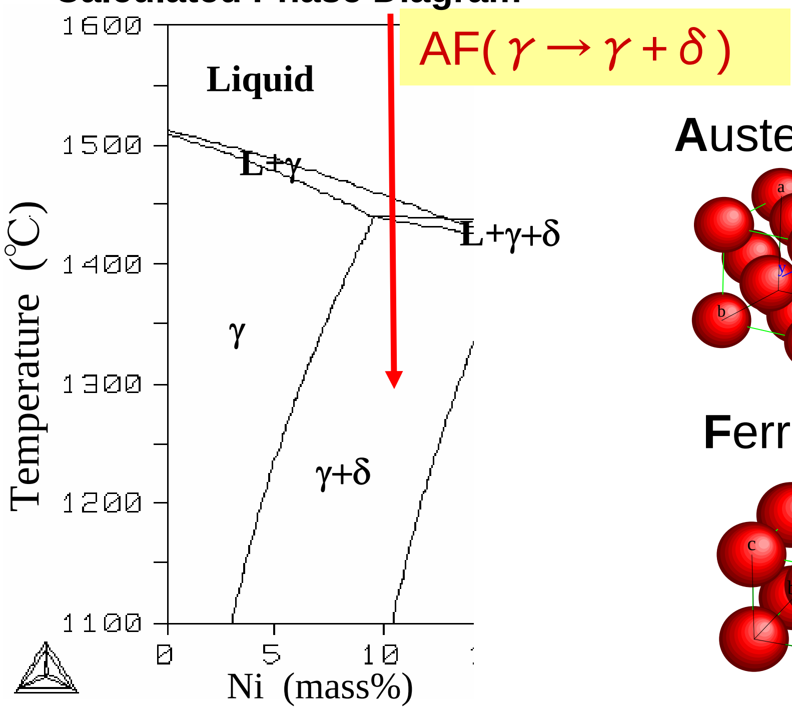


Austenite(γ)

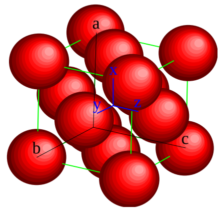


Ferrite(δ)

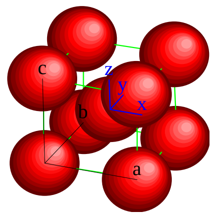


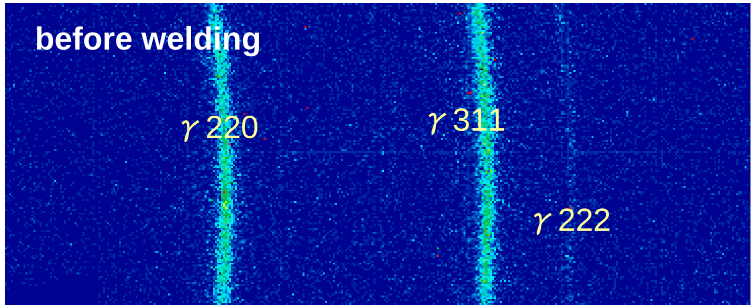


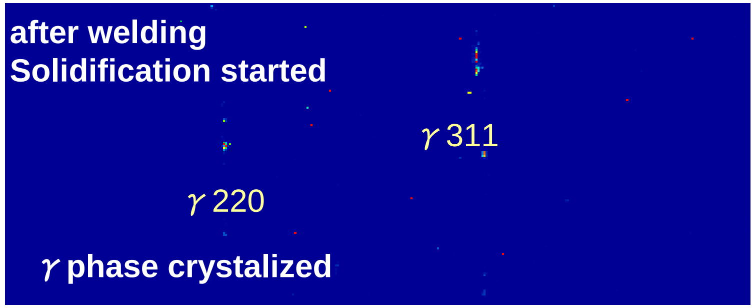


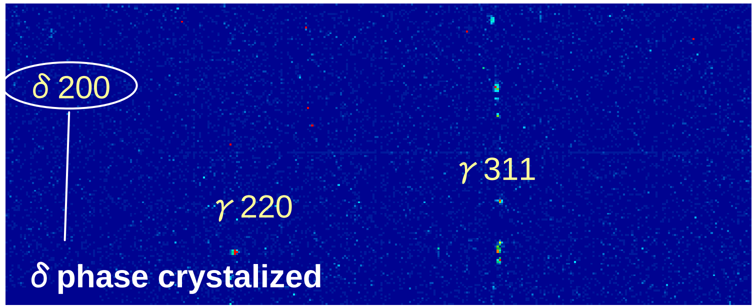


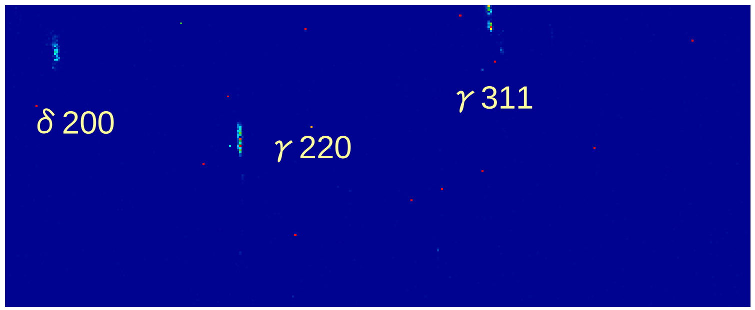

# *In-situ* observation of weld solidification process using synchrotron radiati n

SPring-8

## Summary

Time dependence ffraction s d eld c cation in a few seconds is successfu ng-8 with **High flux** and **Pixel detecto**

This experimental result provides an important information for the development of welding process of high performance steel.

- High allo cation during rapid
- Low alloy stee apid cooling wh ventional method was succes

➡ Important i orm n fo velop nt of weld process of nigh p orma steel

~Å

State Analysis

XAFS

# XAFS
# (X-ray Absorption Fine Structure)

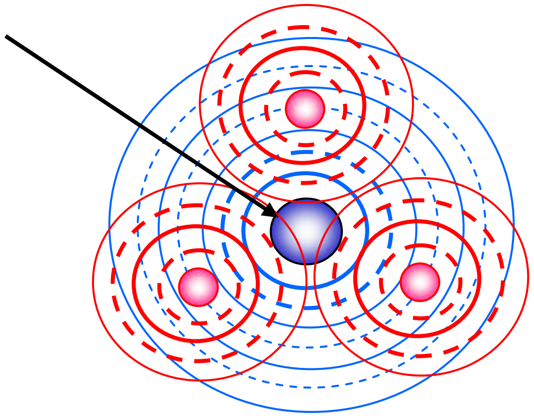

XANES : X-ray Absorption Near Edge Structure
EXAFS : Extended X-ray Absorption Fine Structure

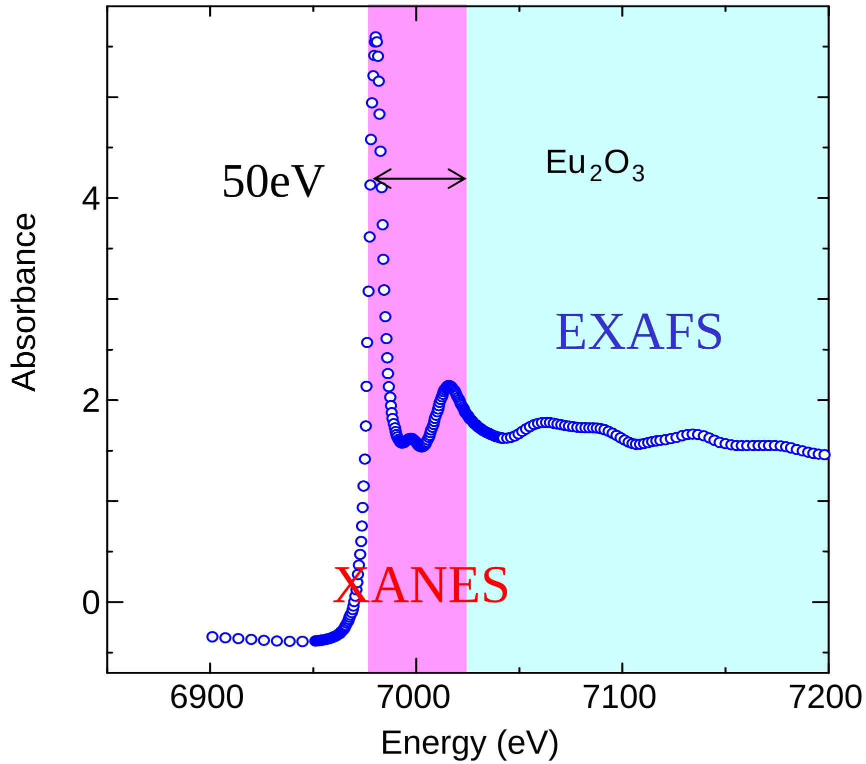


XANES: electronic state (valence)
EXAFS: local structure (coordination number, distance)

# Principle schemes of XAFS measurements

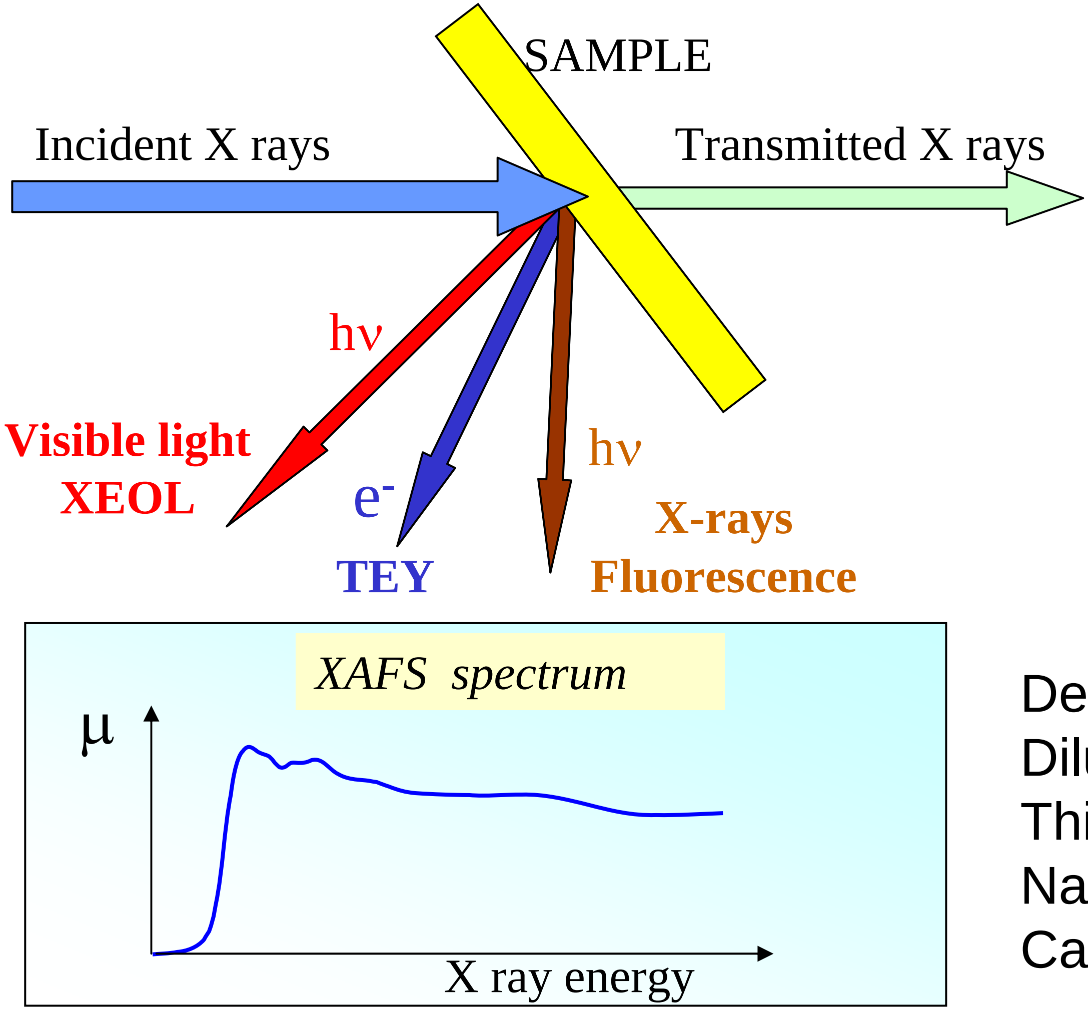


Dense samples
Diluted samples
Thin films
Nanocrystalline materials
Catalysts
…….

# Characterization of blue phosphor for PDP by XAFS

**Study of fading of light emitting from $BaMgAl_{10}O_{17}$ during production of PDP panel**

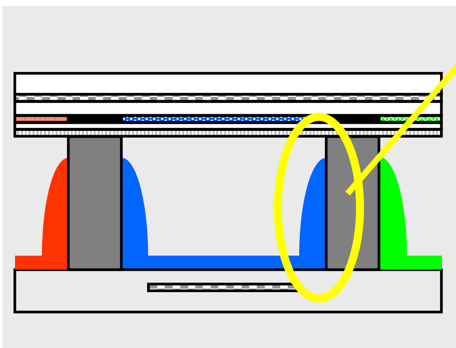

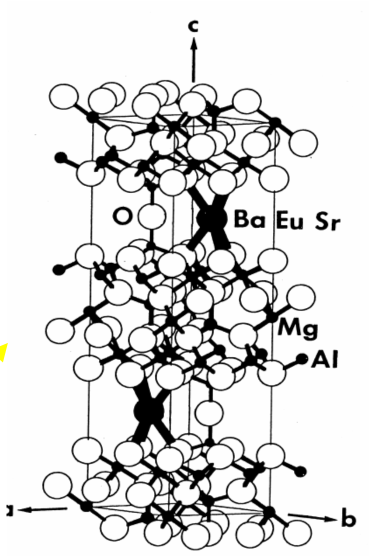


**$BaMgAl_{10}O_{17}$:Eu**

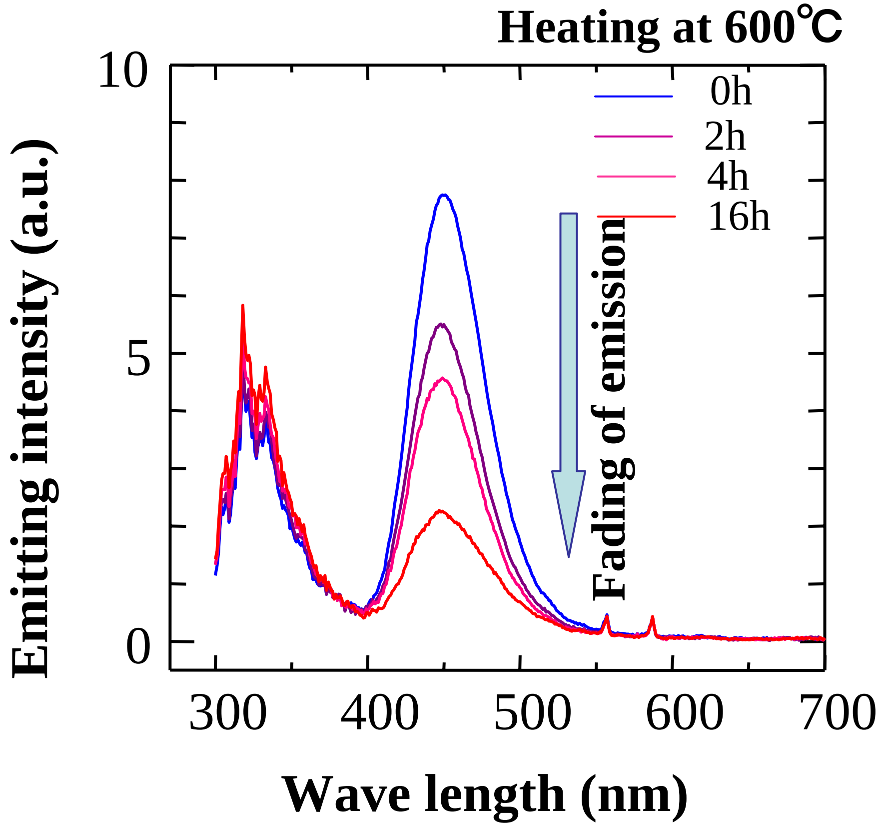


**<u>Change of emitting spectrum during heating</u>**

# Cell structure of PDP

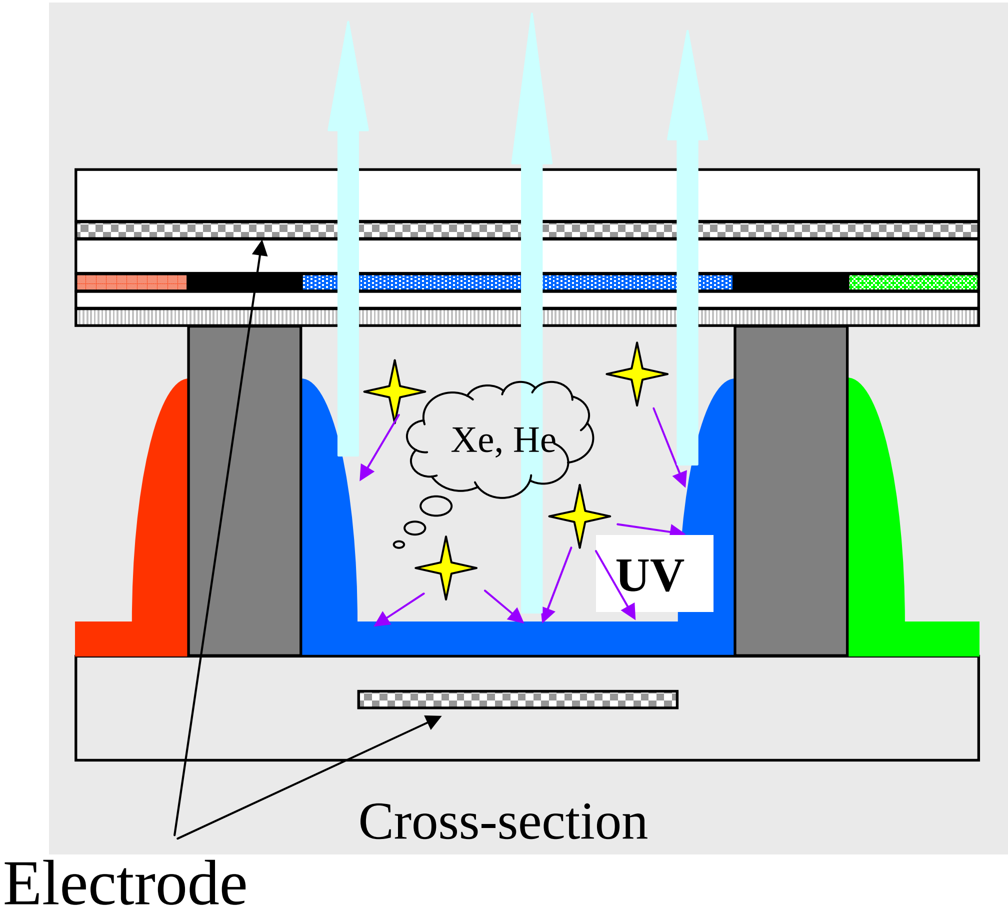


Visible light is emitted from UV irradiated phosphor.

Blue Phosphor :
**$Ba_{1-x}Eu_xMgAl_{10}O_{17}$ (BAM)**

**What occurs in phosphor by UV irradiation?**

Effect of irradiation was investigated by XAFS

# Experimental condition of XAFS of Eu-$L_3$

1st Station of BL19B2

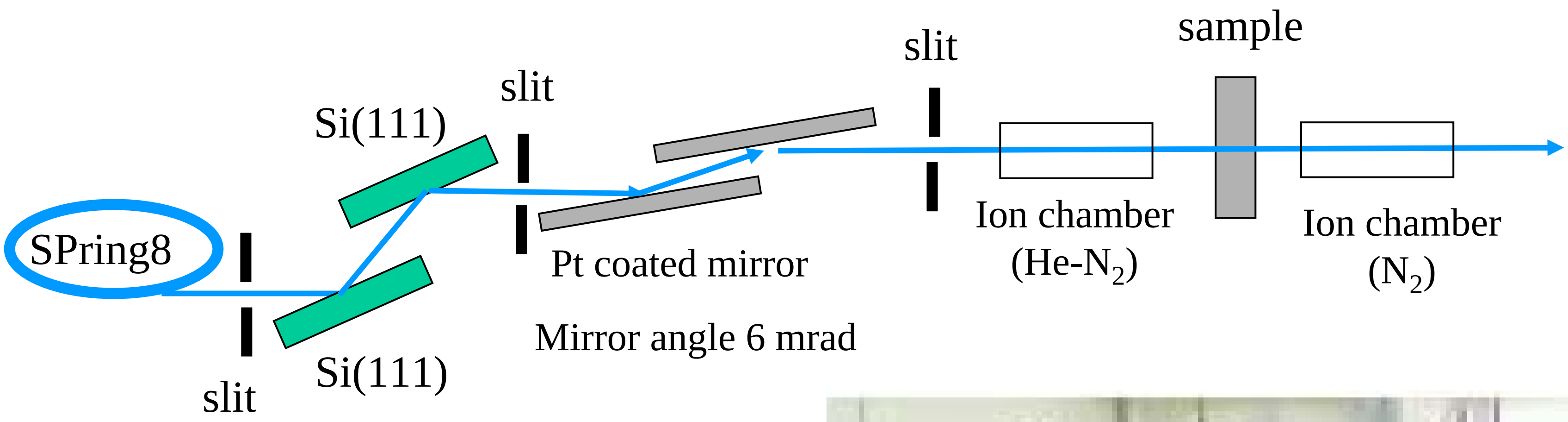


<u>Samples</u>

Irradiated $(BaEu)MgAl_{10}O_{17}$

Non-irradiated $(BaEu)MgAl_{10}O_{17}$

<u>References</u>

$EuCl_2$

$EuCl_3$

# Change of the local structure of Eu in $BaMgAl_{10}O_{17}$ during heating by XAFS

Heating condition : 4 hours / 600℃

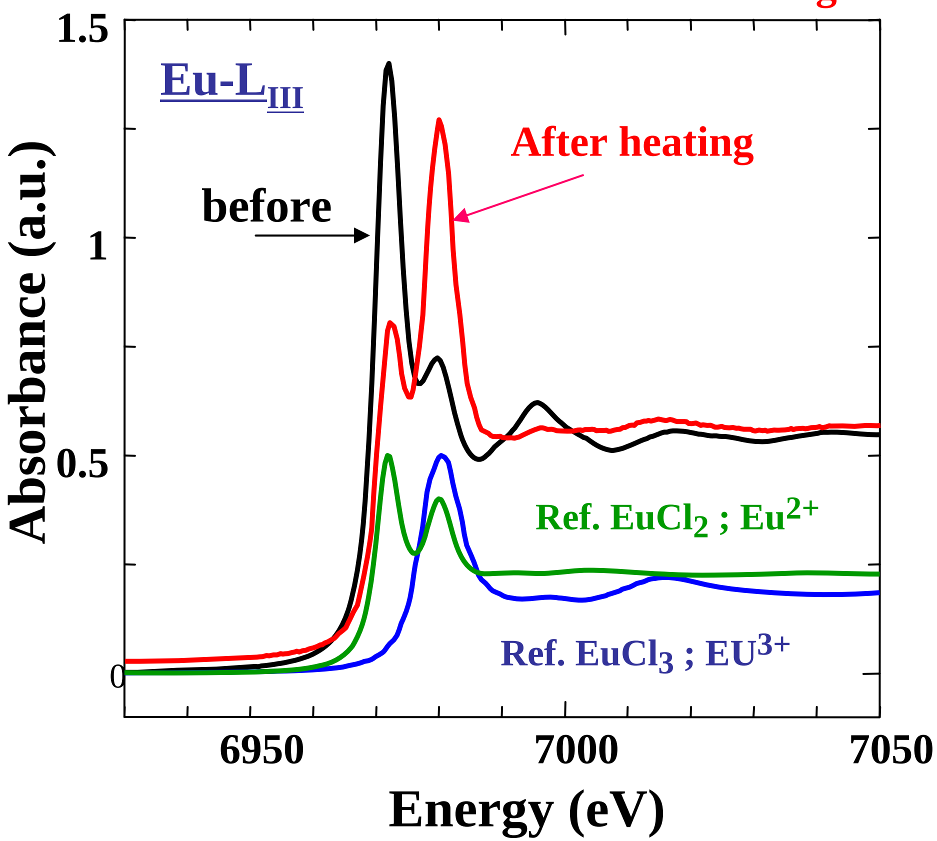


Change of XANES spectrum after heating

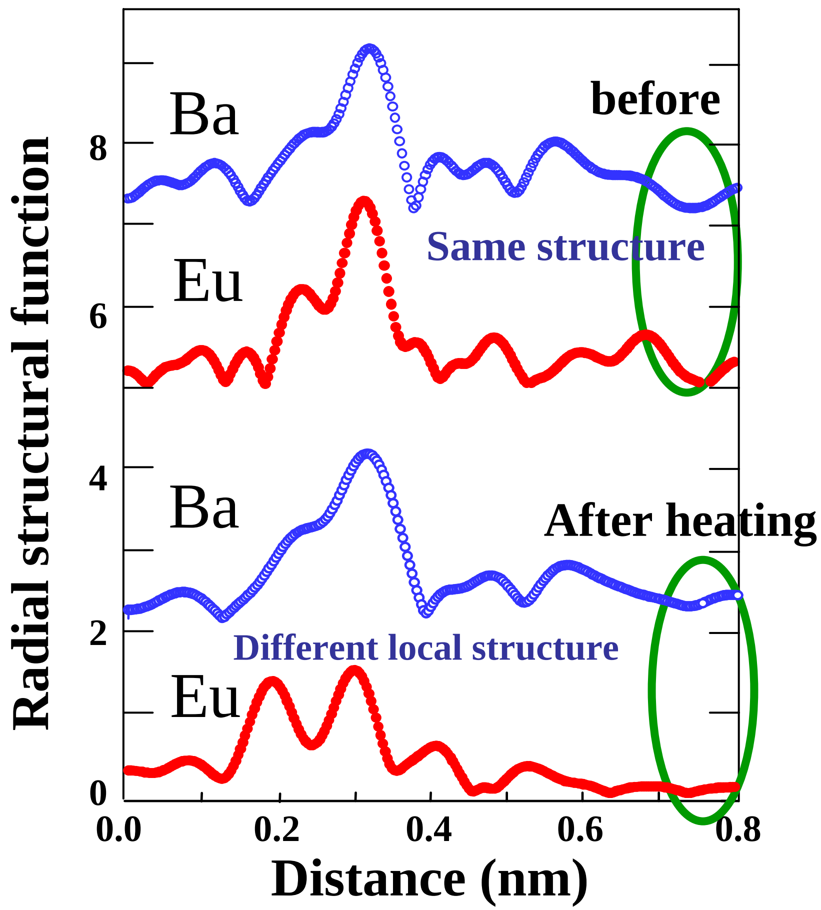


Change of RSF after heating

**Heating ⇨ Oxidization of Eu ⇨ Change of the local structure around Eu**

(Appendix)

# Mechanism of fading of light emitting from $BaMgAl_{10}O_{17}$:Eu during heating

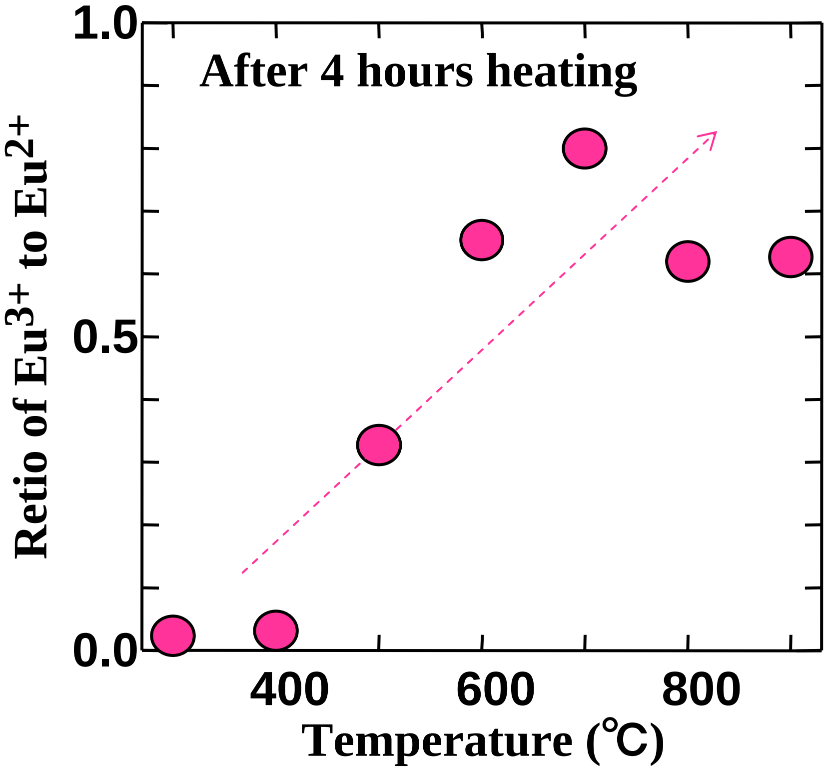


Temperature dependence of $Eu^{3+}$

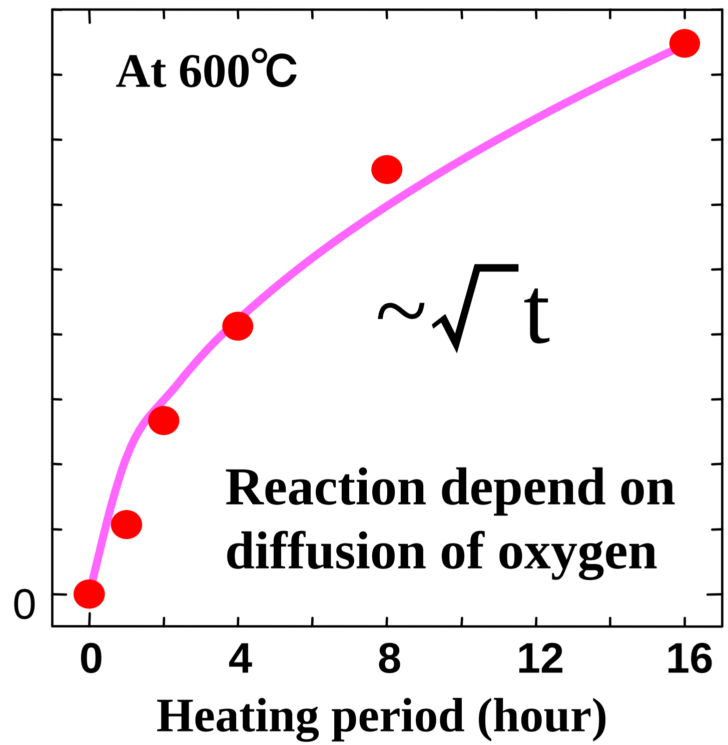


Time dependence of $Eu^{3+}$

**Fading of light emitting during heating is caused by selective oxidation of Eu controlled by oxygen diffusion from atmosphere.**

I. Hirosawa, J. SID . 12, 269 (2004)

# Characterization of blue phosphor for PDP by XAFS

## Summary

- **The fading of blue light is originated in oxidation of Eu in the phosphor.**

$$Eu^{2+} \xrightarrow{\text{Irradiation}} Eu^{3+}$$

- Next step: Clarification of change of local structure around Eu by irradiation.

SPring-8

# INDUSTRIAL APPLICATIONS

## Outline

1. Why did we start promoting industrial use?
2. Industrial support organization
3. Program for the industry supported by MEXT
   a. *Trial Use Program*
   b. *Strategic Program for Utilization of Advanced Large-Scale Research Facilities*
4. Public Beamlines for industrial applications
5. Highlights of industrial research works
6. User satisfaction
7. Summary

**Norimasa Umesaki**
Industrials Application Division, JASRI/SPring-8

10th SPring-8 Anniversary

# Industrial User Evaluation of "*Trial Use* Program"

- The answer to the questionnaire by the industrial users :

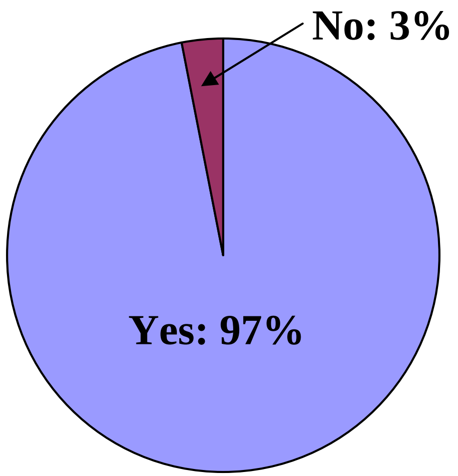


**Was this program useful to your research?**

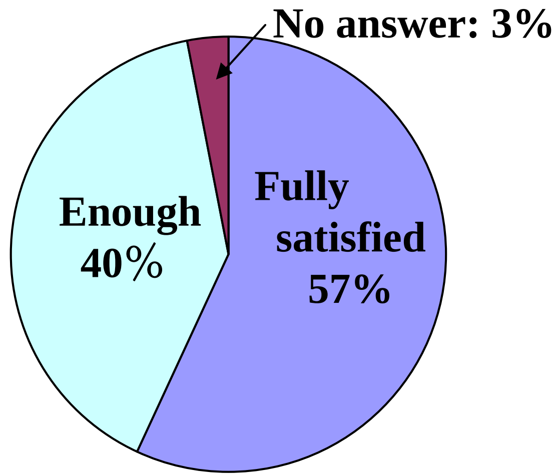


**Was there enough technical support?**

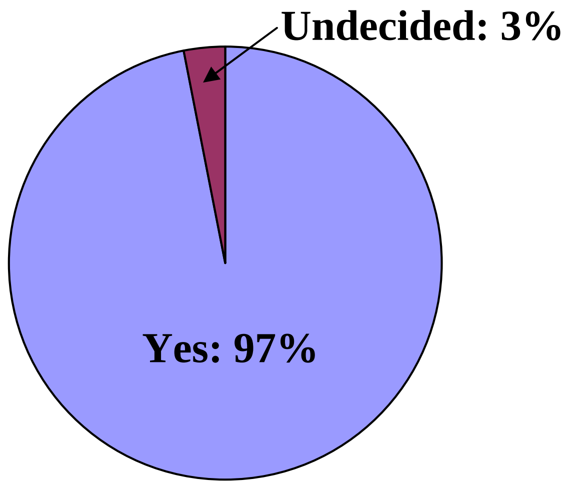


**Will you participate next chance?**

- Result of this program:
  - **Many new industrial users joined the program.**
- Unresolved subject:
  - **Beam time is not enough to create direct contribution for the development of actual products.**

# Industrial User Evaluation of "*Strategic Program for Utilization of Advanced Large-scale Research Facilities*"

**Questions**

**Was the technical consultation appropriately done?**

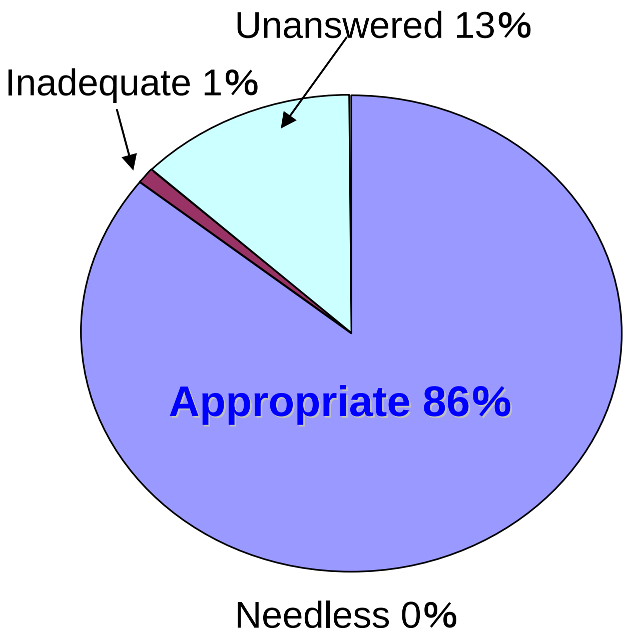


**Was the technical support appropriately done?**

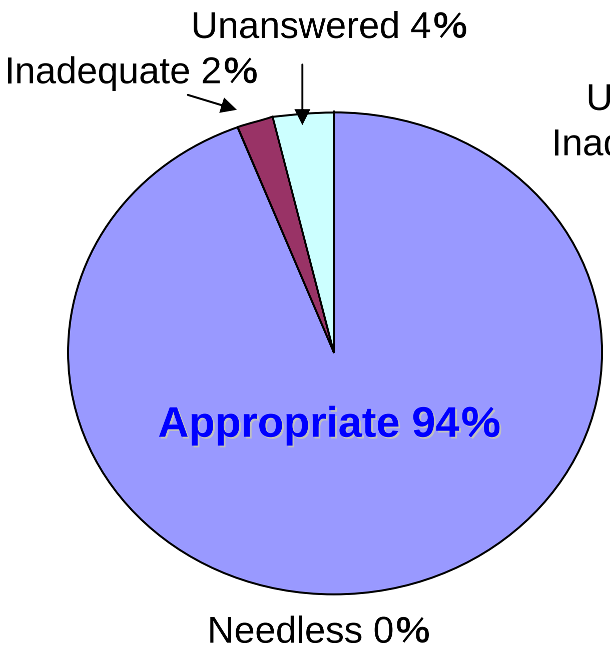


**During and after the period of the users' experiments, was the technical support for data analysis appropriately done?**

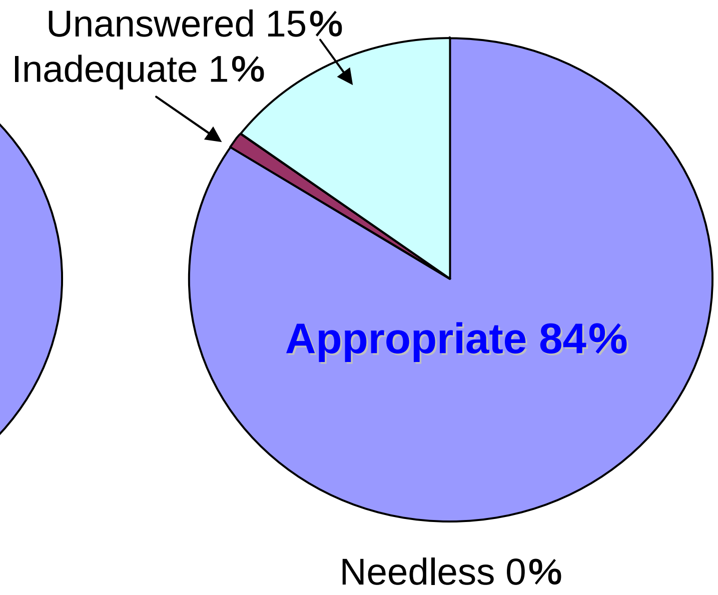


Realization of barrier-free of the users' experiments by reinforcement of the support system

Answer rate of the questionnaire:75% (85 replied proporsa1s / 117 sent proposals)

# Summary

- Industrial applications have been steadily increasing for these five years, as a result of the MEXT programs and the effort of our staff and users. Utilization of SPring-8 has become familiar to the industry, and there has been an active entry of new businesses and from new fields, resulting in a total of 2,200 users from 170 companies visiting SPring-8 to perform experiments in 2005.
- Expansion in utilization and accumulated results suggest various issues and direction for the future. The main issues are the promotion of utilization by non-specialists, and utilization that leads directly to business and the way to secure utilization opportunities for such purposes.
- It is now essential to reconstruct the beamlines, experimental equipment, utilization system and the organization comprehensively to accept various users and to produce good results.


Thank you for listening.
Special thanks to:
Staff of the Industrial Application Division
Industrial Users

(Appendix)

# Small-angle X-ray diffraction using a microbeam at BL40XU (High Flux Beamline)

- Two pinholes
- CCD camera combined with an imaging intensifier

Experiment

Hair cuticle (Inoue *et al.* Kanebo Cosmetics Inc.)

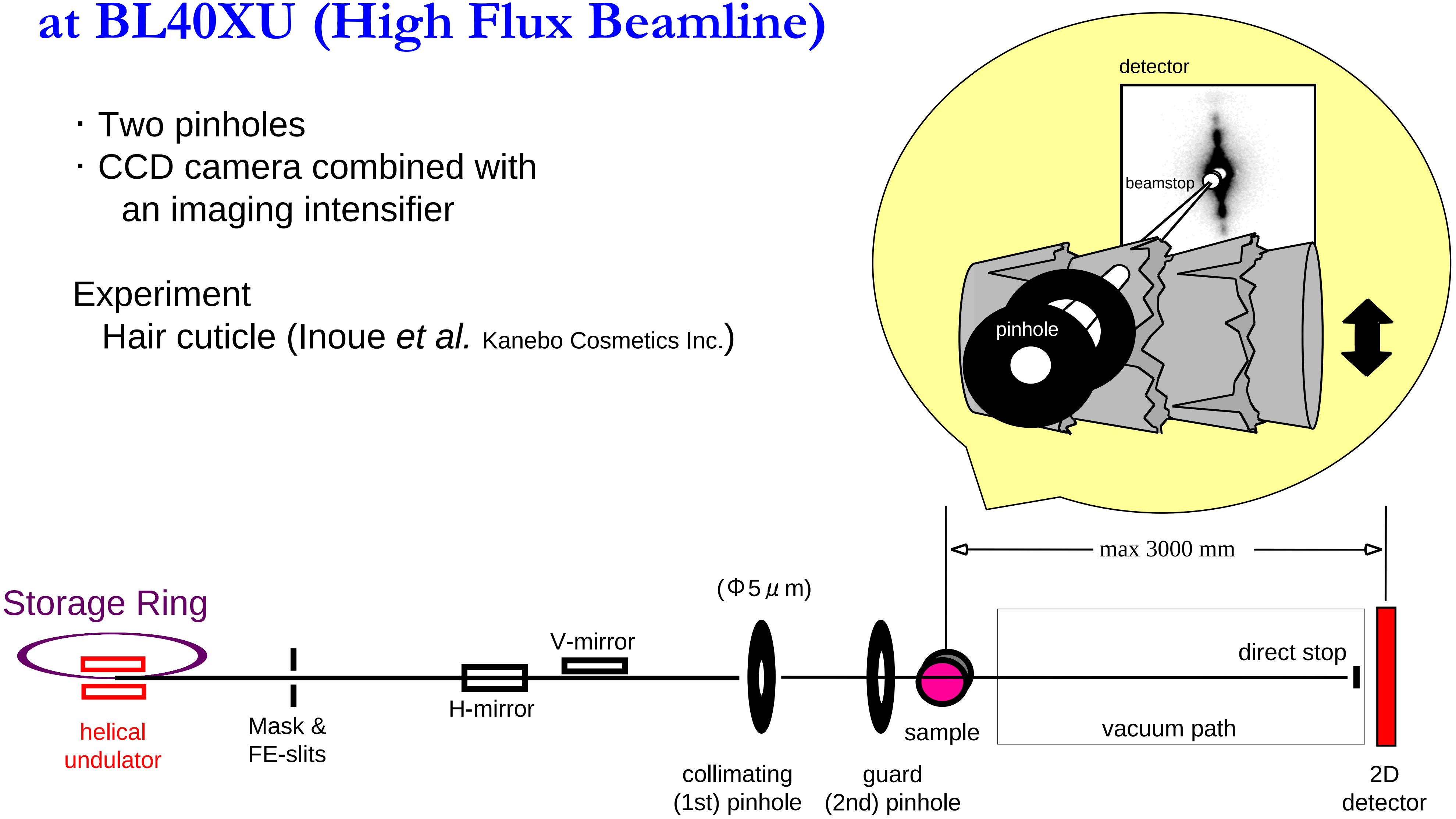

(Appendix)

# Structural Analysis of Human Hair Cuticle using Micro-beam X-ray Diffraction

## - Relationship with Effects of Hair Dyeing (T. Inoue *et al.*) -

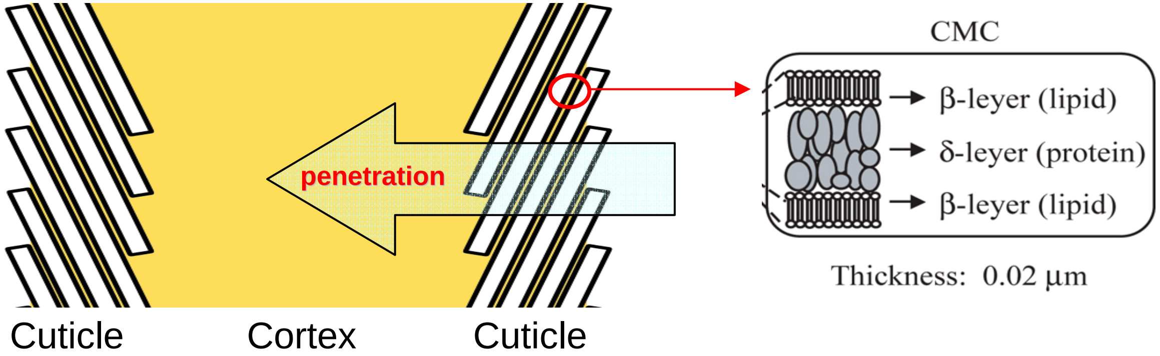


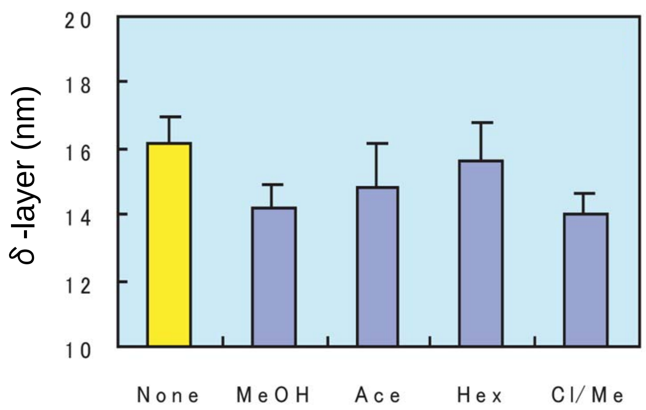


Effects of extraction

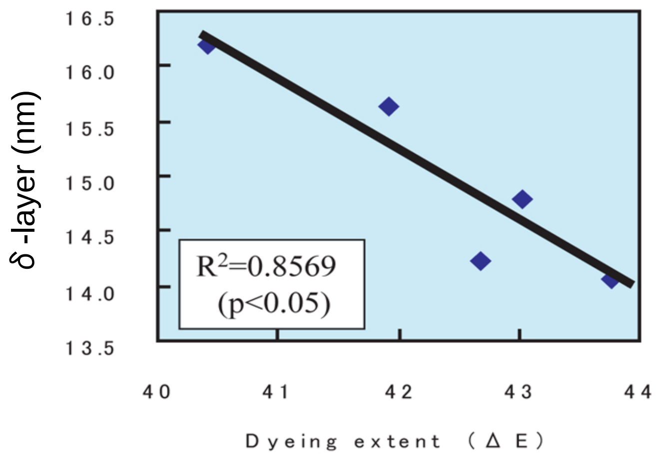


δ -layer thickness and dyeing extent

(Appendix) "Development of Ecological and High-performance Tire"

SRI R&D Ltd. Sumitomo Rubber Industries group Confidential

Nano-particle (Filler) such as Carbon Black and Silica


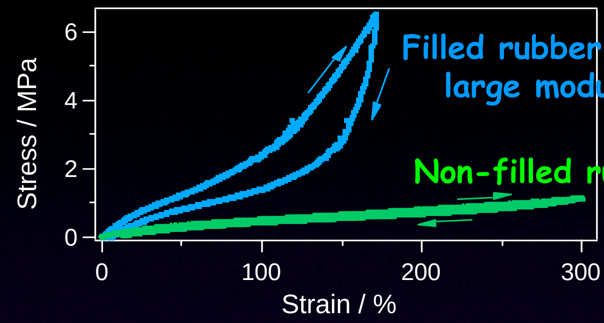


Filled rubber shows "Reinforcement Effect"

## What is the origin of reinforcement effect ?

It is important to clarify
- the filler network structure,
- the change in its structure under stretch.

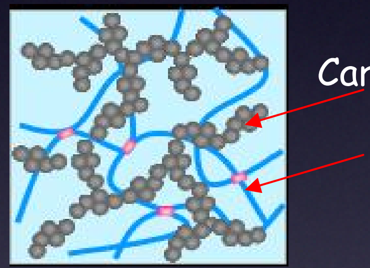


## Time-resolved 2D-USAXS / SAXS / WAXSat BL20XU and BL40B2 in Sring-8

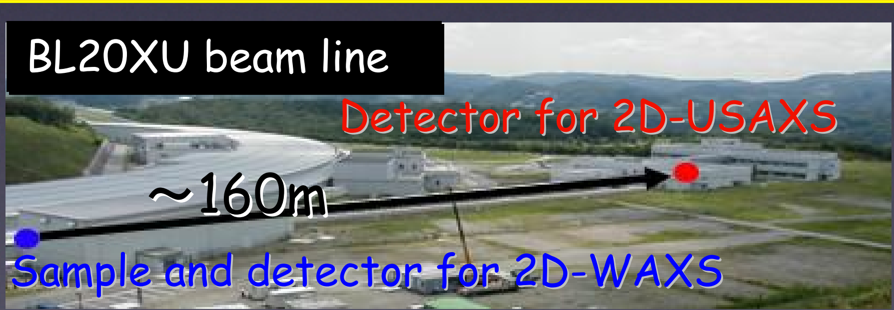


- Camera length : ~ 160m
- Wide q-range : $10^{-4}$ ~ $10^{-1}$ Å$^{-1}$
- Exposure time : < 100 ms

(Appendix)

## 2D-USAXS pattern of rubber filled with spherical silica ( 100 nm in diameter, $\phi$ = 0.2 ) in 2004

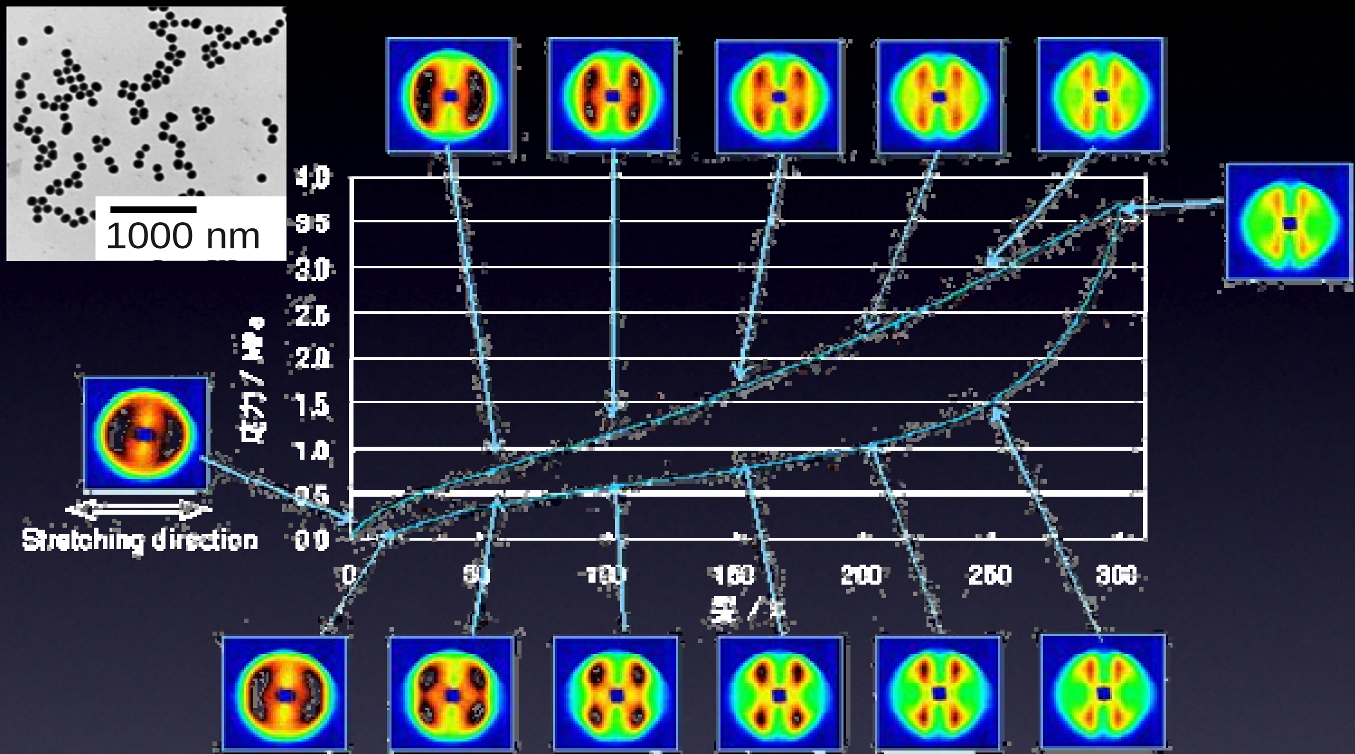


Modeling of filler 3D-configuration with the Earth Simulator

2D-USAXS pattern

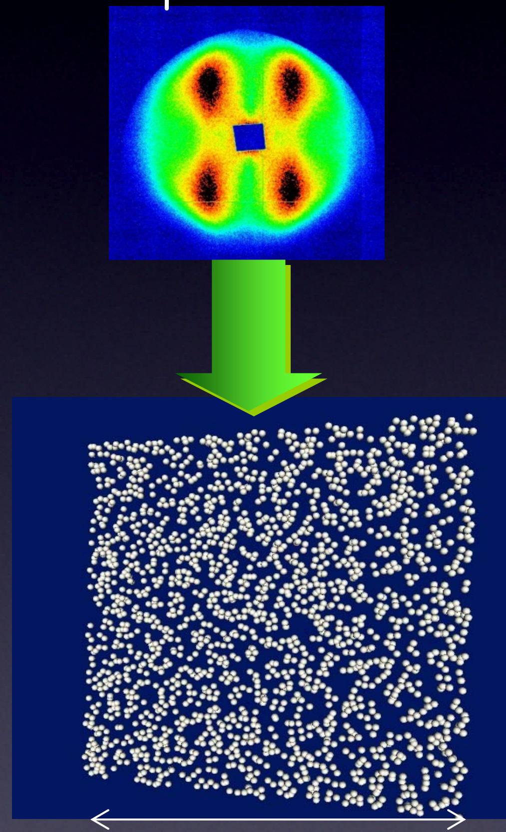


2D-RMC ( slice image)

- Four-spots-like patterns appear at the strain above 100 %, it shows the change from random structure to zigzag structure

The spatial configuration of fillers is changed like pantograph by stretch

We developed 2Dp-RMC in 2005

(Appendix)

# *In situ* XAFS study on cathode materials for Li-ion batteries

SPring-8、BL16B2(The industrial consortium beam line)

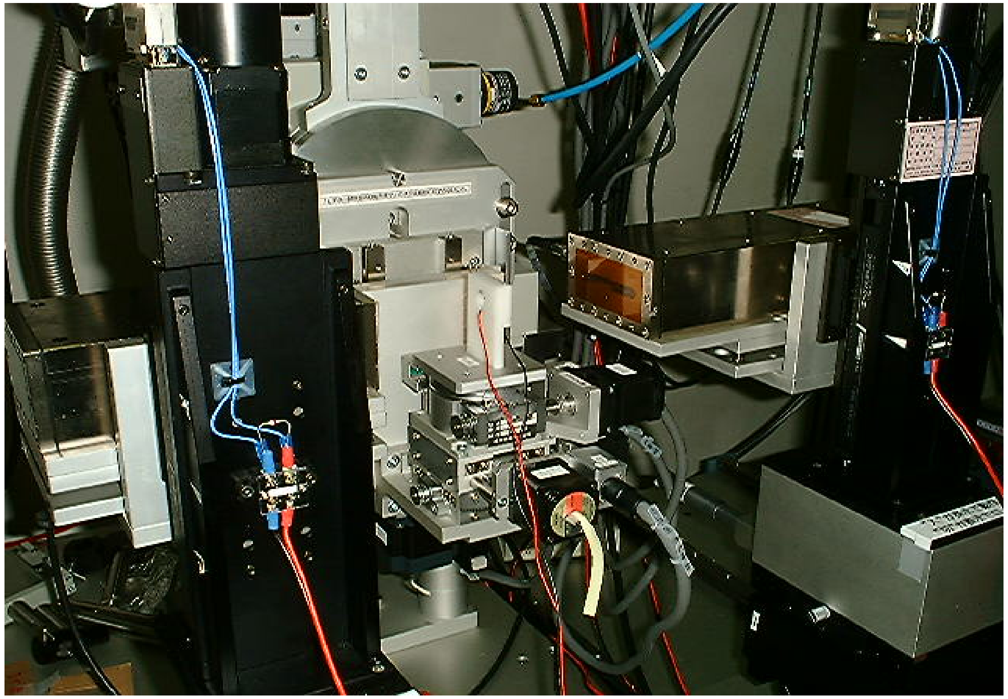

The experimental setup for Ni K-edge XAFS measurements in a transmission mode.

(Appendix)

# *In situ* XAFS study on cathode materials for Li-ion batteries

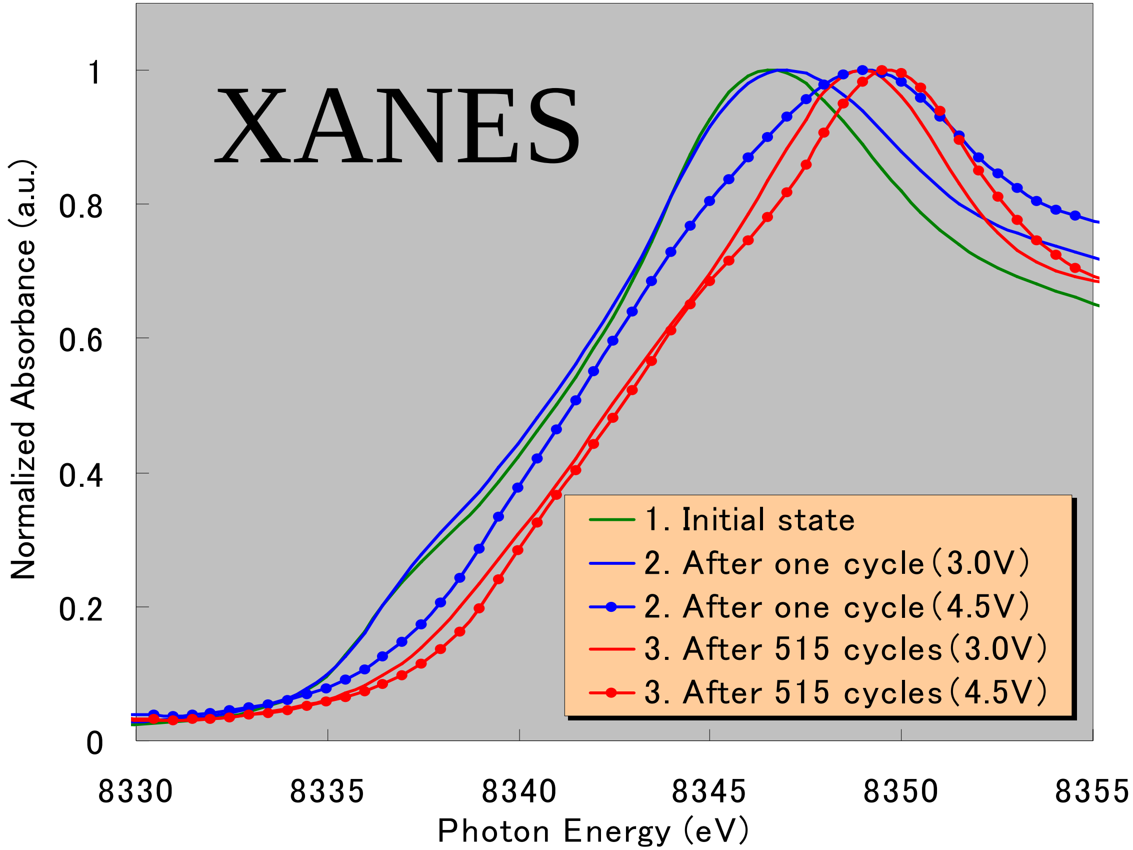


Ni K-edge XANES spectra for $LiNi_{0.8}Co_{0.2}O_2$.

Chemical shift to higher energy

Oxidization of Ni

($Ni^{3+} \rightarrow Ni^{4+}$)

(Appendix)

# *In situ* XAFS study on cathode materials for Li-ion batteries

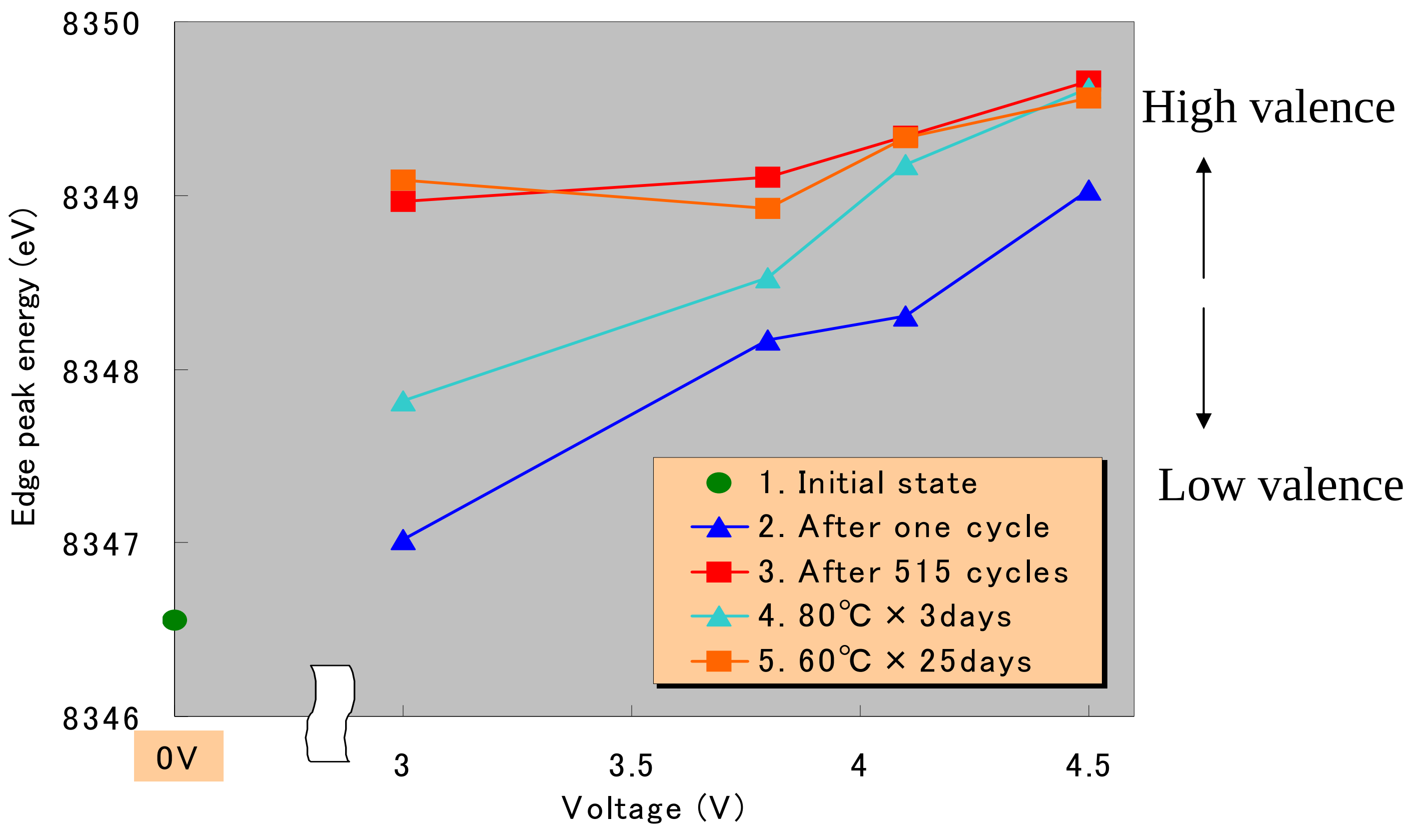


Comparison of Ni K-edge peak energies as a function of the cell voltages.

(Appendix)

# *In situ* XAFS study on cathode materials for Li-ion batteries

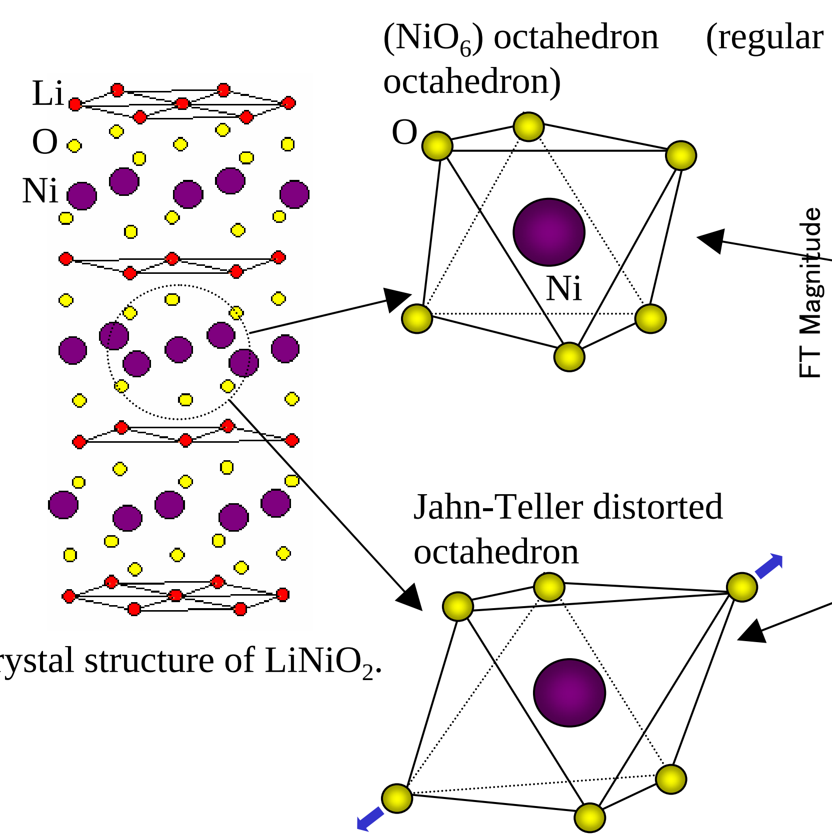


Crystal structure of $LiNiO_2$.

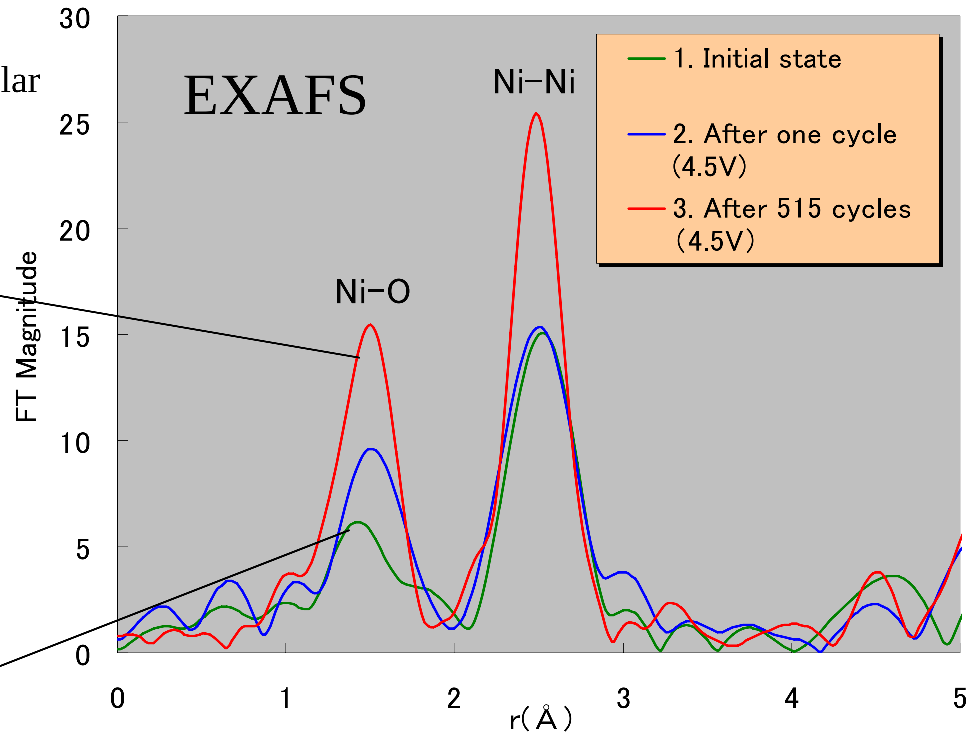


Fourier-transforms of Ni K-EXAFS spectra for $LiNi_{0.8}Co_{0.2}O_2$.

(Appendix)

# *In situ* XAFS study on cathode materials for Li-ion batteries

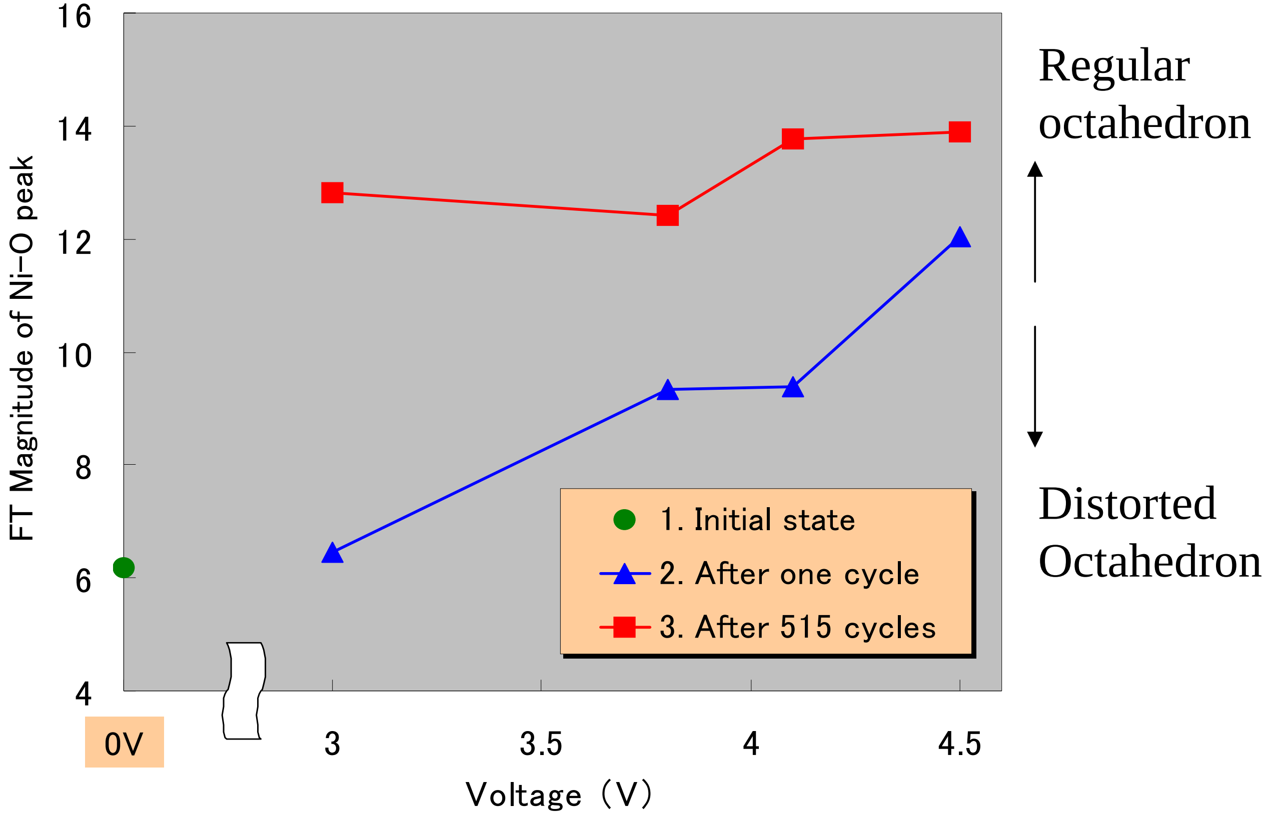


Comparison of the heights of Ni-O peaks in FT spectra as a function of cell voltage.

(Appendix)

# *In situ* XAFS study on cathode materials for Li-ion batteries

## Initial state

Ni valence･･･lower → higher valence upon charging

($NiO_6$) octahedron･･･distorted → regular

## Deteriorated state (Capacity fading)

Ni valence･･･high valence

($NiO_6$) octahedron･･･regular

Li ions can not come back to the cathode?

**By using these in situ XAFS methods, they are now studying some modified cathode materials.**